OXIDATIVE DEHYDROGENATION OF ETHANOL TO ACETALDEHYDE OVER

MAGNESIUM ALUMINIUM LAYERED DOUBLE HYDROXIDES CATALYST

Mr. Piriya Pinthong

A Dissertation Submitted in Partial Fulfillment of the Requirements

for the Degree of Doctor of Engineering in Chemical Engineering

Department of Chemical Engineering

Faculty of Engineering

Chulalongkorn University

Academic Year 2018

Copyright of Chulalongkorn University

ออกซิเดทีฟดีไฮโดรจิเนชันของเอทานอลเป็นอะซิทัลดีไฮด์บนตัวเร่งปฏิกิริยาแมกนีเซียม
อะลูมิเนียมเลเยอร์ดับเบิลไฮดรอกไซด์

นายพิริยะ ปิ่นทอง

Thesis Title	OXIDATIVE DEHYDROGENATION OF ETHANOL TO ACETALDEHYDE OVER MAGNESIUM ALUMINIUM LAYERED DOUBLE HYDROXIDES CATALYST
By	Mr. Piriya Pinthong
Field of Study	Chemical Engineering
Thesis Advisor	Professor BUNJERD JONGSOMJIT, Ph.D.

Accepted by the Faculty of Engineering, Chulalongkorn University in Partial Fulfillment of the Requirement for the Doctor of Engineering

.... Dean of the Faculty of Engineering

(Professor SUPOT TEACHAVORASINSKUN, D.Eng.)

DISSERTATION COMMITTEE

.... Chairman

(Assistant Professor Sasiradee Jantasee, D.Eng.)

.... Thesis Advisor

(Professor BUNJERD JONGSOMJIT, Ph.D.)

.... Examiner

(CHUTIMON SATIRAPIPATHKUL, D.Eng.)

.... Examiner

(Professor MUENDUEN PHISALAPHONG, Ph.D.)

.... Examiner

(Assistant Professor SUPHOT PHATANASRI, Ph.D.)

พิริยะ ปิ่นทอง : ออกซิเดทีฟดีไฮโดรจิเนชันของเอทานอลเป็นอะซิทัลดีไฮด์บนตัวเร่งปฏิกิริยา
แมกนีเซียมอะลูมิเนียมเลเยอร์ดับเบิลไฮดรอกไซด์ . (OXIDATIVE DEHYDROGENATION OF
ETHANOL TO ACETALDEHYDE OVER MAGNESIUM ALUMINIUM LAYERED DOUBLE
HYDROXIDES CATALYST) อ.ที่ปรึกษาหลัก : ศ. ดร.บรรเจิด จงสมจิตร

     งานวิจัยนี้ได้ทำการศึกษาคุณลักษณะและประสิทธิภาพการเร่งปฏิกิริยาของแมกนีเซียม
อะลูมิเนียมเลเยอร์ดับเบิลไฮดรอกไซด์ (Mg-Al LDH) และออกไซด์ผสมที่ปรับปรุงด้วยโลหะ โดยงานวิจัยนี้
แบ่งออกเป็น 3 ส่วน ในส่วนแรกเป็นการศึกษาผลของอุณหภูมิการแคลไซน์ต่อประสิทธิภาพการเร่งปฏิกิริยา
ออกซิเดทีฟดีไฮโดรจิเนชันของเอทานอล ผลการศึกษาพบว่าอุณหภูมิการแคลไซน์มีผลต่อคุณลักษณะของ
แมกนีเซียมอะลูมิเนียมเลเยอร์ดับเบิลไฮดรอกไซด์ (Mg-Al LDH) โดยเฉพาะอย่างยิ่งความเป็นเบสของตัวเร่ง
ปฏิกิริยา นอกจากนี้อุณหภูมิในการแคลไซน์ก็ยังมีผลต่อประสิทธิภาพการเร่งปฏิกิริยาออกซิเดทีฟดีไฮโดรจิเน
ชันของเอทานอล ของแมกนีเซียมอะลูมิเนียมเลเยอร์ดับเบิลไฮดรอกไซด์ (Mg-Al LDH) อีกด้วย ซึ่งผลการ
ทดลองนั้นสอดคล้องกับความเป็นเบสของตัวเร่งปฏิกิริยา ในส่วนที่สองนั้น ออกไซด์ผสมของแมกนีเซียมและ
อะลูมิเนียม (Mg-Al) ที่ได้จากการแคลไซน์แมกนีเซียมอะลูมิเนียมเลเยอร์ดับเบิลไฮดรอกไซด์ (Mg-Al
LDH) ถูกปรับปรุงโดยการเติมโลหะโมลิบดีนัม (Mo) วาเนเดียม (V) หรือทองแดง (Cu) ลงบนบนพื้นผิว
ผลการวิจัยพบว่าประสิทธิภาพการเร่งปฏิกิริยาของตัวเร่งปฏิกิริยาที่ปรับปรุงด้วยโลหะได้รับการส่งเสริมทั้งใน
กระบวนการดีไฮโดรจิเนชันและออกซิเดทีฟดีไฮโดรจิเนชัน ตัวเร่งปฏิกิริยาที่ถูกปรับปรุงด้วยทองแดง (Cu/Mg-
Al) ให้ผลผลิตอะซิทัลดีไฮด์สูงสุดที่ร้อยละ 41.8 ที่อุณหภูมิ 350 องศาเซลเซียส นอกจากนี้การปรับปรุงด้วย
โลหะนั้น ไม่ส่งผลเสียต่อเสถียรภาพของตัวเร่งปฏิกิริยาต่อปฏิกิริยาออกซิเดทีฟดีไฮโดรจิเนชันของเอทานอล
ในระยะเวลา 10 ชั่วโมง เพื่อเป็นการการศึกษาเพิ่มเติมเกี่ยวกับการประยุกต์ใช้ตัวเร่งปฏิกิริยาที่ปรับปรุงด้วย
ทองแดงกับไบโอเอทานอล ผลของปริมาณน้ำในเอทานอลได้ถูกศึกษาในส่วนที่สาม พบว่าปริมาณน้ำส่ง
ผลเสียต่อประสิทธิภาพการเร่งปฏิกิริยาของตัวเร่งปฏิกิริยาที่ถูกปรับปรุงด้วยทองแดง (Cu/Mg-Al) แต่
ผลกระทบนี้จะถูกกำจัดที่อุณหภูมิสูง ยิ่งไปกว่านั้นผลกระทบของอุณหภูมิในการรีดิวซ์ต่อการเร่งปฏิกิริยา ได้
ถูกศึกษาโดยการรีดิวซ์ตัวเร่งปฏิกิริยาที่อุณหภูมิ 300 และ 400 องศาเซลเซียส ก่อนการทำปฏิกิริยาออกซิเด
ทีฟดีไฮโดรจิเนชันของเอทานอล พบว่าขั้นตอนการรีดิวซ์ก่อนทำปฏิกิริยา ไม่ส่งผลกระทบต่อประสิทธิภาพการ
เร่งปฏิกิริยาอย่างมีนัยสำคัญ

สาขาวิชา	วิศวกรรมเคมี	ลายมือชื่อนิสิต ....
ปีการศึกษา	2561	ลายมือชื่อ อ.ที่ปรึกษาหลัก ....

5771418421 : MAJOR CHEMICAL ENGINEERING

KEYWORD: hydrotalcite, ethanol, oxidative dehydrogenation, acetaldehyde, LDH

Piriya Pinthong : OXIDATIVE DEHYDROGENATION OF ETHANOL TO ACETALDEHYDE OVER MAGNESIUM ALUMINIUM LAYERED DOUBLE HYDROXIDES CATALYST. Advisor: Prof. BUNJERD JONGSOMJIT, Ph.D.

In this research, the characteristic and catalytic activity of Mg-Al LDH and their metal-modified mixed oxide were investigated. This research was divided into three parts. In the first part, the effect of calcination temperature on catalytic performance via oxidative dehydrogenation of ethanol was elucidated. The results showed that calcination temperature affected the characteristic of Mg-Al LDH, especially basicity. Moreover, the calcination temperature also affected the catalytic performance on oxidative dehydrogenation of ethanol over Mg-Al LDH. The result was consistent with the basicity of catalysts. In the second part, the Mg-Al mixed oxide derived from calcination of Mg-Al LDH was modified by loading metal (Mo, V or Cu) on the surface. The results showed that the catalytic activity of metal-modified catalyst was promoted in both dehydrogenation and oxidative dehydrogenation. The copper-modified catalyst (Cu/Mg-Al) exhibited the highest acetaldehyde yield of 41.8% at 350°C. Furthermore, the metal modification not negatively affected the stability of catalyst on oxidative dehydrogenation of ethanol upon time-on-stream for 10 h. According to further investigate the application of catalyst to bioethanol, the effect of water content in ethanol feed was studied in the third part. It revealed that water content negatively affected the catalytic performance of Cu/Mg-Al catalyst, but this effect would be eliminated at high reaction temperature. Moreover, the effect of reduction temperature on catalytic activity was elucidated by varying the pre-reduction temperature of Cu/Mg-Al catalyst (300 and 400°C). It was found that the pre-reduction step insignificantly affected the catalytic performance.

Field of Study:	Chemical Engineering	Student's Signature ....
Academic Year:	2018	Advisor's Signature ....

ACKNOWLEDGEMENTS

Piriya Pinthong

TABLE OF CONTENTS

LIST OF TABLES

จุฬาลงกรณ์มหาวิทยาลัย

CHULALONGKORN UNIVERSITY

LIST OF FIGURES

จุฬาลงกรณ์มหาวิทยาลัย
CHULALONGKORN UNIVERSITY

CHAPTER 1

INTRODUCTION

1.1 General introduction

The alternative energy from renewable resources has presently become attraction due to the problem of fossil fuels utilization such as the greenhouse gas emission of petroleum oil and gas combustion. The agricultural resource is widely used as renewable raw material to produce alternative fuel such as bioethanol from sugar cane, cassava and algae [1-4]. Bioethanol nowadays becomes an attractive renewable feedstock in chemical production process because of their stability and non-toxicity at room temperature [1, 5]. It can be converted to several high valuable chemicals such as acetaldehyde, ethylene, acetic acid, diethyl ether and butanol [6-9]. According to the market prices, acetaldehyde production from ethanol is more profitable than production of acetic acid [10].

Acetaldehyde is commonly used as an chemical feed stock for several industrial such as the production of ethyl acetate, acetic acid, acetic anhydride, crotonaldehyde and butanol [11-13]. The conventional process of acetaldehyde production from ethylene deal with toxic and expensive catalyst and high energy consumption due to high reaction temperature [14, 15]. Thus, the alternative production of acetaldehyde from ethanol is interesting because of lower temperature requirement and mild conditions [16-19]. Ethanol can be converted to acetaldehyde via dehydrogenation over basic metal oxides or noble metal catalysts [20]. Moreover, the oxidative dehydrogenation of ethanol is interesting because it can prevent metal sintering and coke formation [21].

It is known that the basicity of catalyst plays important role in oxidative dehydrogenation of ethanol but the formation of undesirable byproduct, COx, will increase with high basicity. The catalysts with moderate basicity such as Mg containing catalyst are found to be suitable in this reaction [22]. Layered double hydroxides (LDH) or hydrotalcite have been interesting because its structure is a brucite-like [Mg(OH)$_2$] in which some Mg atom are substituted with Al atom lead to positively charge layer and anionic layer in the interlayer [23, 24]. The modification of LDHs or hydrotalcite by calcination to obtain mixed oxide and supported metal catalyst have been studied by many researchers [25]. The different precursors used in the LDHs synthesis result in different obtained mixed oxides catalyst [26, 27]. The basic property of this material is important for the catalytic performance on dehydrogenation reaction [28]. In previous work, the catalytic performance in oxidative dehydrogenation of ethanol over mixed oxide derived from calcination of LDHs seems to be fairly low [29]. Accordingly, the modification of mixed oxide to promote the catalytic activity are studied.

In oxidative dehydrogenation reaction, such as dehydrogenation of propane, vanadium has been considered as one of the most active metals. The highest activity was observed on the mixed oxide derived from decavanadate-exchanged LDH [30]. Furthermore, Vanadium catalysts have been applied on dehydrogenation and oxidative dehydrogenation of ethanol. In the oxidative atmosphere, the highest ethanol conversion (98%) was observed on vanadium oxide over Zr-La/SBA-15, having acetaldehyde yield of 40% at 300°C [14]. The molybdenum-modified LDHs were used in several catalytic reaction such as oxidative dehydrogenation of propane [31], selective oxidation of cyclohexene [32] or alkoxylation reaction [33]. Inmanee et al. [34] have studied ethanol dehydrogenation over Mo-modified mixed phased alumina and the results showed that Mo modification promoted selectivity toward acetaldehyde. The copper-containing

catalysts are accounted for highly active catalyst in various reaction such phenol alkylation [35, 36], selective conversion of ethanol [37] and oxidation of ketone [38]. Furthermore, the modification of activated carbon catalyst by loading copper on the surface exhibited the positive effect in dehydrogenation of ethanol to acetaldehyde [39].

In the production of bioethanol via fermentation process, the distillation process is required to remove water from ethanol. The mixture of ethanol 8% and water 92% is obtained from the fermentation of corn and it is further distilled about 3 distillations to obtain 95% ethanol [40]. This purification process consumes energy and has economic cost. It is interesting to apply the mixture of ethanol and water to produced acetaldehyde via oxidative dehydrogenation of ethanol. The effect of water content on catalytic activity would be investigated.

In this study, the LDHs catalyst was prepare by co-precipitation method and calcined at different temperature. The obtained catalysts were performed in oxidative dehydrogenation of ethanol to investigate the effect of calcination temperature. The calcined catalyst which showed the highest activity would be further modified by metal loading to improve the catalytic performance. Vanadium, molybdenum and copper were added to the catalyst surface. The effect of metal-modification on characteristics and performance of catalyst were elucidated. In addition, the effect of water in the ethanol feed and pre-reduction temperature on catalytic activity in oxidative dehydrogenation of ethanol were investigated.

1.2 Research objectives

1) to investigate the effect of calcination temperatures on the characteristics and catalytic properties of Mg-Al LDH catalyst in the ethanol oxidative dehydrogenation reaction.

2) to elucidate the effect of metal modification on the catalytic performance in dehydrogenation and oxidative dehydrogenation of ethanol.

3) to clarify the effect of water content in ethanol feed and pre-reduction temperature on catalytic performance in oxidative dehydrogenation of ethanol.

1.3 Research scopes

1) Preparation of Mg-Al LDH via co-precipitation method and calcined at 450°C, 600°C and 900°C.

2) Preparation of metal-supported LDH catalysts with V, Mo and Cu by the incipient wetness impregnation method.

3) Characterization of Mg-Al LDH and metal-modified catalysts by the following method: X-ray diffraction (XRD), scanning electron microscopy (SEM) and energy dispersive x-ray spectroscopy (EDX), N_2 physisorption, carbon dioxide temperature programed desorption (CO_2-TPD), fourier transform infrared spectroscopy (FT-IR), inductively coupled plasma (ICP) and X-ray photoelectron spectroscopy (XPS).

4) Investigation of the catalytic activity of Mg-Al LDH and metal-modified catalyst in ethanol oxidative dehydrogenation reaction at the reaction temperature range of 200°C-400°C under atmospheric pressure.

1.4 Research methodology

Part I: Comparative study of catalytic performance of Mg-Al LDH and Mg-Al mixed oxide calcined at various temperatures.

```
┌─────────────────────────────────┐
│  Synthesis Mg-Al LDH catalyst by │
│     co-precipitation method      │
└─────────────────────────────────┘
                 ↓
┌─────────────────────────────────┐
│ Calcination of catalyst at various temperatures │
│      (450°C, 600°C and 900°C)    │
└─────────────────────────────────┘
                 ↓
┌──────────────────┐        ┌──────────────────┐
│ Characterization of │ ---> │ XRD,             │
│    catalysts     │        │ N₂-physisortion, │
└──────────────────┘        │ SEM/EDX,         │
                 ↓          └──────────────────┘
┌─────────────────────────────────┐
│ Ethanol oxidative dehydrogenation │
│           reaction               │
└─────────────────────────────────┘
                 ↓
┌────────────────────────┐   ┌──────────────┐    ┌──────┐
│ Temperature programed  │   │ Time on stream│--> │ TGA  │
│ reaction at 200°C-400°C under │ │           │    └──────┘
└────────────────────────┘   └──────────────┘
                      ↓
              ┌──────────────┐
              │ Discussion and│
              │  conclusion  │
              └──────────────┘
```

Characterization of catalysts: XRD, N_2-physisortion, SEM/EDX,

Calcination of catalyst at various temperatures (450°C, 600°C and 900°C)

Temperature programed reaction at 200°C-400°C under

Part II: Investigation of the effect of metal-modification of Mg-Al catalyst on catalytic activity.

```
┌─────────────────────────────────────────┐
│   Mg-Al mixed oxide derived from         │
│   calcination of Mg-Al LDH at 450°C      │
└─────────────────────────────────────────┘
                    │
                    ▼
┌─────────────────────────────────────────┐
│   Modify Mg-Al mixed oxide with          │
│   metals by impregnation method          │
│   (V, Mo and Cu)                         │
└─────────────────────────────────────────┘
                    │
                    ▼
┌──────────────────────┐    ┌──────────────────────┐
│ XRD, N₂-physisortion, │◁--│ Characterization      │
│ SEM/EDX, CO₂-TPD, ICP,│    │ of catalysts          │
│ XPS, FTIR             │    └──────────────────────┘
└──────────────────────┘              │
                          ┌───────────┴───────────┐
                          ▼                       ▼
           ┌──────────────────────┐  ┌──────────────────────┐
           │ Dehydrogenation      │  │ Oxidative             │
           │ reaction             │  │ dehydrogenation       │
           │ (temperature         │  │ reaction              │
           │ programmed)          │  │ (temperature          │
           │ at 200°C-400°C, 1atm.│  │ programmed)           │
           │                      │  │ at 200°C-400°C, 1 atm.│
           └──────────────────────┘  └──────────────────────┘
                          │                       │
                          └───────────┬───────────┘
                                      ▼
                          ┌──────────────────────┐
                          │ Discussion and        │
                          │ conclusion            │
                          └──────────────────────┘
```

Part III: Investigation of the effect of ethanol concentration and reduction condition of copper-modified Mg-Al catalyst on catalytic activity.

CHAPTER 2

THEORY AND LITERATURE REVIEWS

2.1 Dehydrogenation and oxidative dehydration reactions of ethanol

In the dehydrogenation reaction, hydrogen molecule is removed from the organic molecule. In case of alcohols, the products of aldehyde and/or ketone were formed. The ethanol dehydrogenation reaction generates acetaldehyde and hydrogen molecule which is endothermic reaction as follows in equation (2.1) [41]:

$$C_2H_5OH \longrightarrow CH_3CHO + H_2 \qquad +82.5 \text{ kJ/mol} \qquad (2.1)$$

The reaction mechanism of ethanol dehydrogenation over mixed oxide catalyst is shown in **Figure 1.1**
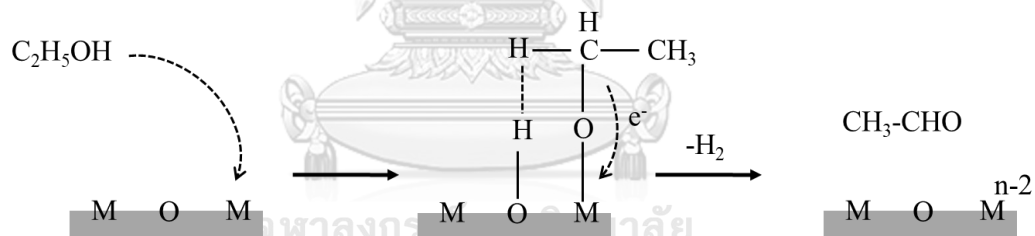
Figure 2.1 Reaction mechanism of ethanol dehydrogenation over mixed oxide catalyst
(rewrite from Lanzafame et al., 2014) [42]

The reaction can also occur on supported metal catalyst. The product selectivity was observed to be dependent on catalysts used and reaction conditions [10, 43]. The different types of alcohols lead to the variety of dehydrogenation products. Primary alcohol is dehydrogenated to aldehyde, while secondary alcohol is dehydrogenated to ketone. The reaction involves the hydrogen molecule removal.

In the oxidative dehydrogenation reaction, ethanol is reacted with oxygen in gas phase and releases energy (exothermic reaction) as follows in equation (2.2) [41]:

$$CH_3CH_2OH + \tfrac{1}{2}O_2 \longrightarrow CH_3CHO + H_2O \qquad -242.0 \text{ kJ/mol} \qquad (2.2)$$
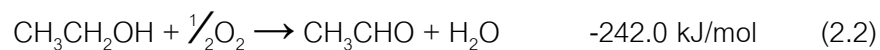
Commonly, acetaldehyde is reported as the main product. Additionally, ethylene, water, hydrogen, methane, carbon dioxide, carbon monoxide, and traces of acetic acid, diethyl ether, and ethyl acetate were detected [44]. Many researchers have also used nickel, iron, cobalt, zinc and manganese in order to increase their dehydrogenation performance [45]. The example mechanism of oxidative dehydrogenation of alcohol is shown in **Figure 1.2**. In this reaction, methanol is dehydrogenated to formaldehyde over molybdenum trioxide [46].
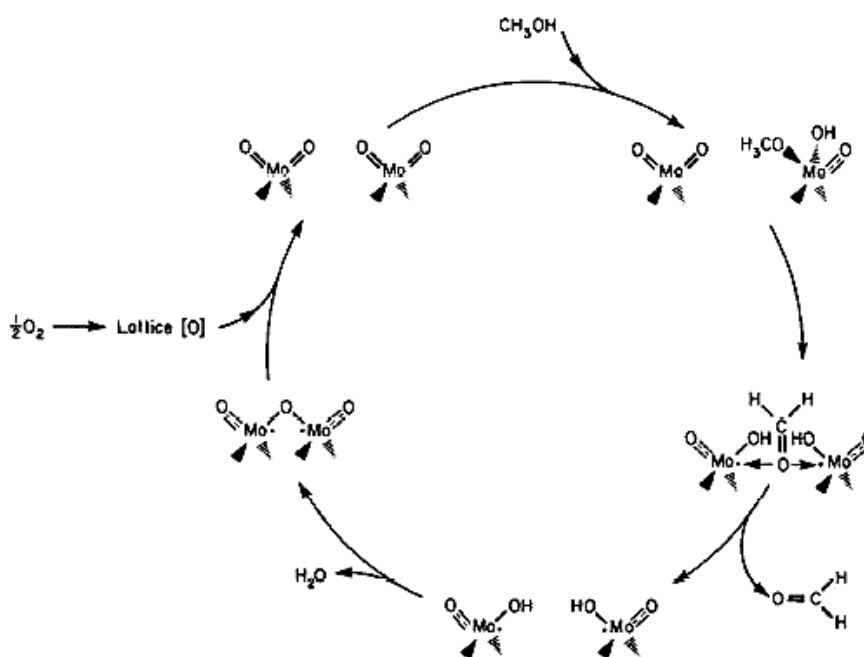
Figure 2.2 The oxidative dehydrogenation reaction of methanol over molybdenum trioxide [46]

2.2 Magnesium aluminium layered double hydroxides catalyst (LDHs)

Layered double hydroxides (LDHs) are known as hydrotalcites (HTs) or anionic clay. It is a white hydrous mineral with a rhombohedral crystalline system. LDHs are rare in nature and can be synthesized in laboratory [47, 48]. They have been acquired great focus in the last decades due to their complex layered structure, reactive surface and the interlayer space, the variety of applications such as ion exchange adsorption (removal of toxic anions or polar organic species), catalyst supports, solid electrode and medicine stabilizer [48, 49]

The general formula of these substances is $[M^{2+}_{1-x}M^{3+}_x.(OH)_2]^{x+}(A^{n-})_{x/n}.mH_2O$, where M2+ represents metallic divalent cations, such as Mg, Co(II), Fe(II), Mn(II) and M3+ represents trivalent cations such as Fe(III) or Al. Hydrotalcite is a layered double hydroxide of general formula $[Mg_3Al(OH)_8][(CO_3)_{1/2}.2H_2O]$. The structure of hydrotalcite is closely related to that of brucite, $Mg(OH)_2$ in which some of Mg^{2+} cations in the brucite layer structure were replaced by Al^{3+} cations. This replacement gives the hydrotalcite layer a positive charge , $[Mg_3Al(OH)_8]^+$, which is balanced with anions, $[(CO_3)_{1/2}.2H_2O]^-$, in the interlayer region between hydrotalcite layer as shown in **Figure 1.3** [50].
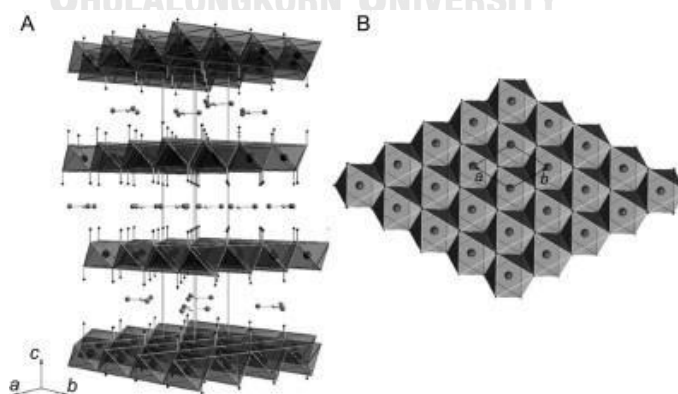
Figure 2.3 (A) The structure of MgAl–LDH with carbonate in the interlayer. (B) the brucite layer viewed from the a–b plane of [50].

The hydrotalcite-like compounds have found many practical applications such as catalyst, catalyst support and ion exchanger. It can be changed into mixed oxides after calcination. The interesting properties of the mixed oxide obtained from calcination process are high surface area, basic properties, stable to thermal treatments and the reconstruction of the original structure (memory effect) [51].

2.2.1 Synthesis of Mg-Al LDH

LDH are inexpensive and easy to synthesize on laboratory and industrial scales by several methods of preparation [50]. An overview of typical methods of synthesis is described in **Figure 1.4**.
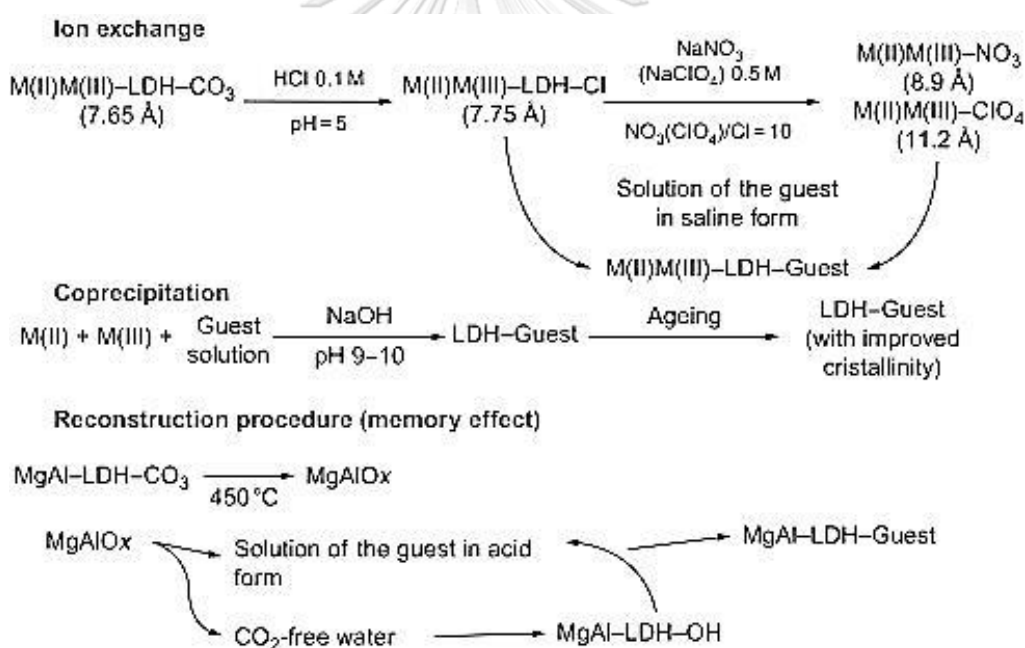
Figure 2.4 The several methods of LDH synthesis [50]

Co-precipitation in aqueous media: this method is one of the most repeatable and reliable methods for the preparation of non-noble metal-based catalysts [51]. The pure and high homogeneity of LDH can be acquired by controlling pH at constant value along the co-precipitation process. The pH of the process is controlled

by synchronously addition of a base solution, e.g. NH_3, KOH, NaOH or a mixed metal salt solution.

The sol-gel method: the synthesis of Mg-Al hydrotalcite by sol-gel method have been studied by Lopez et al. [52]. In this research, magnesium ethoxide, aluminumtri-sec-butoxide and aluminum acetylacetonate were used as precursor. A colloidal solution was obtained which gels and thermally stabilized. The specific surface area of these materials (around 150 m^2/g) was higher than the natural hydrotalcites.

Hydrothermal treatment: the crystallinity and crystal size can be increased by increasing temperature and retention time along the hydrothermal reactions [53, 54]. Furthermore, LDH nanoparticles can be obtained from instant co-precipitation followed by hydrothermal process [55].

Exchange of interlayer anions: The anion exchangeable property of LDH is useful in many applications. Thus, this special property has been applied for modification of LDH. The anion in this process can be organic or inorganic anions such as surfactants [56], polyoxometallates [57], anionic metal complexes [58, 59]. The solvent, the anion ratio and reaction temperature can be adjusted to provide complete anion exchange process.

The reconstruction process: a volatile anion in the LDH structure was decomposed after calcination to form mixed oxide follow by the hydration and intercalation of anion in an aqueous solution. The calcination conditions (temperature, duration time and rate) are essential parameters to control structure restoration. This method was used to prepare several LDH [60] and intercalated oxoanions into Mg-Al LDH [61].

2.3 Supported metal oxide catalyst

2.3.1 Vanadium oxide

Vanadium oxide catalysts are used in several processes in chemical industry such as sulfuric acid and phthalic anhydride production. Moreover, the catalysts contained vanadium oxide are used in the environmental pollution reduction process such as nitrogen oxide from power plant. Most of vanadium oxide catalysts consist of a VO_x on the surface of oxide support (e.g. TiO_2, SiO_2 and Al_2O_3) [62].
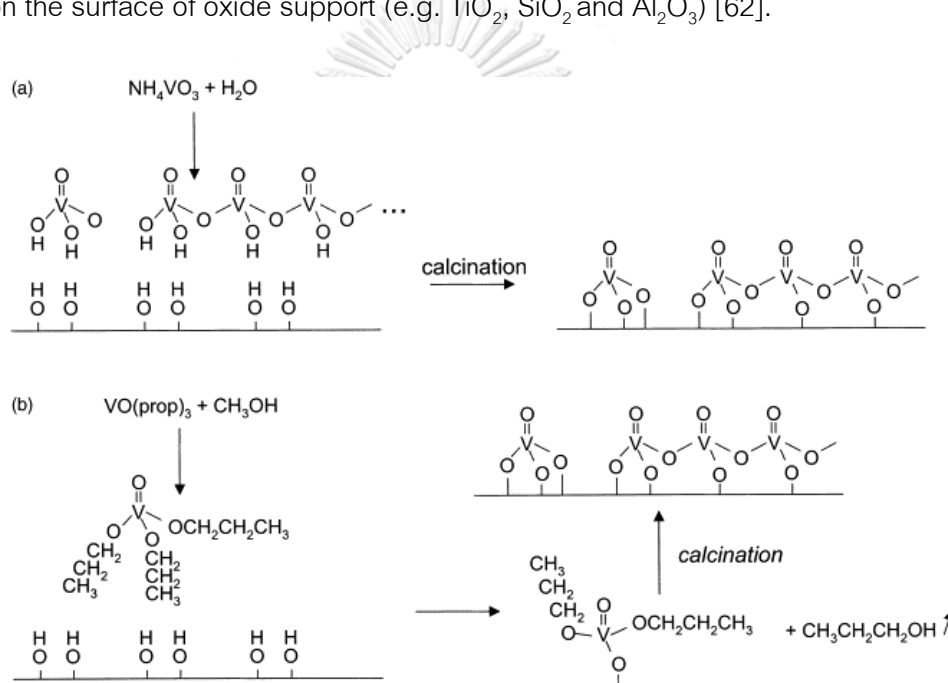
Figure 2.5 Supported VO_x synthesized by (a) impregnation with NH_4VO_3 and calcination (b) impregnation with $VO(OC_3H_7)_3$ and calcination [62].

The simple preparation technique for vanadium oxide catalyst is impregnation which a vanadium compound is adsorbed into the pores of an oxide support. The accurate method for loading vanadium oxide is incipient wetness impregnation which the support is contacted with an appropriate concentration solution. Because V_2O_5 has low solubility in water, many researchers prepare their supported vanadium oxide catalysts by using NH_4VO_3 in water [63, 64] or vanadyl acetylacetonate $(VO(acac)_2)$ or

$VO(OC_3H_7)_3$ or $VO(OC_2H_5)_3$ in methanol or another organic solvent [65, 66] in the impregnation process. The impregnated catalyst is calcined at high temperature (e.g. $500^{\circ}C$) in air to form vanadium oxides on the catalyst surface. The synthesis methods are shown in **Figure 1.5** [62].

2.3.2 Molybdenum trioxide

The molybdenum trioxide (MoO_3) is an oxide of molybdenum of which oxidation state +6. Mo is widely used in various heterogeneous catalytic reactions such as selective oxidation of alcohols and paraffin. The physical and catalytic properties of Mo catalyst was investigated by many researcher [67-69], the surface acidity and catalytic activity mainly depend on the oxidation state of Mo species. The modification of alumina catalyst by loading Mo on the surface exhibited the increase of surface acidity of Rh-Mo/Al_2O_3 catalyst. The acidity of catalyst increased with Mo content [70]. Moreover, in the ethanol dehydration reaction, the Mo species on the surface of HZSM-5 catalyst could be reduced by ethanol. This kind of reduction led to the better catalytic activity, selectivity of ethylene and stability of Mo modified HZSM-5 [71].

2.3.3 Copper oxide

Copper(II) oxide is in the form of monoclinic crystal with 4 oxygen atoms coordinated in the square plana configuration [72]. In the catalytic application, copper is the most selective metal in the dehydrogenation of alcohol [73]. The copper supported on CeO_2 and ZrO_2 were used to improve the production of 1-butanol and ethyl acetate from ethanol. The present of copper affected the basicity and acidity of the metal oxide [74, 75]. Copper nanoparticle was used as a promoter for Mg-Al mixed oxide in the production of 1-butanol via Guerbet reaction of gas-phase ethanol. The effect of Cu nanoparticles on Mg-Al was observed [76, 77]. Furthermore, CuO is used as an effective

support for Au as catalyst for oxidation of alcohols. It was concerned with bi-metallic catalyst with Au and Pt due to the promoting ability [78].

2.4 Literature reviews

2.4.1 Dehydrogenation and oxidative dehydrogenation of alcohols

Inmanee et al. (2016) investigated the effect of calcination temperature and Mo modification of mixed gamma and chi phase alumina on the catalytic ethanol dehydration reaction. Mixed phase alumina was calcined at various temperatures (400-1,000°C) and tested the catalytic activity for ethylene production by gas phase ethanol dehydration reaction at temperature between 200°C to 400°C and atmospheric pressure. The result showed that, acidity of catalyst decreased with the increase of calcination temperature. The mixed phase alumina calcined at 600°C revealed the highest ethanol conversion (complete) and ethylene yield of 98.8% at 350°C. The Mo modification also affected the acidity of catalyst but increased acidity, especially in medium to strong acids. They found that the Mo-modified mixed phase alumina catalyst encouraged ethanol dehydrogenation reaction to acetaldehyde. The catalyst calcined at 600°C and loaded with Mo (15 wt%) exhibit the highest acetaldehyde selectivity (56.35%) at the reaction temperature of 200°C. This can be ascribed to the enhancement of medium to strong acid with metal sites of catalyst [34].

The effect of basicity on catalytic activity of NiMgAl hydrotalcites have been studied by Zhou W. et al. (2016) [28]. All of the catalyst samples were prepared by introducing different magnesium contents. The results showed that the basicity can be efficiently adjusted by introducing Mg^{2+} into NiAl hydrotalcites and the catalytic activity can also be improved. The type of basic sites in the hydrotalcite structure has important effect on the catalytic performance, and only the Bronsted OH basic sites benefit to the

reaction. A proposed mechanism mainly consists of acid-base reaction and hydride transfer step (**Figure 1.6**). The structure of alcohol has an effect on catalytic reaction.
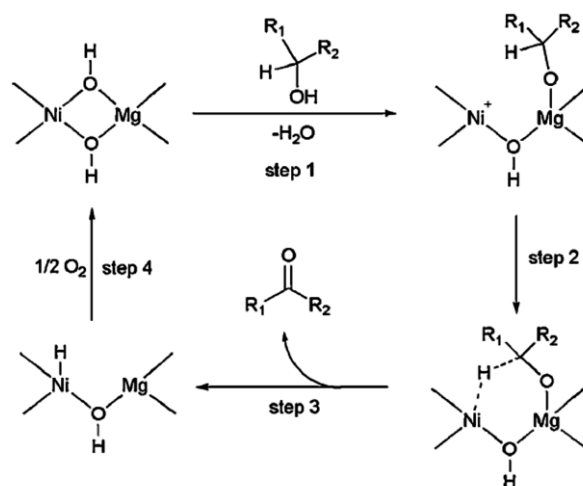
Figure 2.6 The proposed mechanism of the oxidative dehydrogenation of alcohol over Ni$_2$MgAl-LDH [28].

Janlamoon J. and Jongsomjit B. (2015) studied on oxidative dehydrogenation of ethanol over AgLi-Al$_2$O$_3$ catalysts. The catalytic behaviors on AgLi-Al$_2$O$_3$ catalysts with different phase of alumina including gamma, chi and equally mixed phases were investigated. The ethanol conversion and acetaldehyde selectivity depended on the amount of weak basic site of AgLi-Al$_2$O$_3$, phase of alumina, the oxidation state of Ag, and the reduction properties of catalysts. The results showed that AgLi-CHI50 catalyst exhibited higher activity than each pure phase. The ethanol conversion of 80% at reaction temperature below 250°C with good acetaldehyde selectivity was obtained. The reduction state of Ag$^+$ on mixed phase alumina caused weaker interaction resulting increase catalytic activity for oxidative dehydrogenation. Furthermore, increased reaction temperature from 250 to 400°C caused a continuously decrease in acetaldehyde selectivity because of the successive oxidation of acetaldehyde to CO and CO$_2$ [79].

Lippits M.J. and Nieuwenhuys B.E. (2010) investigated the activity of Cu/Al_2O_3 and Ag/Al_2O_3 catalysts in the low temperature oxidative dehydrogenation of ethanol. The promoting effect of adding Li_2O and CeO_x were also studied. The results showed that the appearance of copper nanoparticles and silver on an alumina support are active in the oxidation, dehydrogenation and dehydration of ethanol. Pure alumina acted as an acidic catalyst and produces diethyl ether and ethylene via dehydration reaction. Addition of silver and copper nanoparticles results in a direct conversion of ethanol into ethylene oxide. The addition of Li_2O, affected the selectivity by suppressing the formation of diethyl ether and ethylene. $Ag/Li_2O/Al_2O_3$ and $Cu/Li_2O/Al_2O_3$ catalysts were possible to obtain high selectivity towards ethylene oxide at a temperature of $200\,^{\circ}C$. Moreover, the presence of O_2 was very important for copper based catalysts. It was suggested that at low concentrations the main role of oxygen is to prevent coke formation on the catalytic surface [80].

Deo G. and Wachs I.E. (1994) studied the catalytic activity of vanadium oxide supported catalyst in the partial oxidation of methanol. The reaction was performed in a fixed bed reactor under atmospheric pressure. The mixture of methanol/oxygen/helium of 6/13/81 (mol%) was introduced to the reactor. The reactions were carried out at 473, 503 and 513 K. The result showed that V_2O_5/Nb_2O_5, V_2O_5/TiO_2, and V_2O_5/ZrO_2 selective to formaldehyde (90-99%), while the selectivity around 50% was found for V_2O_5/Al_2O_3. The reactivity of vanadium oxide specie on the surface was determined by the support and was not related to the stability or structure of surface vanadium oxide. The strength of the V-O-support bond determined the number of participating vanadium oxide on the surface [81].

Neramittagapong A. et al. (2008) studied the catalytic ethanol dehydrogenation to acetaldehyde over nickel based catalysts. The reactions were performed at the

temperature range of 200 and 350°C under atmospheric pressure. Ni/SnO$_2$, Ni/Al$_2$O$_3$ and Ni/SiO$_2$ were used as catalysts. The main product of this reaction is acetaldehyde, while secondary products such as ethyl acetate and diethyl ether were found. The results showed that Ni/SnO$_2$ showed the highest ethanol conversion with high selectivity to acetaldehyde. The 10 wt% Ni/SnO$_2$ exhibited the highest yield of acetaldehyde at 300°C. The deactivation of 10 wt% Ni/SnO$_2$ was occurred after 200 minutes on stream due to the formation of Ni – Sn alloy phase [82].

Leon M. et al. (2011) studied the ethanol catalytic condensation over Mg-Al oxides derived from hydrotalcites. They found that acetaldehyde formation can be catalyzed by the medium-strength basic sites of Mg-Al oxide catalyst. Furthermore, the direct condensation reaction of ethanol possibly occurred to form 1-butanol molecule on the catalyst surface. The strongest basic sites catalyzed the condensation reaction of acetaldehyde to form 2-butenal. The hydratalcite material is the most selective for acetaldehyde at low reaction temperature, therefore being higher the surface concentrations of acetaldehyde in the surface. At higher reaction temperature, this trend is reversed. The catalysts prepared at high supersaturation conditions showed the most C4 chemicals selectivity [77].

Ramaswamy A.V. et al. (1970) investigated the dehydrogenation of cyclohexanol on nickel oxide to produce cyclohexanone and phenol. The catalytic reaction was performed in a vertical, fixed bed, flow reactor at reaction temperature 300-410°C. The concentration of cyclohexanone increased to 52 mole% at contact time 1.0 h at 350°C. The rate formation of cyclohexanone was higher than the rate of formation of phenol at lower contact time. At 410°C, the concentration of cyclehexanone was reached the maximum at a contact time of 0.5 h, while the concentration of phenol was reached the

maximum at a contact time of 2.0 h. Cyclohexanone can be further dehydrogenated to form phenol [83].

Gucbilmez Y. and Dogu T. (2006) studied the selective oxidation of ethanol over vanadium-modified MCM-41 catalyst synthesized by direct hydrothermal method. The yield of ethylene production was around 0.66 at 400oC with an O_2/Ethanol feed ratio of 0.5. The overall conversion of ethanol decreased at lower reaction temperature and smaller O_2/ethanol feed ratio. Ethanol conversion increased with the V/Si ratio. The maximum yield of acetaldehyde formation was found at an O_2/ethanol ratio of 0.28 and reaction temperature 400°C. The acetaldehyde yield decreased while carbon dioxide yield increased due to the further oxidation reaction of acetaldehyde in the presence of excess oxygen. The selectivity of acetaldehyde increased when V/Si ratio increased over 0.04. The selectivity of acetaldehyde was 0.7 at 400°C over the catalyst containing a V/Si ratio of 0.133 [84].

Stošić D. et al. (2017) prepared and characterized hydrotalcite catalysts with various Mg/Al ratios (from 2 to 7) which synthesized by ultrasonic assisted co-precipitation method. Moreover, the catalytic activity on 'Guerbet' reaction was investigated in gas phase using methanol/ethanol mixture in order to produce 1-propanol and 1-butanol. The characterization results showed that increasing the Mg/Al ratio from 2 to 3 significantly increase basic sites of catalyst and remain constant for the ratio of 4 and 5. For all materials, their basic sites were higher than acid sites. Among the catalytic activity evaluation, the highest conversion was found on the Mg/Al catalyst with Mg/Al ratio of 3 to 5 which exhibited the highest number of basic sites and acid sites. Furthermore, the highest selectivity of 1-propanol and 1-butanol was observed. The results showed that acidic-basic properties of catalysts correlated with the

selectivity of these products which were the desired products in the Guerbet reaction [85].

Campisano I. S.P. et al. (2017) elucidated the influence of thermal treatment conditions of copper-based hydrotalcite-like compounds on their characteristics and catalytic activity in ethanol dehydrogenation. It was found that copper on the catalyst surface inhibited dehydration and coupling reactions leading to the formation of acetaldehyde. The effect of pretreatment atmosphere on the nature of catalyst was observed using in situ X-ray absorption experiments. The result showed that a mixture of Cu^0/Cu^{+1} species was formed at 750^oC under helium atmosphere while Cu^{2+} species was found under an oxygen/helium atmosphere. Among the reaction, the hydrogen produced from dehydrogenation of ethanol can be consumed to reduce the copper species on the catalyst surface to Cu^0 which is necessary for the dehydrogenation reaction. In this studied systems, the conversion of ethanol to acetaldehyde does not seem to be influenced by the different copper species [86].

Hidalgo J.M. et al. (2016) investigated the vanadium-based catalysts in the ethanol partial dehydrogenation reaction. The catalysts (hydrotalcite, Al_2O_3, TiO_2 and SBA-15) were prepared and loaded with 5% of vanadium. The most active and stable catalyst was V/TiO_2 which exhibited 36.80% ethanol conversion and 72.81% acetaldehyde selectivity at 150^oC. Furthermore, it presented stable activity up to 200 h time on stream. At 250^oC, V/Al_2O_3 catalyst was the most active one. It showed the ethanol conversion of 51.21% and 65.98% in acetaldehyde selectivity. The Mg-Al hydrotalcite catalyst showed the interesting formation of acetaldehyde with 100% selectivity but conversion was lower than 7% at reaction temperature of $150-225^oC$ [87].

2.4.2 Layered double hydroxides applications

Ramasamy K.K. et al. (2015) studied the effect of calcination temperature of MgO-Al$_2$O$_3$ derived hydritalcites in the catalytic condensation of ethanol reaction. Hydrotalcites materials were calcined at various temperatures from 450°C to 800°C. The results showed that, the calcination temperature play a big role in controlling the catalytic activity of this type of catalysts. The basicity of catalysts decreased with the increasing calcination temperature but the acidity was similar with the exception of the calcination temperature of 800°C. In the catalytic condensation reaction, the highest ethanol conversion (44%) and 1-butanol selectivity (50%) were observed for the catalyst calcined at 600°C [88].

El-Raady A.A.Abd et al. (2002) prepared Al-Mg-O mixed oxides catalysts by two methods, wet impregnation and co-precipitation. The catalyst precursors were calcined in air between 500-900°C for 5 h. The surface area, total acidity and basicity of catalyst were determined by N$_2$-physisorption and TPD, respectively. The result showed that, the preparation method has a big influence on selective decomposition of ethanol. The catalysts which prepared by wet impregnation method exhibited more selective in dehydrogenation of ethanol to form ethane due to the higher total acidity of catalyst. Conversely, the catalysts prepared by co-precipitation method were more selective toward acetaldehyde during oxidative dehydrogenation of ethanol because of high concentration of basic sites. Moreover, the trace amount of diethyl ether was also observed [89].

Mitran G. et al. (2012) investigated the effect of cobalt content (from 1 to 20%) in Mg-Al mixed oxide catalyst derived from LDH precursors by calcined at 1023 K. The catalytic activities of catalysts were investigated in the oxidative dehydrogenation of propane at 723 to 873 K. From the catalytic reaction test, the conversion of all of the

catalysts increased with the reaction temperature while the selectivity of propene continuously decreased. In all reaction temperature ranges, the reducibility and catalytic activity of catalysts increased with the cobalt content in catalysts. The highest yields of propene of 10% were found in Co(5)MgAlO and Co(7)MgAlO catalysts at the reaction temperature of 873 K. Furthermore, the propene selectivity at isoconversion was investigated for Co(3)MgAlO and Co(7)MgAlO at 873 K. It was found that the catalyst with lower cobalt content showed higher selectivity of propene because of well-dispersion of cobalt species on the catalyst surface [90].

Dula R. et al. (2002) prepared mixed oxide vanadium catalyst by thermal decomposition of Mg-Al layered double hydroxides (LDHs) with vanadium in the brucite layer and the interlayer for oxidative dehydrogenation of propane. The incorporation methods of vanadium into LDH structure play the important role in the catalytic performance. The catalyst prepared from interlayer-doped precursor was more selective and active than mixed oxides obtained from layer-doped LDHs. The result showed that the different forms of magnesium vanadates were occurred in the mixed oxide after calcination. Pyrovanadate was formed in the case of interlayer-doping, while ortho-vanadate was formed in the case of layer-doping. The covalency of V-O bonds around the reduce V centers might affect the catalytic behavior of catalysts [91].

CHAPTER 3

EXPERIMENTAL

This chapter explains about the experimental procedures, including the preparation of Mg-Al LDH catalysts presented in section 3.1, the characterizations of catalyst presented in section 3.2 and the experimental for ethanol oxidative dehydrogenation reaction presented in 3.3.

3.1 Catalyst preparation

3.1.1 Chemicals and reagents

Table 3.1 The chemicals used in the catalyst preparation

Chemial	Formula	Supplier
Magnesium nitrate hexahydrate	$Mg(NO_3)_2.6H_2O$	Sigma-aldrich
Aluminium nitrate nonahydrate	$Al(NO_3)_3.9H_2O$	Ajax finechem
Sodium hydroxide	$NaOH$	Ajax finechem
Sodium carbonate	Na_2CO_3	Ajax finechem
Vanadyl acetyl acetonate	$OV(C_5H_7O_2)_2$	Sigma-aldrich
Copper (II) nitrate hemi(pentahydrate)	$Cu(NO_3)_2 \cdot 2.5H_2O$	Sigma-aldrich
Ammonium heptamolybdate tetrahydrate	$(NH_4)_6Mo_7O_{24}$	Merck

3.1.2 Synthesis of Mg-Al LDH

The MgAl-LDHs or hydrotalcite catalyst was prepared by the co-precipitation method [92]. Two solutions were prepared: solution A consisted of 0.200 mol of $Mg(NO_3)_2 \cdot 6H_2O$ and 0.100 mol of $Al(NO_3)_3 \cdot 9H_2O$ dissolved in 500 cm^3 of de-ionized

water. solution B consisted of 0.050 mol of Na_2CO_3 and 0.620 mol of NaOH 250 cm^3 of de-ionized water. Then, the solution A and B were mixed at constant flow rate under vigorous stirring for 2-3 h. The synthesis condition was controlled at pH 10 and 65^oC. The gel was aged after stirring for 18 h. The precipitate was washed with DI water until neutral and dried at 110^oC overnight in oven. The obtained Mg-Al LDH catalyst was calcined at different temperature (450^oC, 600^oC and 900^oC) and named as Mg-Al-450, Mg-Al-600 and Mg-Al-900, respectively.

3.1.3 Metal loading on supported-LDH catalyst

The metal supported catalysts were prepared by the incipient wetness impregnation method. The metal precursor, mentioned in **Table 3.1**, was dissolved in de-ionized water (volume of de-ionized water equals to pore volume of catalyst). Mg-Al catalyst was impregnated with the aqueous solution of the metal precursor by the incipient wetness technique. The metal solution was slowly dropped onto 1 g of LDH catalyst to obtain the desired weight percent of the catalyst. Then, the catalyst was dried in the oven at 110^oC overnight and calcined in air at 450^oC for 6 h. The obtained catalysts were denoted as V/LDH, Cu/LDH and Mo/LDH. The calculations are shown in **Appendix A**.

3.2 Catalyst characterization

3.2.1 X-ray diffraction (XRD)

The phase of all catalyst samples was determined by SIEMENS D 5000 X-ray diffractometer. The experimental were performed out using CuK_α radiation with Ni filter in 2θ ranges of 10-80 degree with solution 0.04^o. The crystallite size was calculated from Scherrer's equation.

3.2.2 N_2 physisorption

Pore size and pore volume and specific surface area of all catalyst samples were determined by N_2 physisorption technique. Before analysis process, the catalyst sample was dried in oven at $110^{o}C$ overnight. Then, of catalyst sample (0.1 g) was placed in the sample cell and degassed at $200^{o}C$ for 4h. The N_2 adsorption and desorption isotherm and hysteresis loop were determined using Micromeritics ASAP 2000 automated system at liquid nitrogen temperature ($-196^{o}C$). BET method was applied to determined specific surface area. The average pore diameter was calculated by BJH method.

3.2.3 CO_2 temperature programed adsorption TPD

The basicity of all catalysts was determined using Micromeritics Chemisorb 2750 automated system by CO_2-TPD method. of catalyst sample (0.05 g) was packed in the sample cell and pretreated at $450^{o}C$ under helium flow rate 25 cm^3/min for 1 h prior to analysis. The catalyst sample was saturated with CO_2 at ambient temperature. Then, the catalyst surface was physisorbed by the He flow rate 35 cm^3/min for 30 min. After that, the temperature programmed desotion was carried out from $40^{o}C$ to $500^{o}C$ at heating rate $10^{o}C$/min. the amount of CO_2 in effluent gas was analyzed via thermal conductivity detector (TCD) as a function of temperature.

3.2.4 Scanning electron microscopy (SEM) and energy dispersive X-ray spectroscopy (EDX)

The surface morphology and near-surface (ca. 5 μm) element distribution throughout the catalyst crystallites was investigated by the JEOL mode JSM-6400 scanning electron microscopy (SEM) and energy dispersive X-ray spectroscopy (EDX) respectively. The EDX was performed using Link Isis Series 300 program

3.2.5 Thermal gravimetric analysis (TGA)

The thermogravimetric analysis of catalyst was determined by thermal gravimetric SDT analyzer model Q600. The 10-20 mg of sample was heated from room temperature to 1000°C with a heating rate of 10 $^\circ$C/min. The information about weight loss, derivative weight loss, heat flow and derivative heat flow were obtained from this technique. Moreover, this technique used for determined carbon content in used catalyst.

3.2.6 Fourier transform infrared spectroscopy (FTIR)

The functional groups presented on the catalyst surface was determined using Nicolet 6700 FTIR spectrometer. The IR spectra were recorded in the range of 400 to 4000 cm^{-1} to identify specific structural characteristics of the chemical group from the vibrational properties.

3.2.7 X-ray photoelectron spectroscopy (XPS)

XPS technique provides a quantitative analysis of the surface composition of catalyst samples. This technique was performed by an AMICUS spectrometer using MgK$_\alpha$ X-ray radiation at voltage 15kV and current of 12 mA. The pressure in the analysis chamber was less than 10^{-5} Pa

3.3 Reaction study of ethanol oxidative dehydrogenation

3.3.1 Chemicals and reagents

Table 3.2 The chemicals and reagents used in the ethanol oxidative dehydrogenation reaction

Chemicals and reagents	Supplier
Absolute ethanol (99.9%)	Merck
Ultra-high purity grade nitrogen (99.999%)	Linde
Ultra-high purity grade argon (99.999%)	Linde
Ultra-high purity grade hydrogen (99.999%)	Linde
Synthetic Air (99.999%)	Linde

3.3.2 Instrument and apparatus

The flow diagram of ethanol oxidative dehydrogenation reaction system is shown in **Figure 3.1**. The main system consists of gas controlling system, syringe pump, vaporizer, reactor, electric furnace, temperature controller and gas chromatograph.
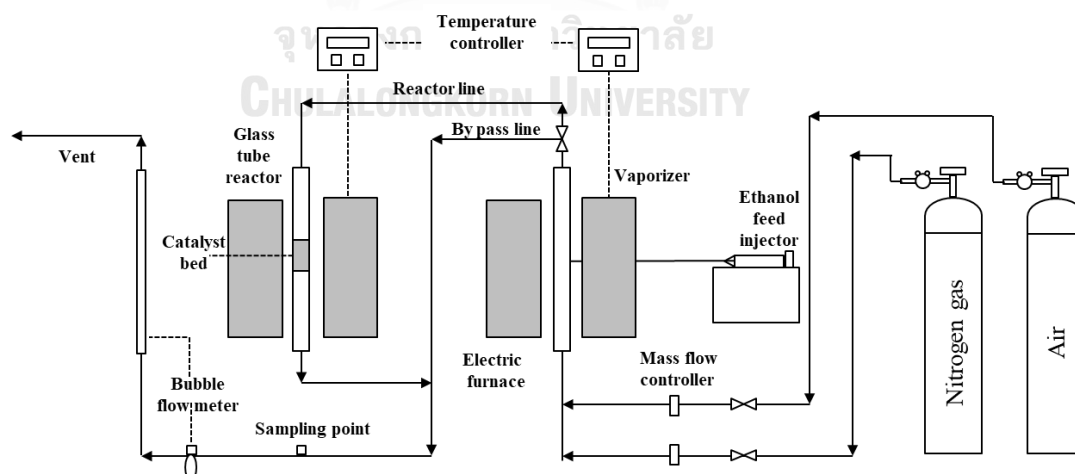
Figure 3.1 Flow diagram of catalytic oxidative dehydrogenation reaction of ethanol

(a) Gas controlling system: The flow rate of carrier gas (N_2) and air are adjusted by mass flow controller. The presser regulator and on-off valve are equipped in this system in order to control gas flow.

(b) Syringe Pump: Liquid ethanol is injected to the vaporizer by syringe pump.

(c) Vaporizer: Liquid ethanol is vaporized in vaporizer at temperature of 120°C.

(d) Reactor: The borosilicate glass tube reactor with inside diameter of 0.7 is used as a reactor. The center of reactor is packed with catalyst on quartz wool layer.

(e) Electric Furnace: the reactor and vaporizer are heated by electric furnace. The temperature of furnace is controlled by temperature controller with the maximum voltage of 220 volt.

(f) Temperature controller: The temperature of electric furnace is set by temperature controller in range between 150°C to 400°C. The temperature controller is connected to variable voltage transformer and thermocouple which attached to the reactor.

(g) Gas Chromatograph (GC): Light hydrocarbon such as ethylene, ethanol, acetaldehyde, etc. are analyzed by a gas chromatograph (Shimadzu GC-14A) equipped with flam ionization detector (FID) and DB-5 capillary column. A Shimadzu GC-8A gas chromatograph equipped with thermal conductivity detector (TCD), molecular sieve 5A and Porapak Q column is used to analyzed carbon dioxide, carbon monoxide and oxygen in the stream. The operating conditions of GC are shown in the **Table 3.3**

Table 3.3 Operating conditions for gas chromatographs

Gas chromatographs	Shimadzu GC-8A		Shimadzu GC 14B
Detector	TCD	TCD	FID
Column	Molecular sieve 5A	Porapak Q	DB5
Maximum temperature	350°C	150°C	350°C
Carrier gas	He	He	N$_2$
	(99.999%)	(99.999%)	(99.999%)
Carrier gas flow	40 cc/min	-	-
Column temperature			
- Initial (^{o}C)	60	60	40
- Final (^{o}C)	60	60	40
Injection temperature (^{o}C)	100	100	150
Detector temperature (^{o}C)	-	-	150
Current (mA)	80	80	-
Analyzed gas	CO, O$_2$, N$_2$	CO$_2$, CH$_4$, C$_2$H$_4$	Ethanol, acetaldehyde, ethylene, diethyl ether

3.3.3 ethanol oxidative dehydrogenation reaction procedure

Catalytic oxidative dehydrogenation reaction of ethanol was performed in the fixed-bed continuous flow reactor. quartz wool bed (0.01 g) and 0.05 g of catalyst were packed in the middle of glass tube reactor. Then the reactor was placed in the electric furnace. The catalyst was preheated at 200°C for 30 min in N$_2$ to remove the moisture prior to reaction test. Ethanol was vaporized at 120°C and mixed with N$_2$ gas and air to

obtained flow rate of 60 ml/min. The mixed-gas stream was introduced to the reactor with WHSV of 22.9 h^{-1} and the reaction was carried out at temperature range from 200°C to 400°C under atmospheric pressure. The gaseous products were analyzed by gas chromatograph with flame ionization detector (FID) and thermal conductivity detector (TCD).

CHAPTER 4

RESULTS AND DISCUSSION

This section aimed to investigate the effect of Mg-Al LDHs on catalytic activity in dehydrogenation and oxidative dehydrogenation of ethanol. The topic was divided to 3 parts. The first part showed the effect of calcination temperature on the characteristics and catalytic performance of LDHs. The effect of metal-modification on characteristics and catalytic activity was explained in the second part. In the final part, the influences of water content in the ethanol feed and pre-reduction conditions on catalytic performance were investigated and discussed.

4.1 Comparative study of catalytic performance of Mg-Al LDHs and Mg-Al mixed oxide calcined at various temperatures.

4.1.1 Catalyst characterization

The effect of calcination temperature on the characteristics of Mg-Al LDH and their mixed oxide (calcined samples) was studied. The XRD patterns of all catalyst samples are shown in **Figure 4.1**. For non-calcined (Mg-Al-000) sample, some common features of layered material, sharp and symmetric diffraction peaks in 2θ range of 10-25° and broad diffraction peaks in 2θ range of 30-50° were found [47, 93, 94]. The basal spacing (d_{003}) reflection of LDH structure was 7.67 Å at 2θ of 11.5°, indicating that the interlayer of non-calcined catalyst was mainly water, hydroxide ion and carbonate ion [28]. For all calcined catalysts, the diffraction peaks of layered structure disappeared and the diffraction peaks were observed at 2θ = 43° and 63°, which attributed to a periclase MgO phase [25, 93]. The diffraction peaks of alumina were not observed

because of a very high dispersion of aluminium in magnesium oxide structures [25, 92]. the sharpening peaks of MgO were observed on the catalyst calcined at $900^{o}C$ (Mg-Al-900), and some diffraction peaks of spinel $MgAl_2O_4$ also appear [93]. The XRD results revealed that the LDH structure was destroyed and Mg-Al mixed oxide was formed For all calcined catalysts.
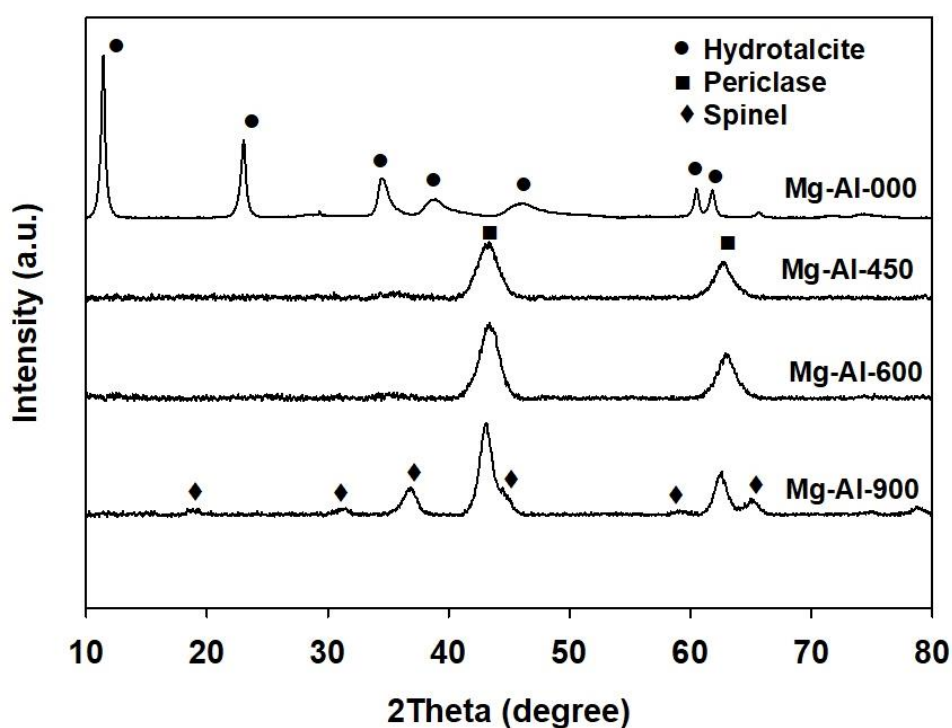
Figure 4.1 XRD patterns of Mg-Al catalysts calcined at different temperatures

The morphology (SEM image) of all catalysts are shown in **Figure 4.2**. The morphology of non-calcined catalyst (Mg-Al-000) was more compact than the calcined catalysts. The catalyst calcined at $450^{o}C$, $600^{o}C$ and $900^{o}C$ (Mg-Al-450, Mg-Al-600 and Mg-Al-900) showed the plate-like morphology. Some agglomerated particles were formed on the catalyst calcined at $900^{o}C$ (Mg-Al-900), the result was consistent with the BET surface area which lower than the other calcined samples. The elemental compositions of all samples determined by EDX are reported in **Table 4.1**. The ratios of

Mg to Al (Mg/Al) of all Mg-Al catalysts were in the range of 1.88-2.18 indicating that Mg/Al ratios were not change along calcination precess.
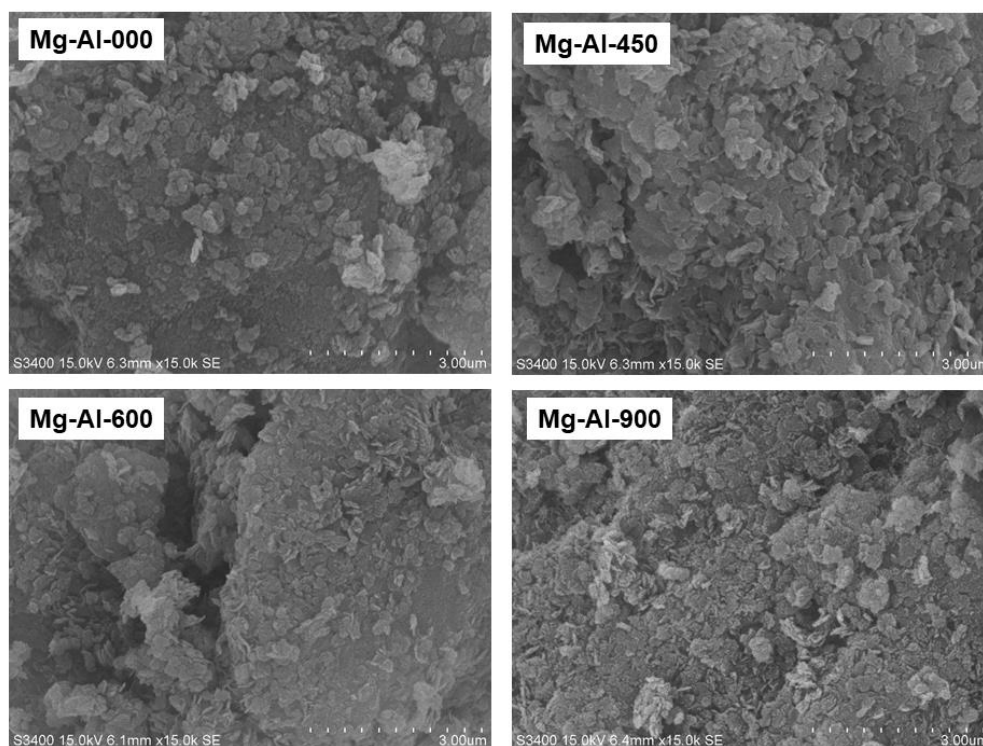
Figure 4.2 SEM image of all Mg-Al catalysts calcined at different temperatures

Table 4.1 The near-surface chemical composition Mg-Al catalysts and their calcined derivatives obtained from EDX.

Samples	%atom					
	%Mg	%Al	%C	%N	%O	Mg/Al
Mg-Al-000	27.96	13.66	8.19	2.13	48.06	2.04
Mg-Al-450	30.26	16.08	7.40	2.59	43.67	1.88
Mg-Al-600	29.11	13.35	7.00	1.77	48.77	2.18
Mg-Al-900	30.11	14.23	5.08	1.20	49.38	2.10

The N_2-physisortion results (BET surface area, pore size and pore volume of all Mg-Al catalyst samples are shown in **Table 4.2**. When calcination temperature increased, BET surface area gradually decreased. The BET surface area of calcined Mg-Al samples was in range of 95-168 m^2/g, which higher than the non-calcined Mg-Al sample (51 m^2/g). **Figure 4.3** shows the N_2 adsorption-desorption isotherms of all Mg-Al catalyst sample. The hysteresis loop was observed at high relative pressure ($P/P_0 > 0.7$) representing the mesoporous structure of all samples corresponding to Type IV (IUPAC). The pore volumes decreased whereas calcination temperature increased, resulting in the increase of average pore size diameter (**Table 4.2**). The average pore size diameters were in the range of 12-20 nm. The pore size distribution of Mg-Al catalysts is shown in **Figure 4.4**. It was found that most pores were ranged between 2 and 50 nm for all samples indicating the mesoporous materials.

Table 4.2 BET surface area, pore volume, and pore size diameter of Mg-Al LDH.

Sample	Basicity (μmol CO_2/g)	BET surface area (m^2/g)	Pore volume (cm^3/g)	Pore size diameter (nm)
Mg-Al-000	224	51	0.27	20
Mg-Al-450	212	168	0.60	12
Mg-Al-600	184	110	0.45	13
Mg-Al-900	146	95	0.40	18

Figure 4.3 N_2 adsorption–desorption isotherms of all Mg-Al catalysts calcined at different temperatures
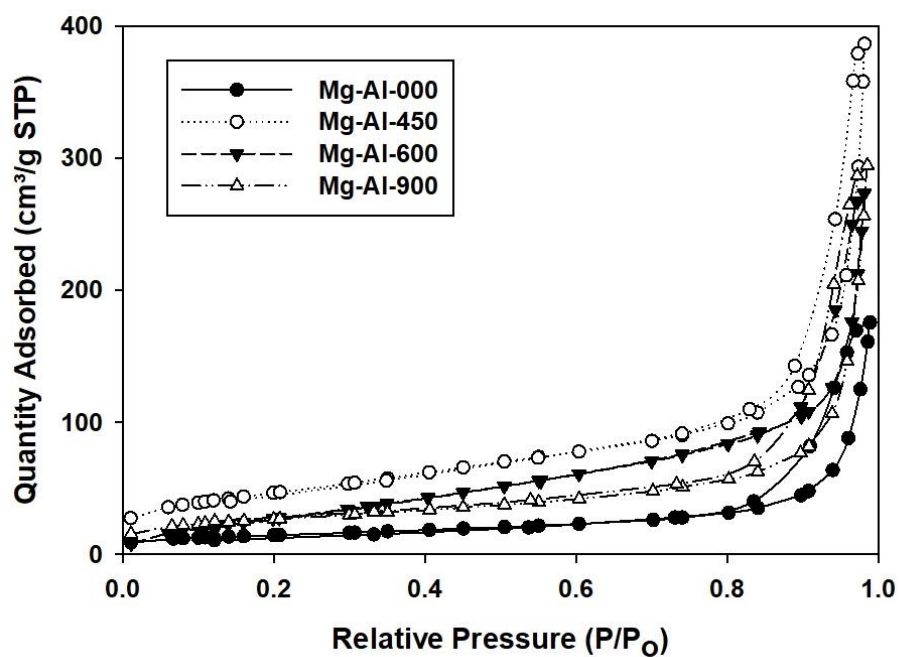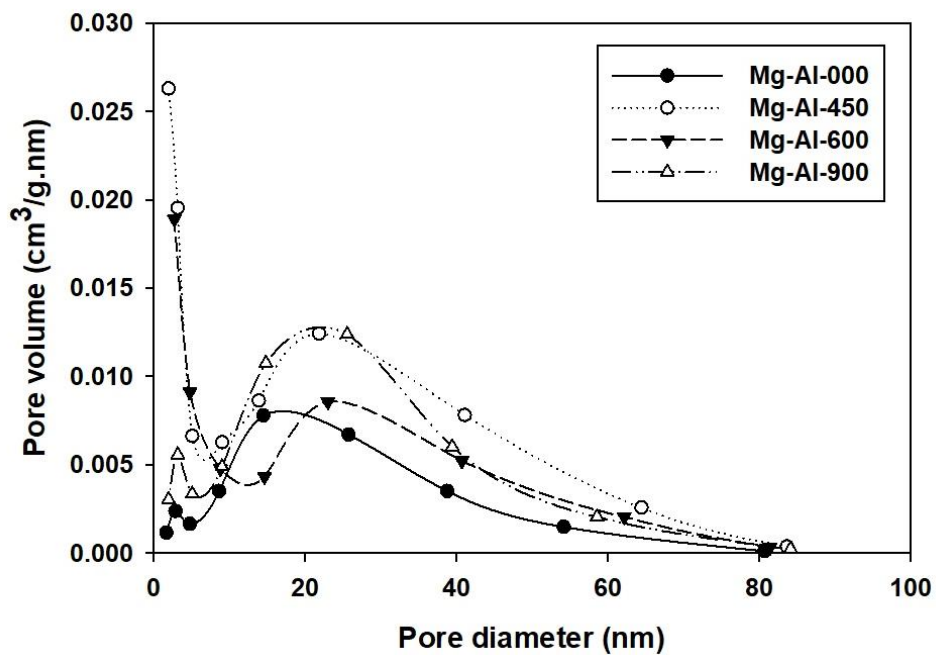

Figure 4.4 Pore size distribution of all Mg-Al catalysts calcined at different temperatures

The chemical groups on the Mg-Al catalysts surface were determined by FT-IR as seen in **Figure 4.5**. The IR spectra show broad absorption band at 3420 cm^{-1} of O-H stretching absorption of hydroxyl groups in the structure and interlayer water molecules [94] and the bands at 1640 cm^{-1} and 3000 cm^{-1} represent the interlayer water [95]. The sharp peak at 1359 cm^{-1} with a shoulder at 1559 cm^{-1} corresponded to symmetric and asymmetric stretching absorption of C-O and C=O in interlayered carbonate ion [24, 94]. The broad peaks in the range of 400-1000 cm^{-1} correspond to stretching absorption of Mg-OH or Al-OH [28, 96]. As calcination temperature increased, the absorption bands of interlayer water and OH- groups decreased indicated the removal and dehydroxylation of water and OH- groups via calcination process. Moreover, The same trend was found on C-O and C=O absorption bands due to decarboxylation of carbonate ion in the layer [25].
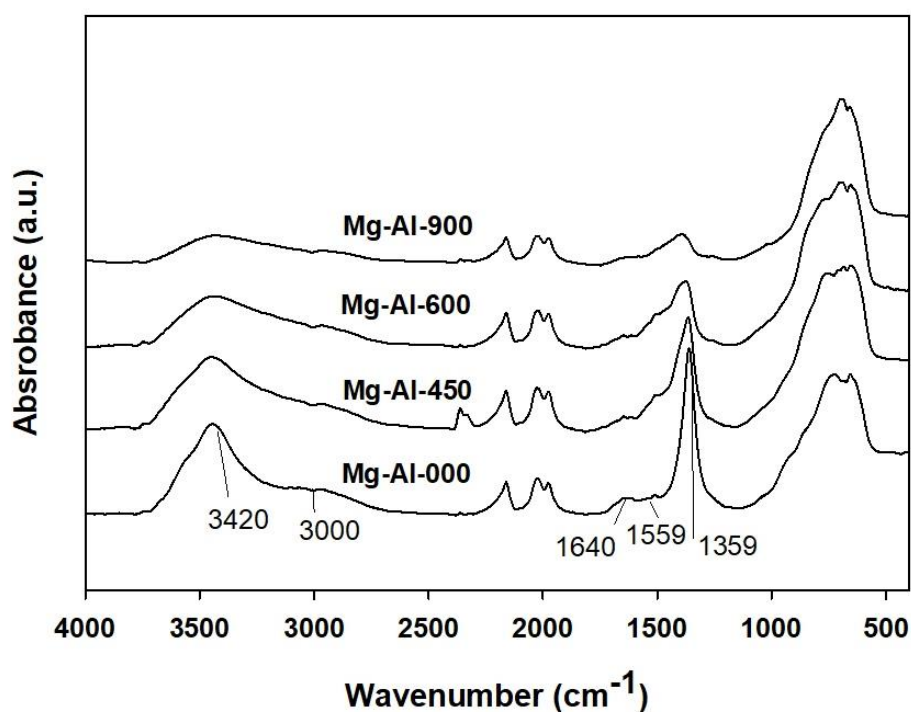

Figure 4.5 FT-IR spectra of Mg-Al catalysts calcined at different temperatures.

It has been well known that in oxidative dehydrogenation of alcohols, the basic site of catalyst is required [97-99]. Thus, CO_2-TPD analysis was applied to determine the basic sites of catalysts. The CO_2-TPD profiles are shown in **Figure 4.6**. It exhibited broad desorption peak extending from 50-450°C accounting for weak, medium and strong basic site associated with surface OH^- groups, M^{2+}-O^{2-} or Al^{3+}-O^{2-} acid-base pairs and surface O^{2-} ions, respectively [100, 101]. **Table 4.2** show the number of basic sites. The results showed that the basic sites decreased with increased calcination temperature. the highest basicity of 297 μmolCO_2/g was observed on non-calcined catalyst (Mg-Al-000). For calcined catalysts, the catalyst calcined at 450°C (Mg-Al-450) revealed the highest basicity of 227 μmolCO_2/g catalyst.

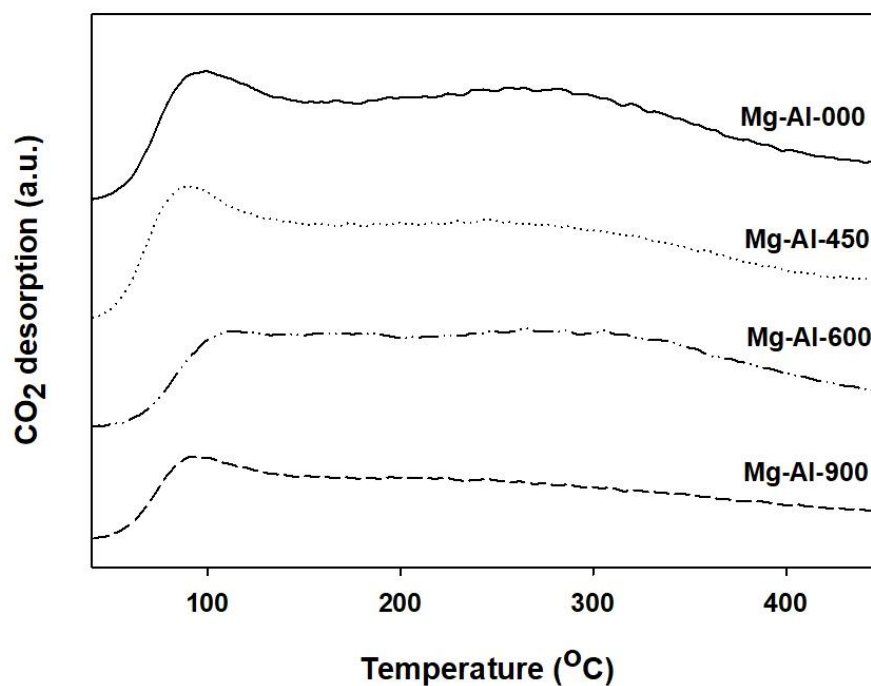**Figure 4.6** CO_2-TPD profiles of Mg-Al catalysts calcined at different temperatures.

4.1.2 Reaction study

First, the reactions were performed on Mg-Al-000 in the absence and presence of oxygen atmosphere in order to compare the catalytic activity of Mg-Al LDH catalyst on dehydrogenation and oxidative dehydrogenation. The result showed that the activity of non-calcined catalyst (Mg-Al-000) in the presence of oxygen was higher than that of without oxygen (**Figure 4.7**). This is probably due to reoxidization on the catalyst surface by oxygen from the feed [98]. Therefore, all Mg-Al catalysts was determined via oxidative dehydrogenation of ethanol at the reaction temperature from 200-400°C in order to investigate the catalytic activity. The results of ethanol conversion on different reaction temperature are shown in **Figure 4.7**. The ethanol conversion increased with reaction temperature for all catalysts. The ethanol conversion decreased in the order of Mg-Al-450 > Mg-Al-600 > Mg-Al-000 > Mg-Al-900 catalysts. The highest ethanol conversion of 65% was found on Mg-Al-450 at 400°C among other catalysts. Non-calcined catalyst (Mg-Al-000) showed the highest ethanol conversion of 5.57-8.90% at lower reaction temperature range (200-300°C). This probably because the catalyst was layered structure, which contained carbonate (-CO$_3^{2-}$) and hydroxyl groups (-OH$^-$) at external surface that can interact with the ethanol [101, 102]. In the temperature range of 350-400°C, Mg-Al-450 showed the highest ethanol conversion (deal with the basicity of catalyst), which was higher than Mg-Al-000 because of the destruction of layered structure of Mg-Al-000 at high reaction temperature (> 350°C). Furthermore, the catalyst was in the partially dehydroxylated and decarbonated LDH formed resulting in lower activity than the mixed oxide phase of Mg-Al-450 [102].
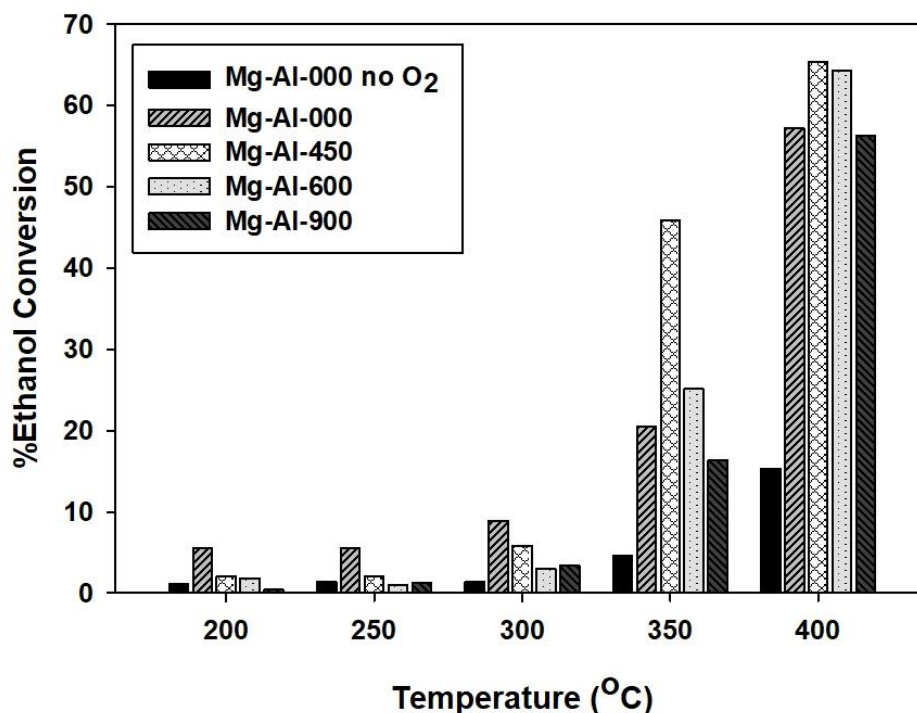
Figure 4.7 Ethanol conversion of Mg-Al catalysts calcined at different temperatures.

The acetaldehyde selectivity at different reaction temperatures is shown in Figure 4.8. Acetaldehyde was found as the main product in the reaction temperature range of 200-350°C, selectivity higher than 90%. The acetaldehyde selectivity decreased with the increase of reaction temperature due to the formation of byproducts such as diethyl ether, ethylene, ethyl acetate, CO_x. At 400°C, carbon dioxide was observed as a major product due to the successive oxidation of acetaldehyde [79]. The proposed mechanism for oxidative dehydrogenation of ethanol to acetaldehyde is shown in Figure 4.10. In the first step, ethanol is adsorbed on acid-base pair site and the O-H bond is broken to form surface ethoxide species [101, 103]. In the next step, the α-hydrogen is abstracted by M-OH group on the surface to form water and the lattice oxygen is removed. Then, acetaldehyde is desorbed and the surface is reoxidixed by oxygen from the feed [98].

The acetaldehyde yield was considered as shown in **Figure 4.9** in order to determine the suitable condition for acetaldehyde production from ethanol over Mg-Al catalyst. Except Mg-Al-000 in the absence of oxygen atmosphere, all Mg-Al catalysts exhibited the maximum acetaldehyde yield at $350^{\circ}C$. When the reaction temperature increased to $400^{\circ}C$, acetaldehyde yield decreased due to the formation of mainly carbon dioxide. At reaction temperature of $350^{\circ}C$, Mg-Al-450 catalyst exhibited the highest acetaldehyde yield of 29.7%.
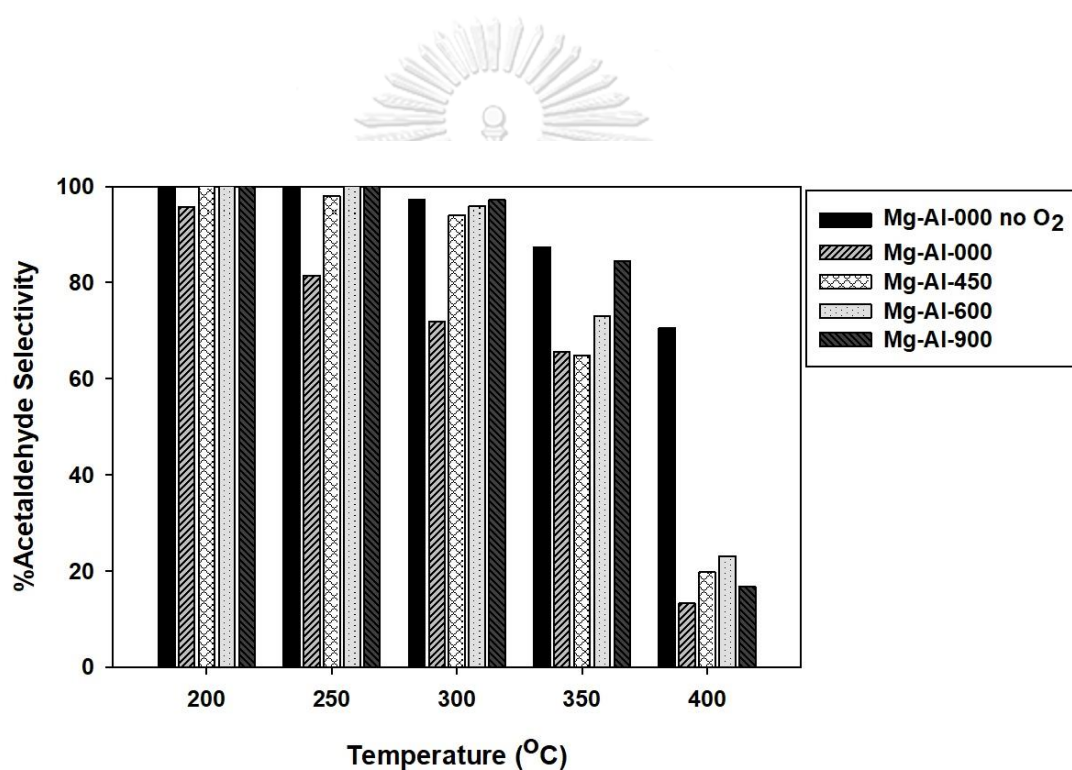

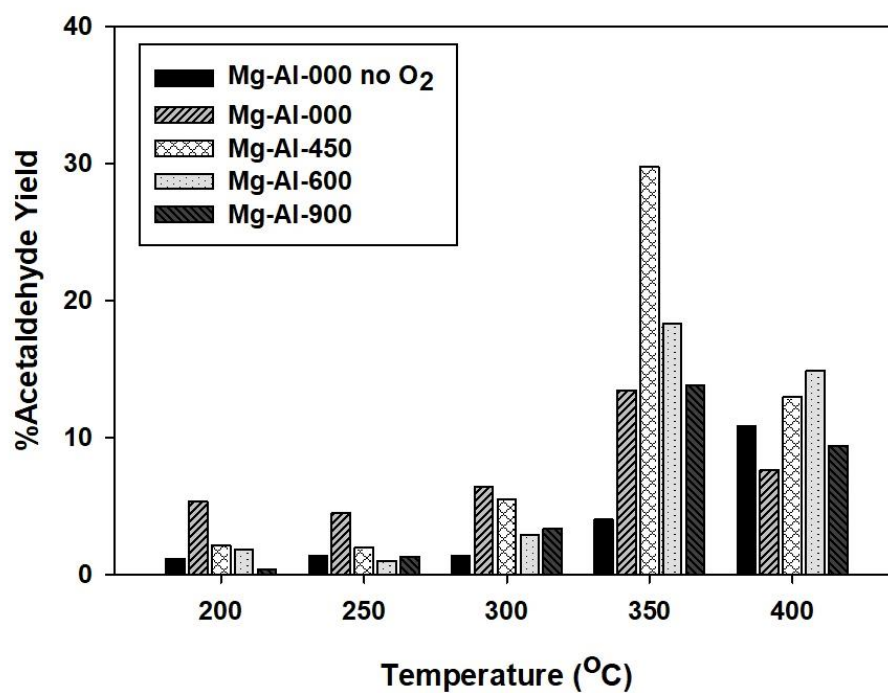**Figure 4.8** Acetaldehyde selectivity of Mg-Al catalysts calcined at different temperatures.

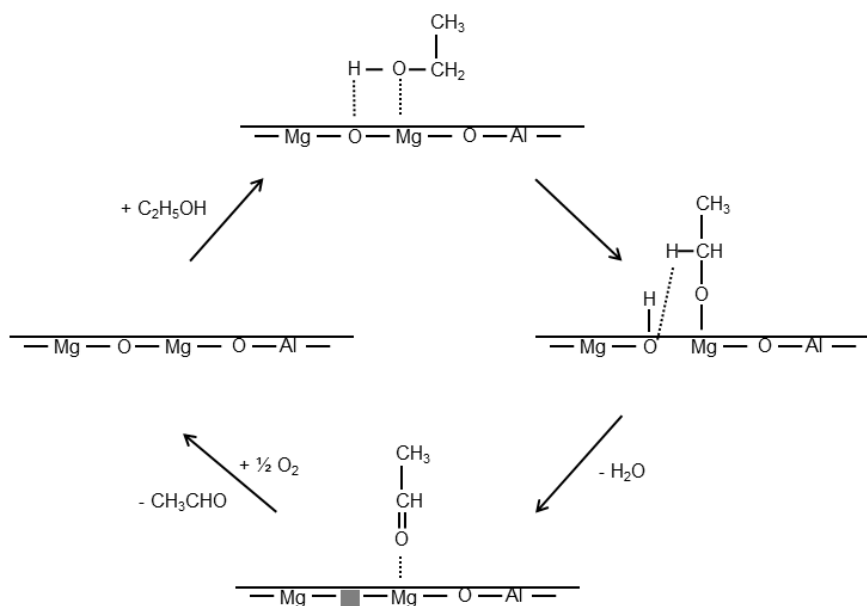Figure 4.9 Acetaldehyde yield of Mg-Al catalysts calcined at different temperatures.

Figure 4.10 Proposed mechanism for oxidative dehydrogenation of ethanol to

acetaldehyde over Mg-Al catalyst.

There are many researches focus on oxidative dehydrogenation of ethanol to acetaldehyde over various catalysts such as mixed phase (chi and gamma) alumina catalyst with silver and lithium addition [79], manganese oxide octahedral molecular sieves modified with cobalt [104], grafted vanadium based catalysts on titania–silica supports [105], vanadium-incorporated MCM-41 [84], gold nanoparticle on $MgCuCr_2O_4$ spinel-supported catalyst [21], zeolite-encapsulated gold nanoparticles [106] and gold nanoparticle on TiO_2 catalyst [107]. The catalytic activities of various catalysts for oxidative dehydrogenation of ethanol to acetaldehyde are summarized in **Table 4.3** in order to compare the catalyst performance with this work. It was found that the calcined Mg-Al catalyst (Mg-Al-450) is quite competitive among other catalysts without any pre-reduction step and promising for further modification and study in oxidative dehydrogenation of ethanol to acetaldehyde.

Table 4.3 Comparison of catalytic activity of various catalysts for oxidative dehydrogenation of ethanol to acetaldehyde.

Catalyst	Reaction temperature (^{o}C)	Ethanol conversion (%)	Acetaldehyde selectivity (%)	Ref.
Mg-Al-450	200-400	2-65	20-100	This work
AgLi-Al$_2$O$_3$	150-400	20-100	20-100	[79]
[Co]-OMS	300	83	81	[104]
V$_2$O$_5$/TiO$_2$-SiO$_2$	100-200	0.2-92	38-100	[105]
Au/MgCuCr$_2$O$_4$	250	96	99	[21]
Au/Recryst-S1	200	50	98	[106]
V4b-MCM-41	300-400	24-99	6-72	[84]
Au/TiO$_2$	100-250	30-95	45-65	[107]

4.2 Investigation of the effect of metal-modification of Mg-Al catalyst on catalytic activity.

4.2.1 Catalyst characterization

From XRD results in **Figure 18**, the characteristic peak of MgO (periclase) were found at $2\theta \approx 37^{\circ}$, 43° and 63° in all samples indicated that the Mg-Al mixed oxide was formed after calcination process [108]. The distinguished peak of V and Mo species were not found in XRD patterns of modified catalysts due to it was in the amorphous state or in small crystallite [109] and well dispersion on Mg-Al catalyst surface [34]. The XRD pattern of Cu/Mg-Al catalyst (**Figure 4.11**) revealed the characteristic peaks at $2\theta \approx 43^{\circ}$ and 63°, which can be assigned to MgO periclase [25, 93] and peaks at $2\theta \approx 35.5^{\circ}$ and 38.8° indicating the presence of crystalline CuO on the catalyst surface [110].
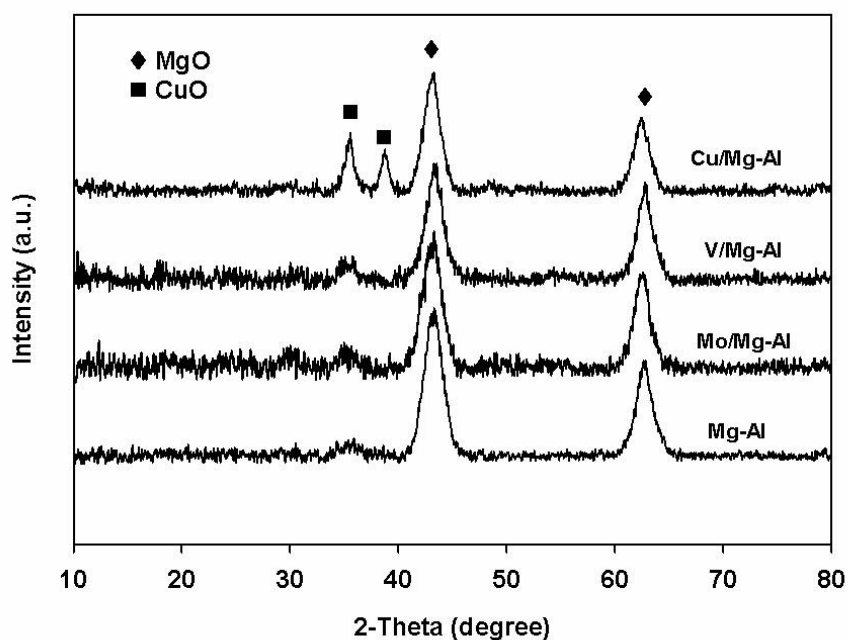
Figure 4.11 XRD patterns of catalysts.

The N_2-physisorption adsorption-desorption isotherms of all catalyst are shown in Figure 4.12. Type IV isotherm with hysteresis loops were observed on all catalysts indicated a mesoporous material. Furthermore, the pore size distribution was evaluated as shown in Figure 4.13. Most pores of Cu/Mg-Al and Mo/Mg-Al catalyst were range between 2 and 50 nm, and 2-60 nm for V/Mg-Al catalyst indicating the mesoporous materials [111]. Simultaneously, when V was loaded on the Mg-Al catalyst (V/Mg-Al), the pore size distribution curve broadened. It was possibly caused by blockage of smaller pore of VO_x particles. This result was consistent with the decrease in BET surface area (Table 4.4).
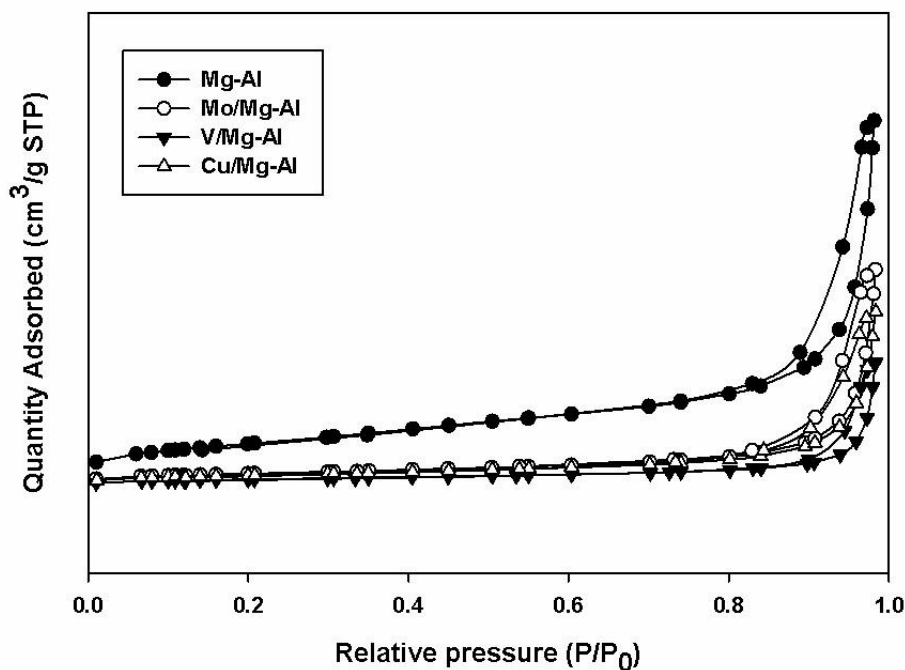
Figure 4.12 N_2 adsorption–desorption isotherms of catalysts.
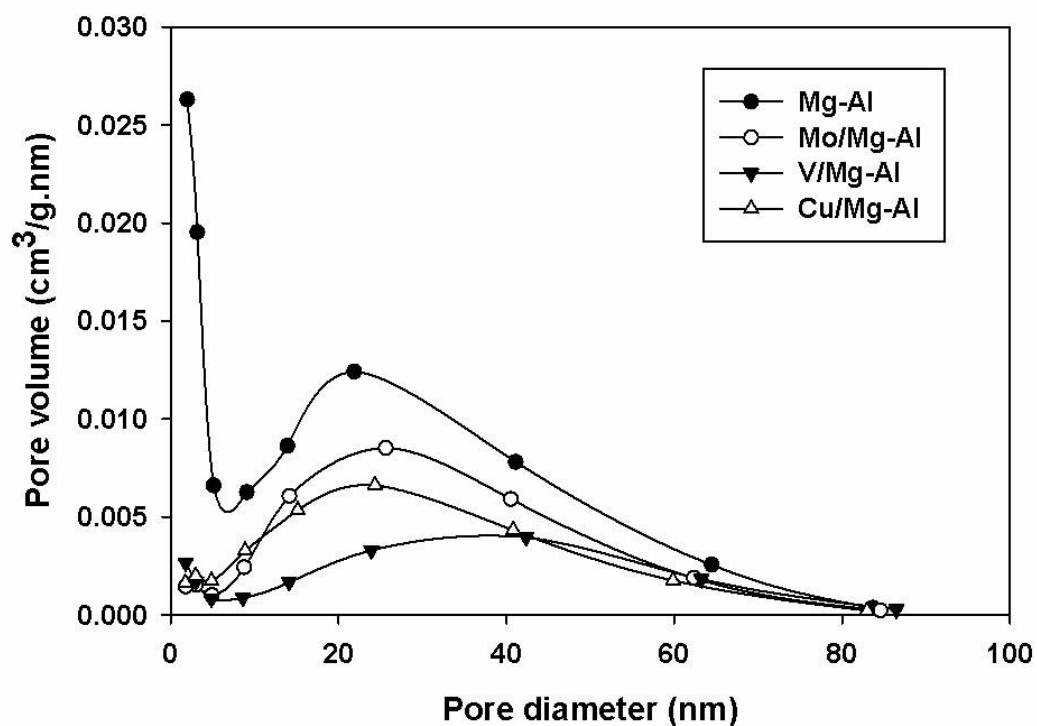
Figure 4.13 Pore size distribution of catalysts.

Table 4.4 BET surface area, pore volume, and pore size diameter of all catalysts.

Sample	BET surface area (m^2/g)	Pore volume (cm^3/g)	Pore size diameter (nm)	Basicity (μmol CO_2/g)	Base density (μmol CO_2/m^2)
Mg-Al	168	0.60	12	253.5	1.51
Cu/Mg-Al	47	0.29	21	251.8	5.36
V/Mg-Al	32	0.20	24	196.1	6.13
Mo/Mg-Al	53	0.36	24	148.4	2.80

The oxidation states of vanadium, molybdenum and copper on the catalyst surface were measured by X-ray photoelectron spectroscopy (XPS). For V/Mg-Al catalyst (**Figure 4.14**), the peak at 525 eV was observed, corresponding to $V^{5+} 2p^{1/2}$ [14]. The Mo 3d spectrum (**Figure 4.15)** showed a doublet peak corresponding to $3d^{3/2}$ and $3d^{5/2}$ states. These results indicated the presence of mainly Mo^{6+} on the Mo/Mg-Al catalyst surface [112]. The XPS spectra of Cu/Mg-Al is shown in **Figure 4.16**. The peaks of Cu 2p core level transition was observed at 933.8 and 942.5 eV. This result indicated that Cu(II) species was formed on the Cu/Mg-Al surface [78].
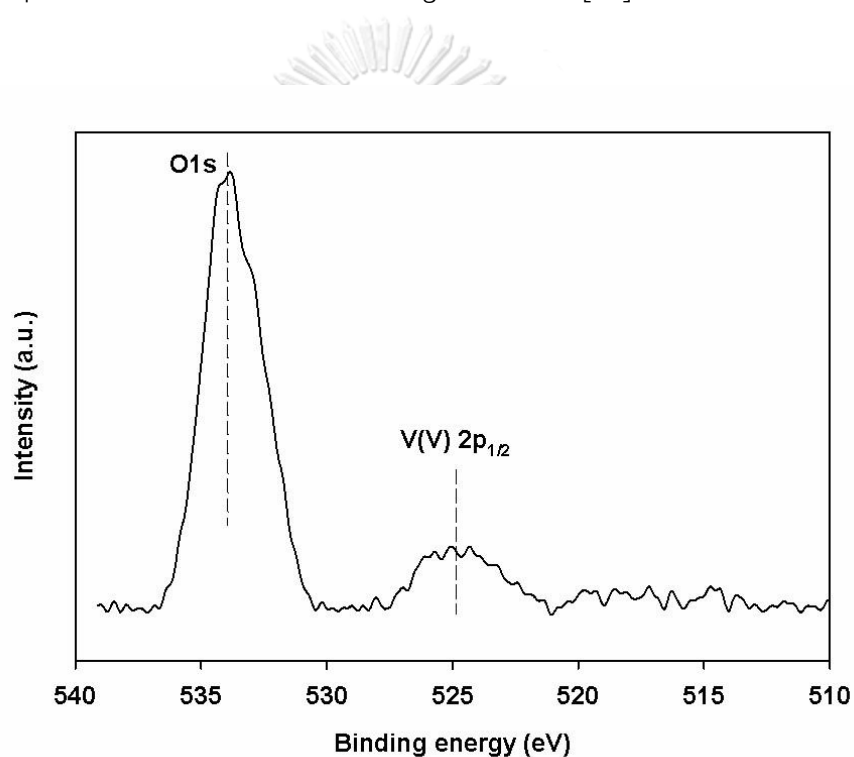
Figure 4.14 XPS spectra of V-modified catalysts (V/Mg-Al) in the V 2p regions.
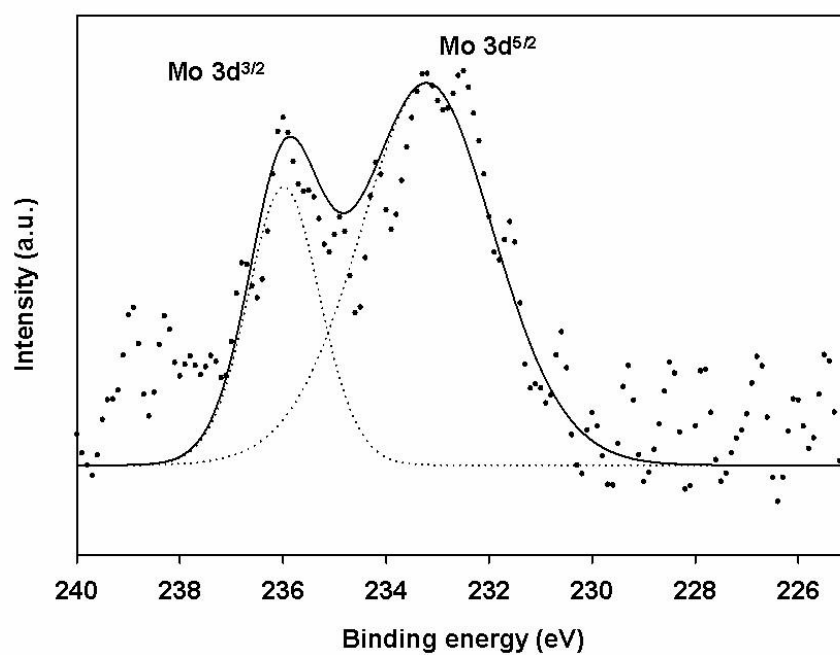
Figure 4.15 XPS spectra of Mo-modified catalysts (Mo/Mg-Al) in the Mo 3d regions.
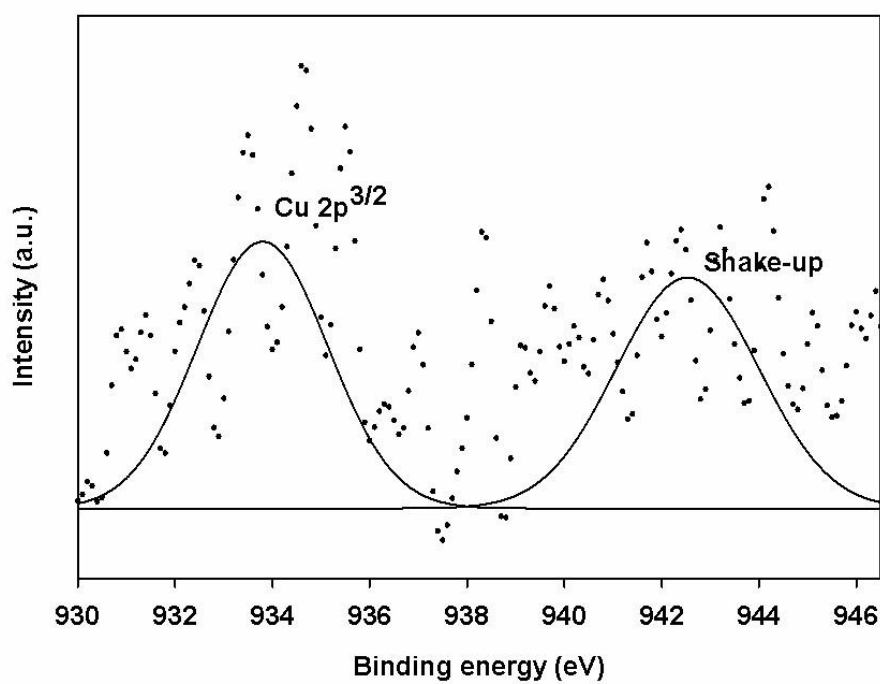
Figure 4.16 XPS spectra of Cu-modified catalysts (Cu/Mg-Al) in the Cu 2p regions.

The morphology of all catalysts was explained by SEM image in **Figure 4.17**. It indicated that the agglomeration of particles was observed in case of vanadium loading, while the addition of copper or molybdenum did not significantly change the Mg-Al morphology. The near-surface element distribution of all catalysts measured by EDX are shown in **Table 4.5**. The Mg/Al molar ratio of Mg-Al catalyst was around 2.00 as expected from the synthesis. The ratio was slightly changed when vanadium was loaded. The measurement of metal loading by EDX exhibited 2-fold to 3-fold higher metal content than the result obtained by ICP technique (**Table 4.5**). This result indicated that the metal particles were located mainly near the catalyst surface.

Figure 4.17 SEM image of catalysts.

Table 4.5 The near-surface chemical composition of all catalysts obtained from EDX.

Samples	%wt						atomic ratio[a]
	Mg	Al	O	V	Mo	Cu	Mg/Al
Mg-Al	38.40	21.27	40.33	-	-	-	2.06
V/Mg-Al	30.61	18.95	39.69	10.75 (5.27[a])	-	-	1.91
Mo/Mg-Al	31.07	16.65	41.19	-	11.09 (4.64[a])	-	2.03
Cu/Mg-Al	32.11	16.52	33.93	-	-	17.46 (4.25[a])	2.16

[a] Obtained from ICP (bulk chemical composition)

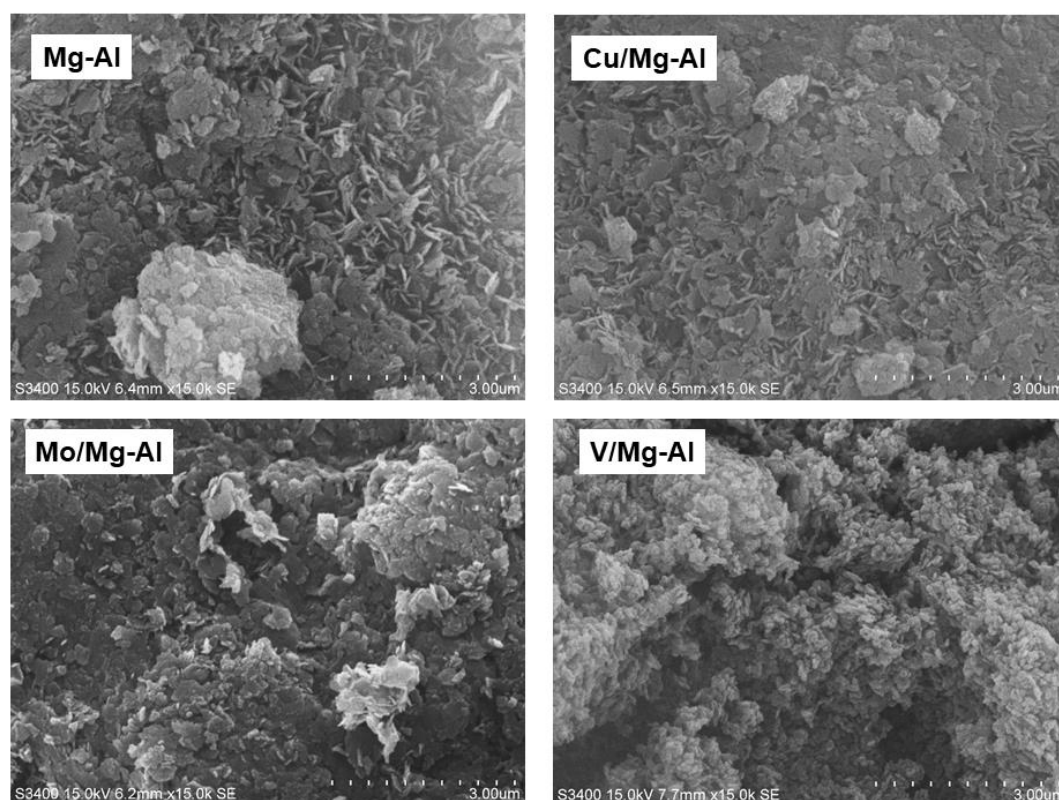The surface basicity of catalysts is the key factor to determine the catalytic activity of dehydrogenation and oxidative dehydrogenation of ethanol [97-99]. Consequently, the basicity of catalysts of all catalyst was determined by CO_2-TPD. The CO_2-TPD profiles of all catalyst were shown in **Figure 4.18**. Two desorption peaks were observed in the range of 40-200°C and over 200°C indicated weak basic site (OH$^-$ groups) and medium and strong basic site (Al^{3+}-O^{2-} or M^{2+}-O^{2-} acid-base pairs and surface O^{2-} ions, respectively [100, 101]). The basicity decreased when the metal was added. The Mg-Al catalyst exhibited the highest basicity of 253.5 μmolCO$_2$/g catalyst as seen in **Table 4.4**. When base density was calculated from basicity and surface area of catalyst, it was found that V/Mg-Al showed the highest base density of 6.13 μmol CO$_2$/m^2. The base density tended to decrease in the order of V/Mg-Al > Cu/Mg-Al > Mo/Mg-Al > Mg-Al.
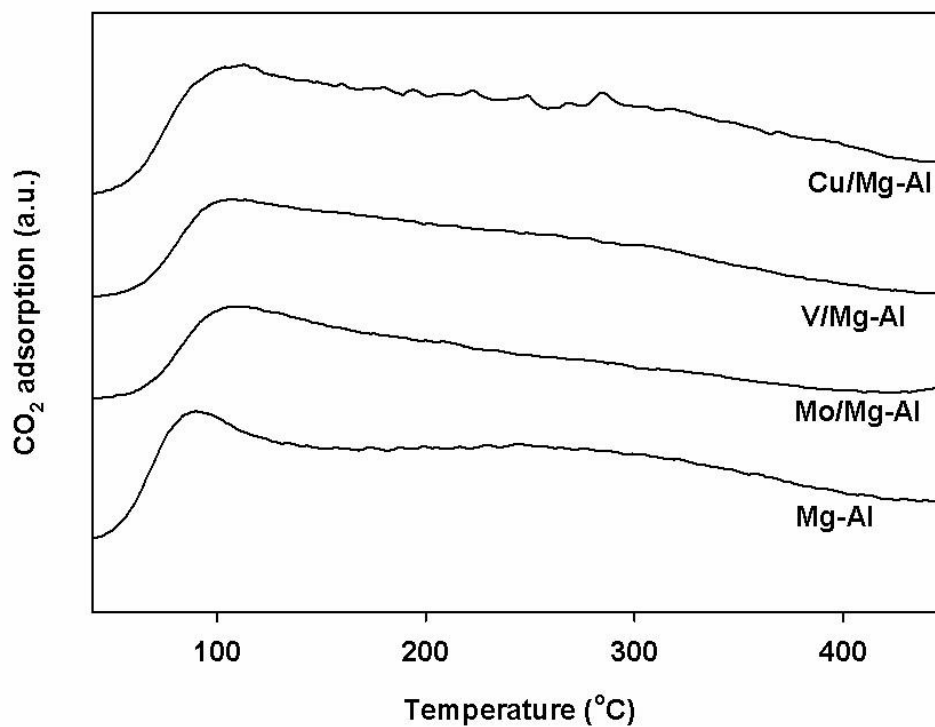
Figure 4.18 CO_2-TPD profiles of catalysts.

4.2.2 Reaction study

catalytic dehydrogenation and oxidative dehydrogenation of ethanol were performed at temperature 200 to 400°C in order to investigate catalytic activity of all catalysts. The ethanol conversion and acetaldehyde selectivity of each catalysts is presented in **Figure 4.19** and **4.20**. The ethanol conversion increased with reaction temperature in both dehydrogenation and oxidative dehydrogenation of ethanol.
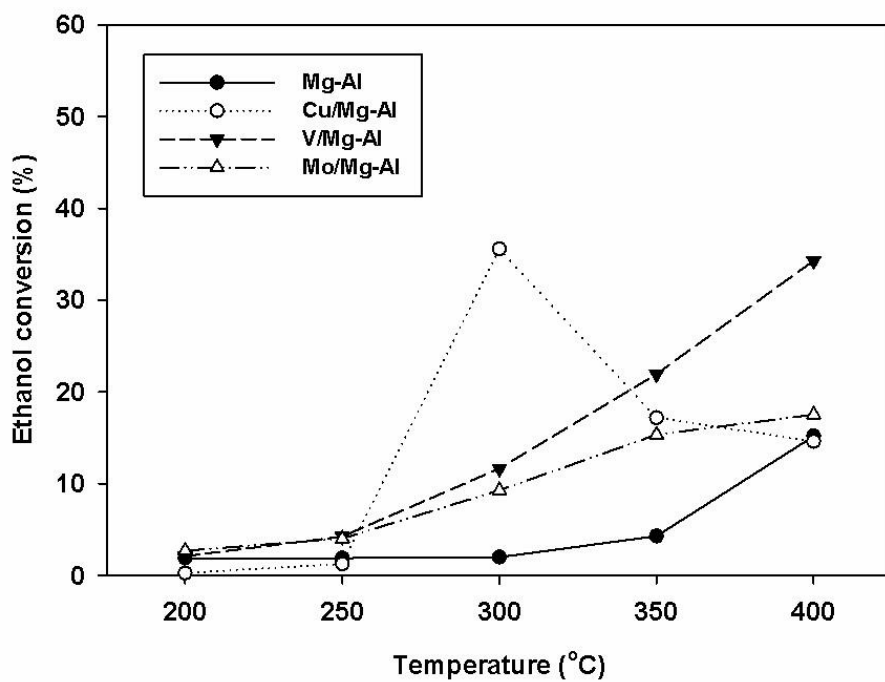
Figure 4.19 Ethanol conversion of all catalysts under non-oxidative dehydrogenation.
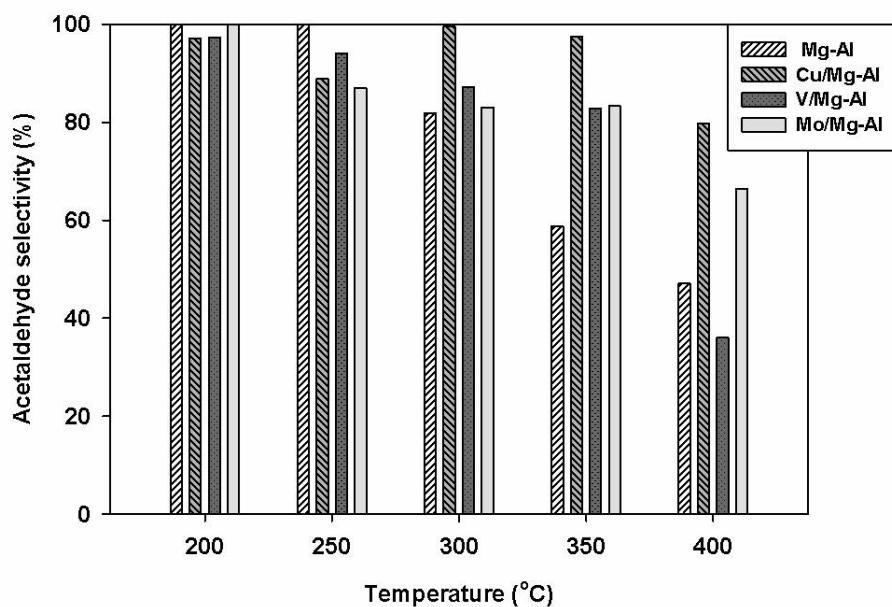
Figure 4.20 Acetaldehyde selectivity of all catalysts under non-oxidative

dehydrogenation.

4.2.2.1 Non-oxidative dehydrogenation of ethanol

In the absence of oxygen, the metal-modified Mg-Al catalysts exhibited higher activity than Mg-Al catalyst (**Figure 4.19**). The copper modified catalyst (Cu/Mg-Al) exhibited the highest conversion of 75.6% at 300°C and then rapidly decreased at high temperature. The catalyst with vanadium (V/Mg-Al) showed the highest ethanol conversion in the temperature range of 350-400°C and the maximum conversion of 34.3% was found at 400°C. Excepted Cu/Mg-Al catalyst, the activity tended to decrease in the order of V/Mg-Al > Mo/Mg-Al > Mg-Al. This trend was consistent with the base density of catalyst as shown in **Table 4.4**. The reduction of CuO species on the Cu/Mg-Al catalyst surface by hydrogen from ethanol led to maximum conversion at 300°C. The greatly decrease of ethanol conversion at 350-400°C probably due to the deactivation by coke formation [39]. The products of ethanol dehydrogenation mainly consisted of acetaldehyde (selectivity > 80%), ethylene and trace amount of diethyl ether at temperature range 200-300°C. The acetaldehyde selectivity of all catalyst decreased with increased temperature due to the formation of a competitive product (ethylene), especially on V/Mg-Al catalyst (**Figure 4.20**). The highest acetaldehyde yield of 15.5% was observed on V/Mg-Al catalyst due to the highest conversion although the V/Mg-Al catalyst showed the lowest selectivity at 400°C (**Figure 4.21**). This result indicated that in the absence of oxygen, the presence of Cu, Mo and V on the surface of Mg-Al catalyst enhanced the rate of dehydrogenation of ethanol. It was probably due to the enhancement of surface base density of modified catalysts [113]. The proposed mechanism of dehydrogenation of ethanol over V/Mg-Al catalyst is described as followed. In the first step, ethanol is adsorbed on acid-base site of Mg-Al oxide and vanadium oxide on the catalyst surface [103, 114]. The O-H bond of ethanol dissociates and form an ethoxide species, then the α-hydrogen is abstracted by Mg-OH group. The acetaldehyde is desorbed as product and H atom on the surface recombines to form H_2.

The proposed mechanism is shown in **Figure** 4.22. Although low acetaldehyde yield was observed in non-oxidative dehydrogenation reaction, the production of hydrogen as byproduct was considered as the advantage of this reaction.
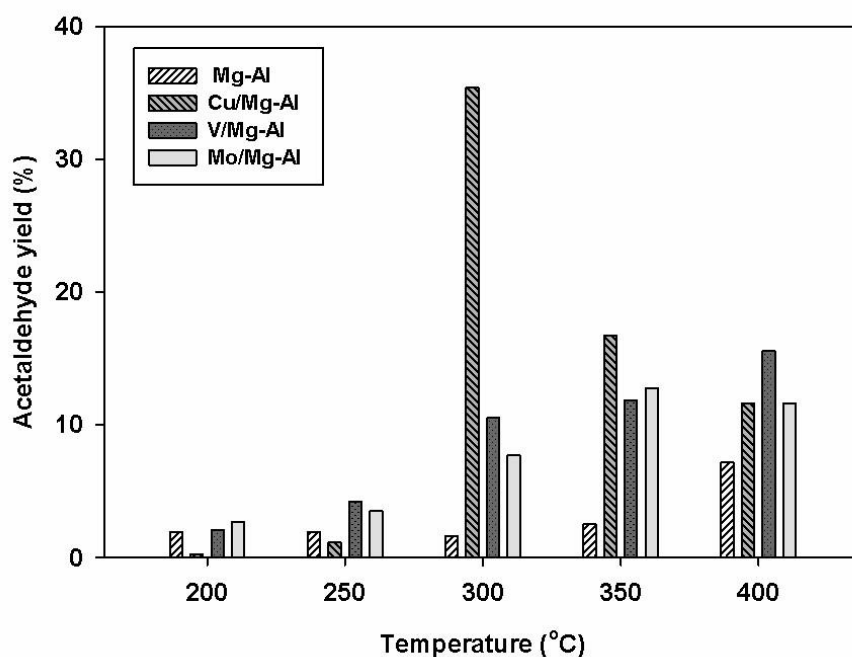

Figure 4.21 Acetaldehyde yield of all catalysts under non-oxidative dehydrogenation.
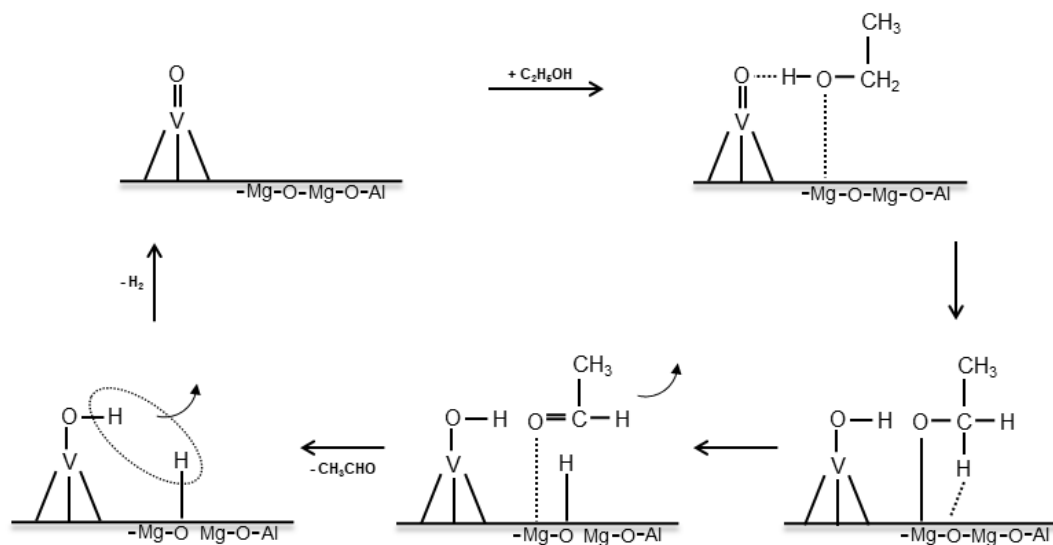

Figure 4.22 Proposed mechanism of non-oxidative dehydrogenation of ethanol over V/Mg-Al catalyst.

4.2.2.2 Oxidative dehydrogenation of ethanol

When the reaction was performed in the presence of oxygen (oxidative dehydrogenation), the ethanol conversion of all catalysts was higher than those in the absence of oxygen. The higher ethanol conversion in all reaction temperature was observed on Cu/Mg-Al catalyst. The ethanol conversion of Cu/Mg-Al extremely increased at 300°C (75.6%) and slightly increased at the temperature range of 300 to 400°C as shown in **Figure 4.23**. The maximum ethanol conversion of 93.0% was observed at 400°C, while the maximum ethanol conversion of Mg-Al catalyst was 65.3%. In contrast, the acetaldehyde selectivity on Cu/Mg-Al catalyst highly decreased at 300°C due to CO_2 formation (**Figure 4.24**). The enhancement of catalytic activity of Cu/Mg-Al catalyst was suggested that copper oxide species on the surface and the base density affected the catalytic performance on dehydrogenation of ethanol [73, 113].

The oxidative dehydrogenation products differed from in the dehydrogenation. Acetaldehyde was observed as a major product at low temperature range (200-300°C) (**Figure 4.24**), but various byproducts (such as ethylene, diethyl ether, ethyl acetate, acetic acid and carbon dioxide) were formed at high temperature range (350-400°C). The acetaldehyde selectivity greatly decreased at 400°C due to further decomposition to form mainly CO_2. Except Cu/Mg-Al, the V/Mg-Al catalyst showed the maximum acetaldehyde yield of 29.5% at 400°C. It was suggested that both basic site and vanadium oxide species on the catalyst surface affected the catalytic activity on this reaction in oxidative atmosphere [62]. The proposed mechanism of oxidative dehydrogenation of ethanol is shown in **Figure 4.25**. The ethanol molecule adsorption and acetaldehyde formation step are like the first step of non-oxidative dehydrogenation mechanism as mentioned in **Figure 4.22**. However, in the oxidative atmosphere, H from the V-O-H group combines with OH from Mg-OH group to produce H_2O leading to the

oxygen vacancy on the catalyst surface. Then, the surface is re-oxidized by oxygen in the feed [98]. This mechanism is probably faster than the non-oxidative dehydrogenation, thus the observed activity of catalyst in oxidative dehydrogenation is higher than non-oxidative one.
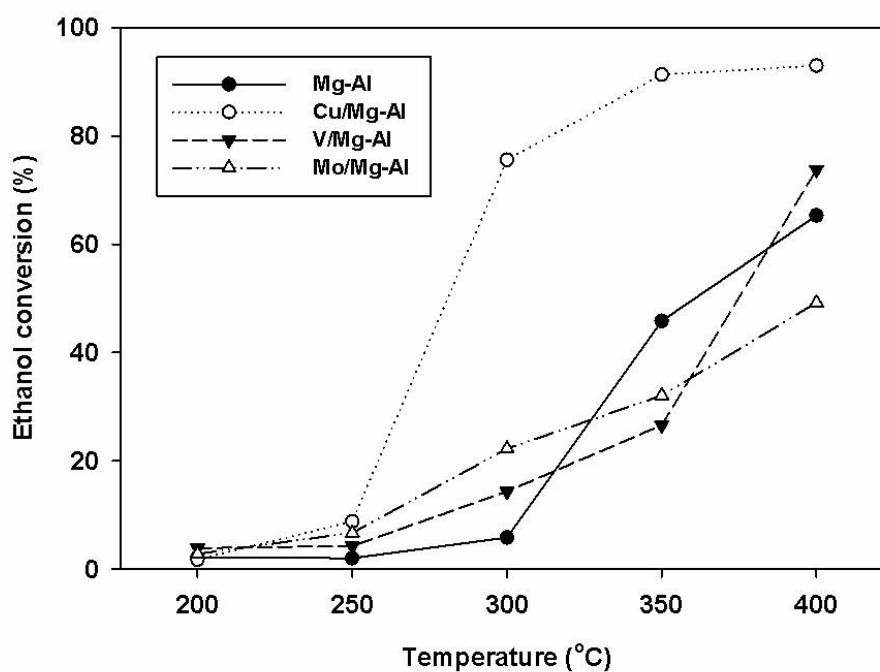

Figure 4.23 Ethanol conversion of all catalysts under oxidative dehydrogenation.
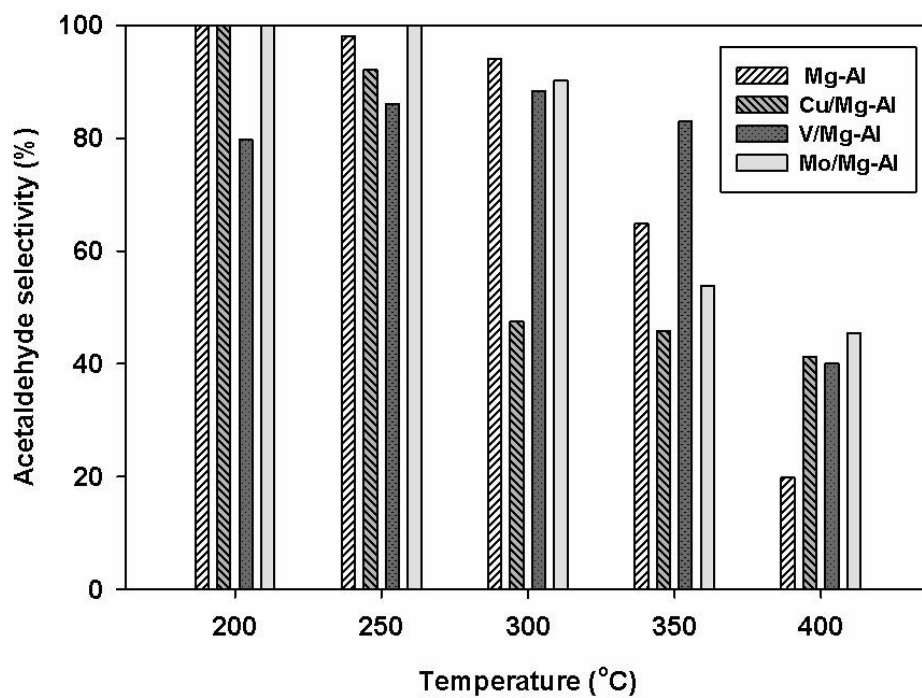
Figure 4.24 Acetaldehyde selectivity of all catalysts under oxidative dehydrogenation.
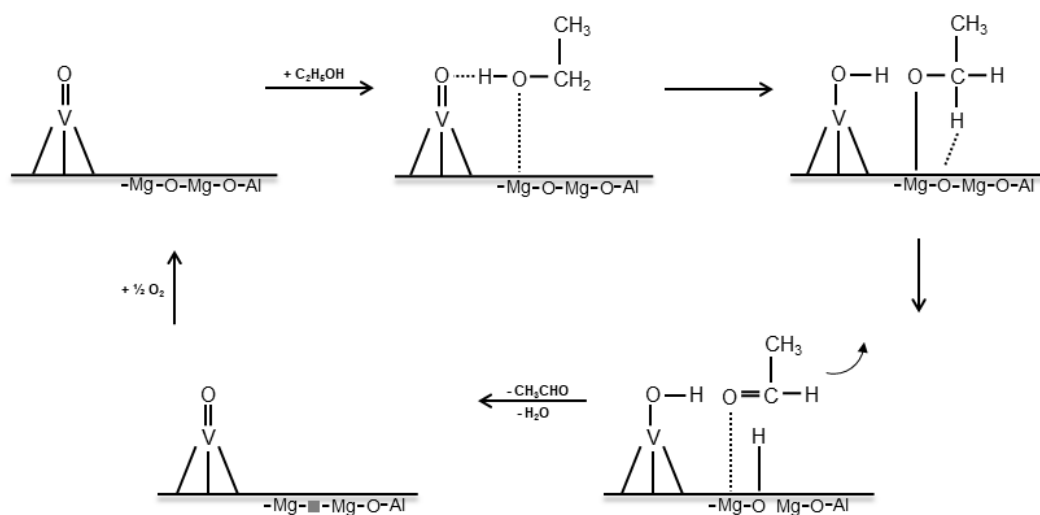
Figure 4.25 Proposed mechanism of oxidative dehydrogenation of ethanol over V/Mg-Al catalyst.

The proposed mechanism in the presence of Cu is likely shown in **Figure 4.26**. The reaction starts with the adsorption of ethanol molecule on the acid/base site of Mg-Al oxide surface [103, 114]. The ethoxide specie is formed by the dissociation of O-H bond of ethanol [101, 102]. The α-hydrogen is abstracted by CuO to form acetaldehyde and Cu-O-H group. Then, acetaldehyde molecule is desorbed, and the H from Cu-O-H group combines with H from O-H group on the Mg-Al surface to produce water resulting in the Cu^0 formation on the surface. The Cu^0 is consecutively oxidized to CuO by oxygen in the feed [98].
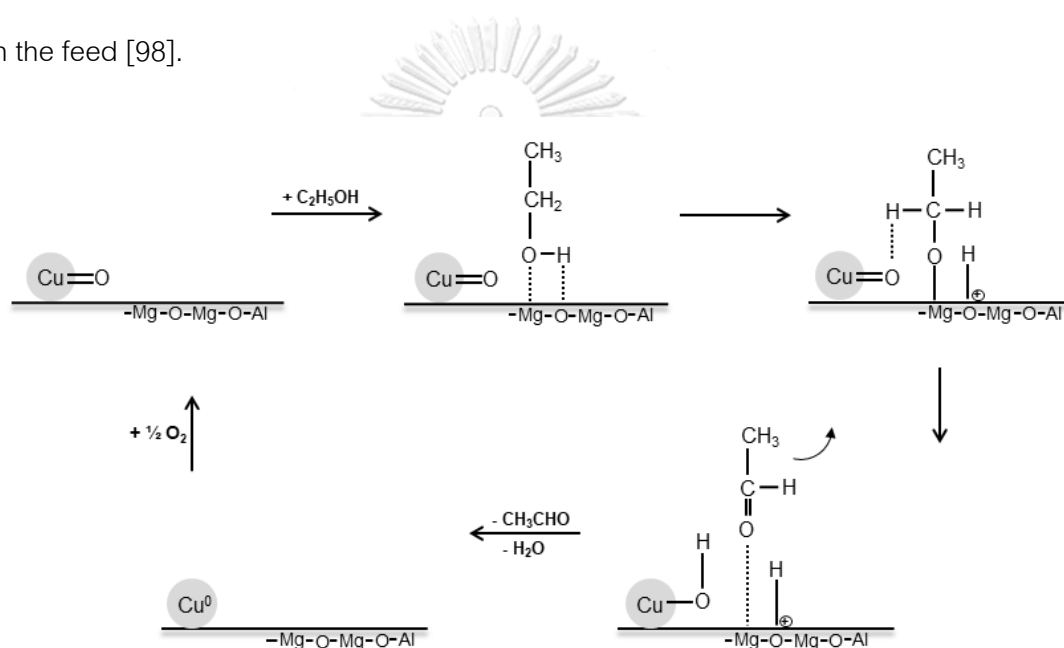
Figure 4.26 Proposed mechanism for oxidative dehydrogenation of ethanol over Cu/Mg-Al catalyst.

The stability of all catalysts was performed with time on stream (TOS) for 10 h (**Figure 4.27**). The reaction temperature was fixed for each catalyst (350°C for Mg-Al catalyst, 375°C for V/Mg-Al catalyst and 400°C for Mo/Mg-Al catalyst) in order to control the ethanol conversion approximately 40-60% [8]. For Cu/Mg-Al catalyst, it would be test at the temperature with provide ethanol conversion of ca. 80% (at 300°C) because it was

hard to control the ethanol conversion at 40-60%. The result showed that all catalysts were relatively stable upon 10 h. The Mo/Mg-Al exhibited higher deactivation than others due to high reaction temperature and the lowest activity of catalyst. the thermogravimetric analysis was applied in order to investigate the carbon deposition on the spent catalyst from TOS. The result of weight loss as a function of temperature was presented in **Figure 4.28**. The first region of weight loss at $200^{\circ}C$ referred to the removal of water. The weight loss in the temperature range of 200 to $400^{\circ}C$ can be attributed to the dehydroxylation and decarbonation of hydrotalcite structure [95, 115]. The carbon deposition or coke formation on catalyst surface was calculated in the temperature range of 400 to $800^{\circ}C$, which is de-coking process period [116]. It was found that the weight loss of spent catalyst in this region was insignificantly different showing less amount of carbon deposition.
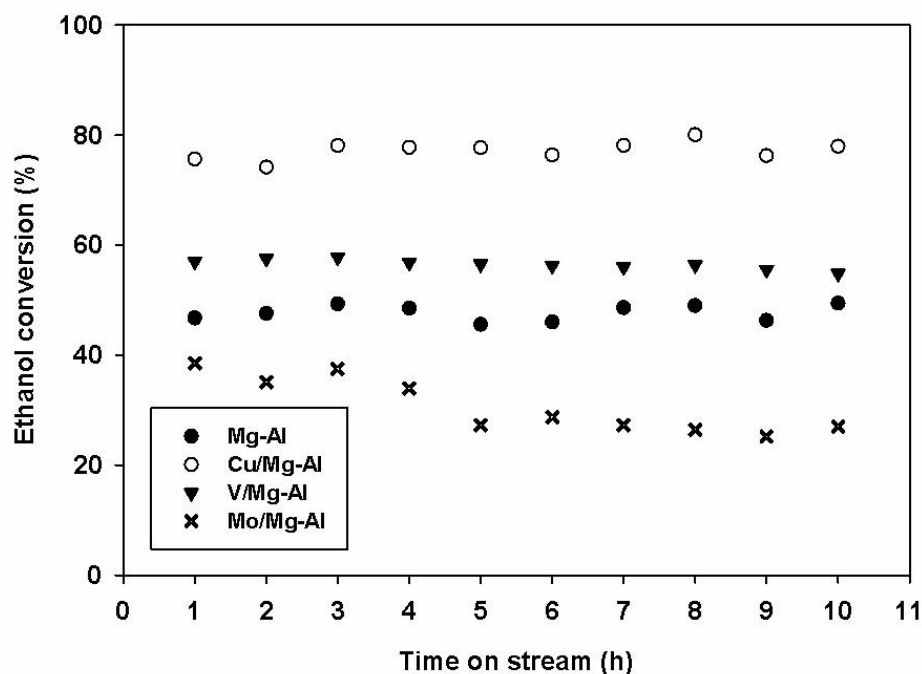
Figure 4.27 Stability test for all catalysts under oxidative dehydrogenation.
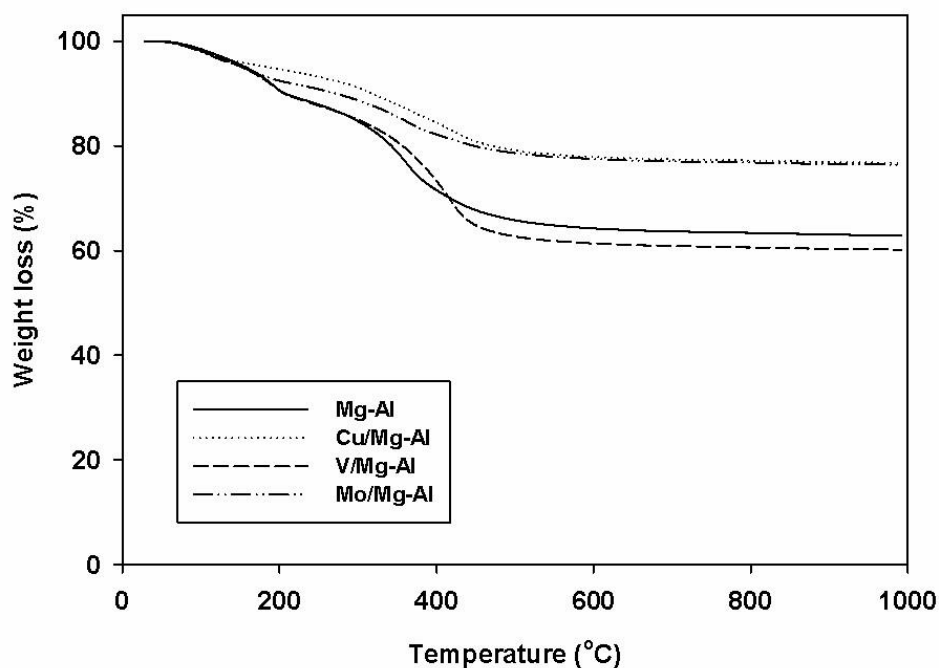
Figure 4.28 Thermogravimetric analysis of spent catalysts.

4.3 Investigation of the effect of ethanol concentration and reduction condition of copper-modified Mg-Al catalyst on catalytic activity.

4.3.1 Charateristics

The reducibility of Cu/Mg-Al catalyst was determined by H_2-TPR and the profile is shown in **Figure 4.29**. The TPR profile indicated reducibility of the surface copper species in two steps at maximum temperature (T_{max}) of ca. $205^{o}C$ and $370^{o}C$ corresponding to the reduction of CuO to Cu_2O and Cu_2O to Cu^{0}, respectively [117].
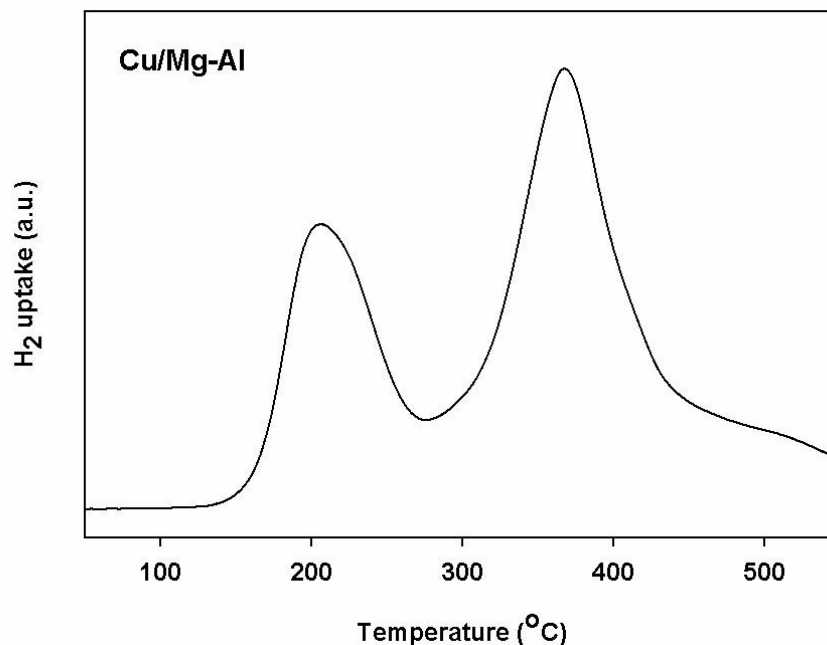
Figure 4.29 H_2-TPR profile of Cu/Mg-Al catalyst.

4.3.2 Reaction study

4.3.2.1 Effect of ethanol concentration on catalytic activity

It is known that the production of bioethanol by fermentation process leads to formation of water in the ethanol solution. Therefore, the effect of ethanol concentration has to be evaluated. There are some researchers investigated on this effect on catalytic activity such as Krutpijit et al. [118] and Wu et al. [119]. In this study, the various ethanol concentration was used as reactant (99.9%, 75% and 50% by weight) in the oxidative dehydrogenation reaction. The ethanol solution was prepared by mixing the absolute ethanol (99.9%) with DI water to obtain ethanol concentration of 75% and 50%. The result in **Figure 4.30** shows that the conversion of absolute ethanol and diluted ethanol was greatly different at 300°C. The conversion of diluted ethanol (75% and 50%) of only ca. 12% was observed. It suggested that water content negatively affected the ethanol

conversion of Cu/Mg-Al catalyst. It can be ascribed that there was competitive adsorption of water molecule on the active site [120]. At high temperature range (350-400°C), the ethanol conversion only slightly decreased with decreased ethanol concentration. It can be noticed that water content slightly affected the catalytic activity at high reaction temperature range [121]. It might be due to the water adsorption ability of Cu/Mg-Al catalyst decreased with increased temperature.
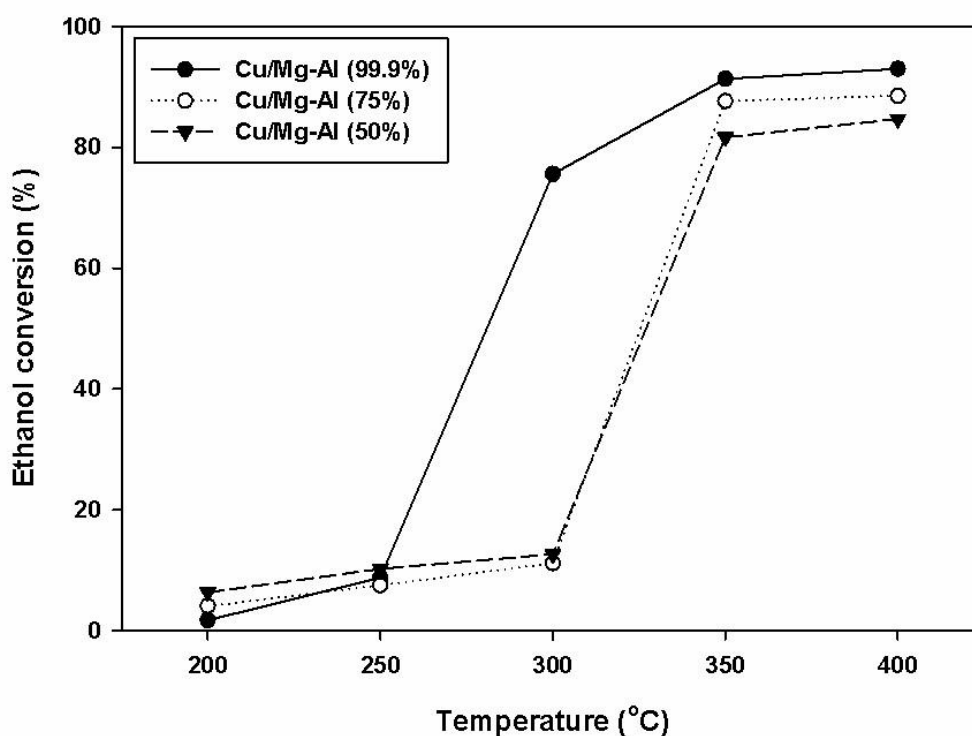
Figure 4.30 Ethanol conversion of Cu/Mg-Al catalyst under various ethanol concentration.

The acetaldehyde selectivity decreased with increased reaction temperature for all conditions (**Figure 4.31**) because of the formation of byproduct such as CO_2, ethylene, diethyl ether, acetic acid and ethyl acetate. The formation of CO_2 increased with increased reaction temperature (**Figure 4.32**) due to complete oxidation of ethanol.

This result was obviously observed at high ethanol conversion on Cu/Mg-Al. In contrast, the ethylene selectivity increased with the water content in the feed (**Figure 4.33**). It revealed that the dehydration pathway increased because of the formation of Brønted acid site by the reaction of water and catalyst surface [120, 121]. The CO_2 byproduct was also observed on Mg-Al at high temperature range (350-400°C). However, the highest acetaldehyde yield of 41.8% was observed on Cu/Mg-Al catalyst at 350°C (**Figure 4.34**).
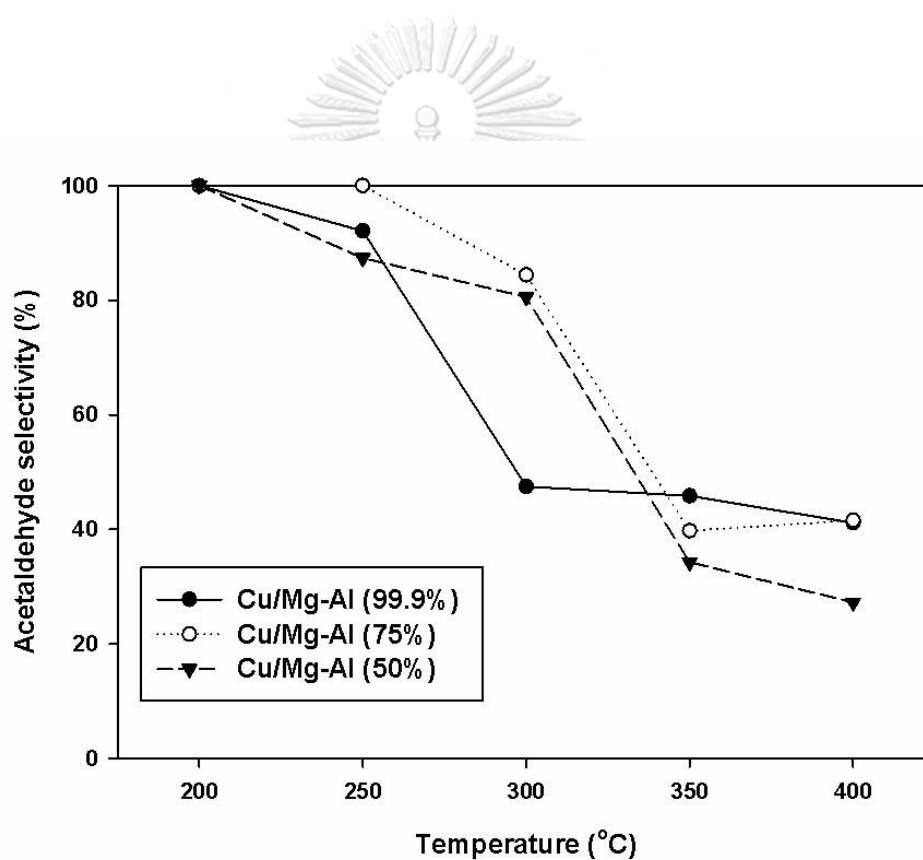
Figure 4.31 Acetaldehyde selectivity of Cu/Mg-Al catalyst under various ethanol concentration.
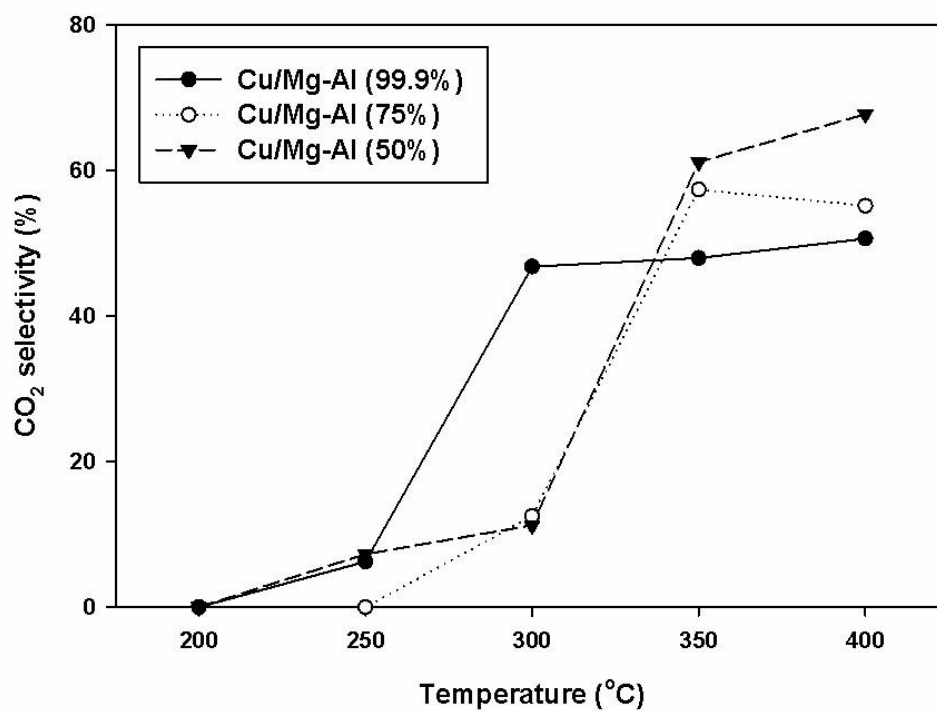
Figure 4.32 CO_2 selectivity of Cu/Mg-Al catalyst under various ethanol concentration.

Figure 4.33 Ethylene selectivity of Cu/Mg-Al catalyst under various ethanol
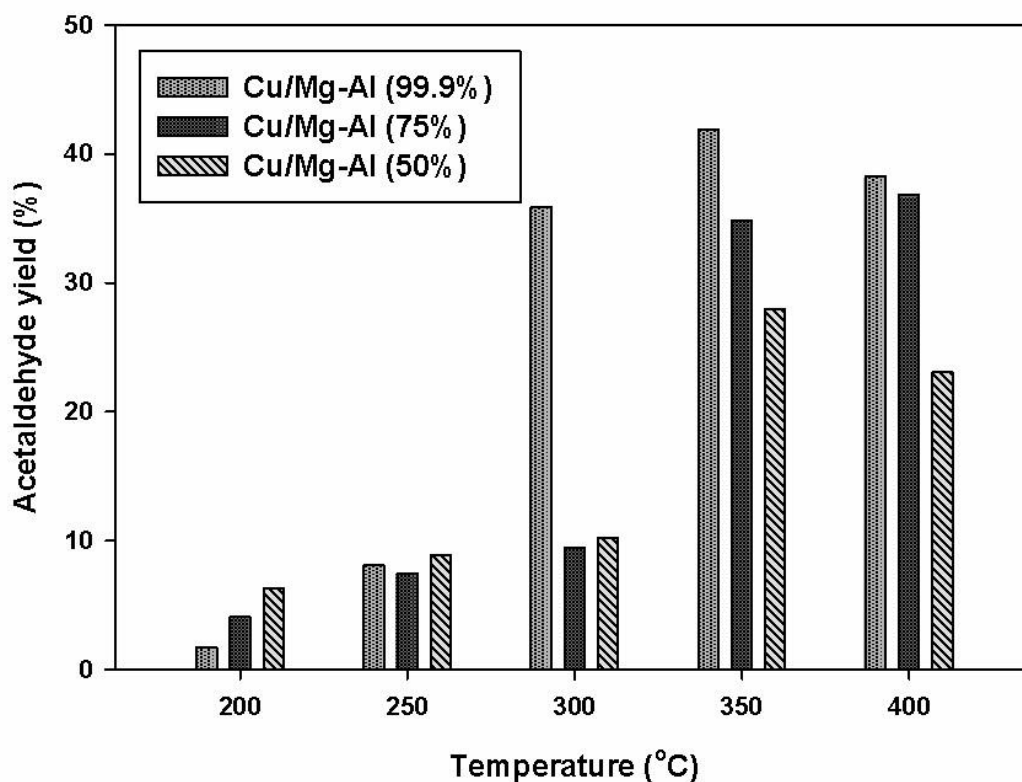
concentration.

Figure 4.34 Acetaldehyde yield of Cu/Mg-Al catalyst under various ethanol concentration.

4.3.2.2 Effect of reduction temperature on catalytic activity

From the proposed mechanism in **Figure 4.26**, it might be implied that the Cu/Mg-Al catalyst could be used in oxidative dehydrogenation of ethanol without pre-reduction step. It would be reduced by the hydrogen atom from ethanol via dehydrogenation reaction [115] and reoxidized to CuO by oxygen in the feed. In an additional experiment, the effect of pre-reduction temperature was investigated to support this hypothesis and the results are shown in **Figure 4.35**. It was found that ethanol conversion was slightly different in high reaction temperature range (350-400°C). Non-reduced Cu/Mg-Al catalyst showed the highest ethanol conversion, while the

reduced catalyst showed about 5-10% lower. The same trend was observed in the acetaldehyde selectivity (**Figure** 4.36) and the results were slightly different. The formation of CO_2 at high temperature led to the decrease of acetaldehyde selectivity. The acetaldehyde yield of catalysts was calculated and shown in **Figure** 4.37. It was found that of non-reduced and reduced catalyst could confirm that the pre-reduction step of Cu/Mg-Al catalyst was not necessary in oxidative dehydrogenation of ethanol.
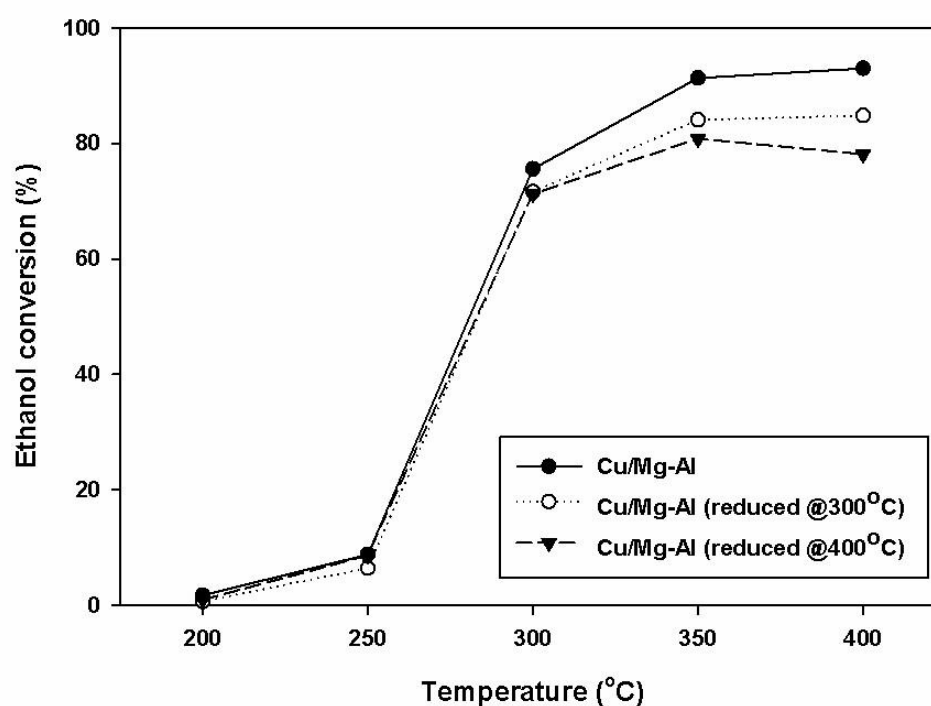
Figure 4.35 Ethanol conversion of Cu/Mg-Al catalyst under various pre-reduction conditions.
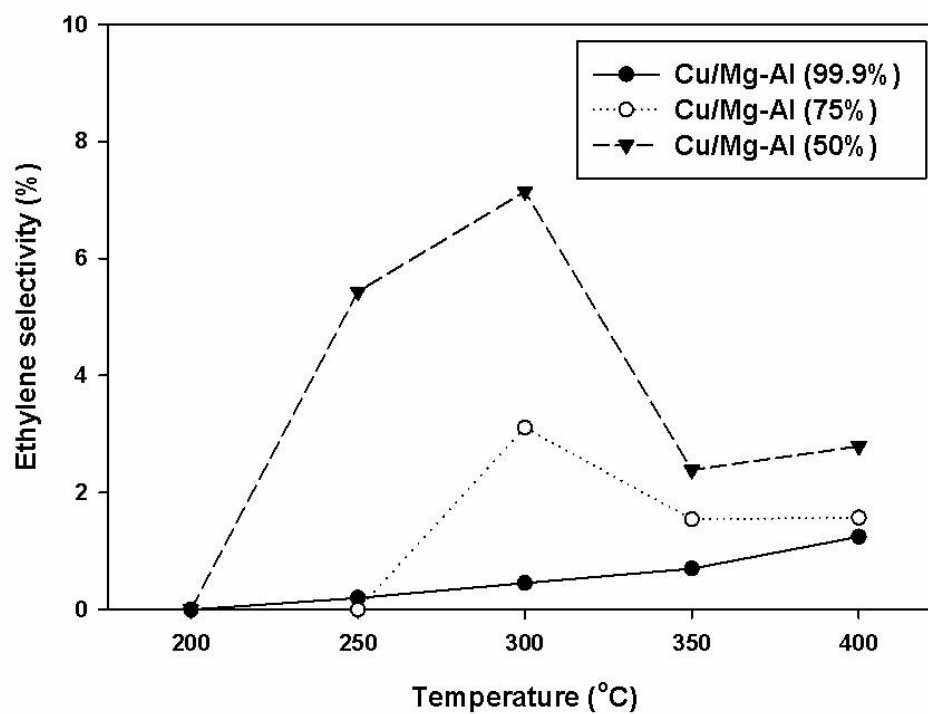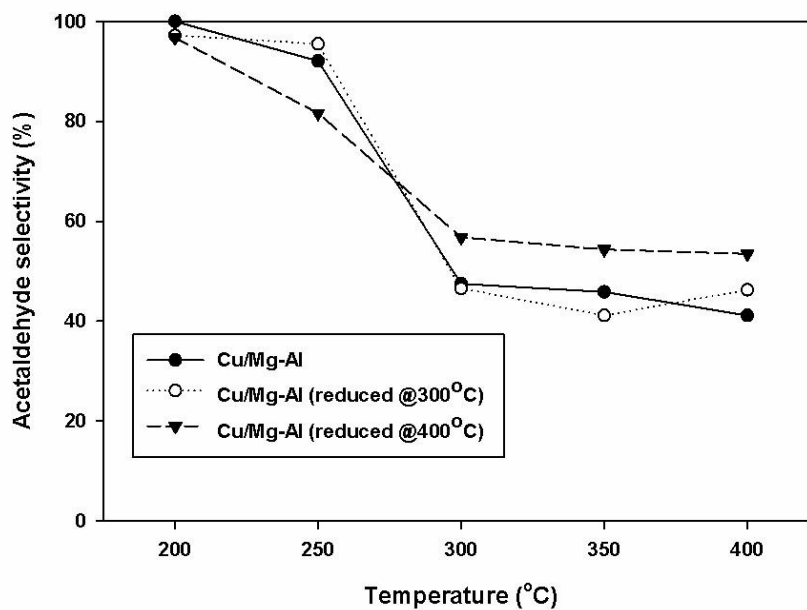
Figure 4.36 Acetaldehyde selectivity of Cu/Mg-Al catalyst under various pre-reduction conditions.
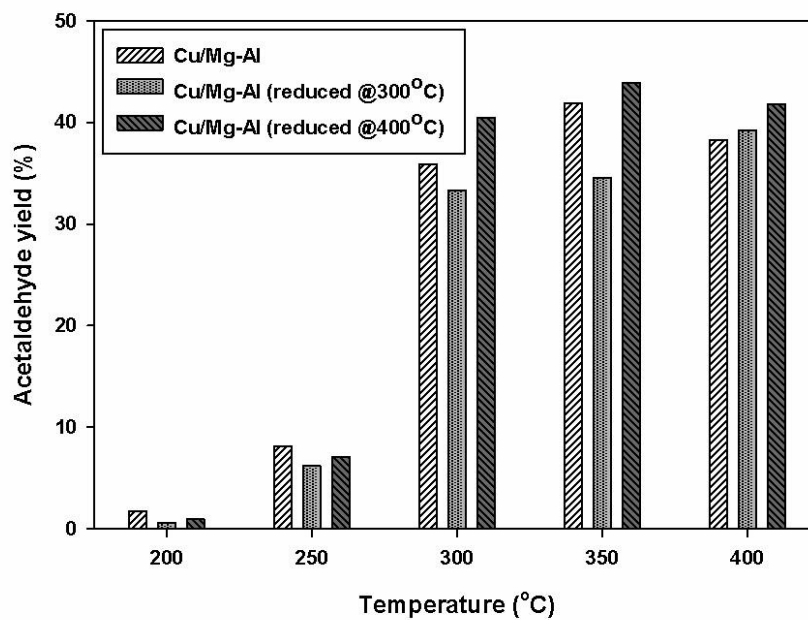
Figure 4.37 Acetaldehyde yield of Cu/Mg-Al catalyst under various pre-reduction conditions.

CHAPTER 5

CONCLUSION AND RECOMMENDATIONS

5.1 Conclusion

　　In the first part, Mg-Al LDHs catalyst was synthesized by co-precipitaion method and calcined at various temperatures from 450 to 900°C. The result showed that calcination temperature played an important role on the characteristics and catalytic performance of Mg-Al catalysts. The BET surface area and basicity of calcined catalysts decreased with increased calcination temperature. This result led to the decrease of catalytic performance in oxidative dehydrogenation of ethanol. When considering at low reaction temperature range (200-300°C), the non-calcined Mg-Al LDHs catalyst (Mg-Al-000) showed the highest ethanol conversion involving with the hydroxyl groups on the surface. At high reaction temperature range (350-400°C), the catalysts calcined at 450°C and 600°C exhibited the highest ethanol conversion because of their basic mixed oxide form. The acetaldehyde selectivity decreased with increasing the reaction temperature due to byproducts formation, especially carbon dioxide. In this study, the highest acetaldehyde yield of 29.7% at 350°C was observed on the catalyst calcined at 450°C (Mg-Al-450). This catalyst would be further modified to promote the catalytic activity.

　　In the second part, the copper-, vanadium- and molybdenum-modified Mg-Al catalysts obtained from LDHs were prepared by incipient wetness impregnation. They were characterized and investigated the catalytic activity for dehydrogenation and oxidative dehydrogenation of ethanol. It was found that the metal loading affected the characteristic and activity of catalyst. The surface area and basicity of catalyst decreased when the metal was added. Considering the base density of catalysts, the

V/Mg-Al catalyst exhibited the highest base density of 6.13 μmol CO_2/m^2. This result was consistent with the activity of V/Mg-Al catalyst for both non-oxidative dehydrogenation and oxidative dehydrogenation. For copper-modified catalyst (Cu/Mg-Al), the characterization result showed that only CuO presented on the surface and the basicity slightly decreased. Under non-oxidative condition, Cu/Mg-Al catalyst showed the maximum acetaldehyde yield of 35.4% at 300°C then rapidly decreased at high temperature. V/Mg-Al catalyst exhibited the highest acetaldehyde yield of 15.5% at 400°C. In the oxidative dehydrogenation, the catalytic activity of Cu/Mg-Al increased at $300-400^{o}$C. The maximum acetaldehyde yield was 41.8% at 350°C while V/Mg-Al catalyst showed the highest acetaldehyde yield of 29.5% at 400°C. The results showed that the present of metal species as well as basicity of catalysts play an important role in both non-oxidative and oxidative dehydrogenation.

In the third part, the effect of water content in ethanol feed was investigated by varying ethanol concentration. The result indicated that water content greatly affected the catalytic performance of Cu/Mg-Al at 300°C. The ethanol conversion decreased about 6-fold due to the competitive adsorption of water molecule. However, the negative effect decreased at high temperature ($350-400^{o}$C). The effect of reduction condition was examined by pre-reducing catalyst at 300 and 400°C. It was found that the reduction step showed insignificant effect on catalytic activity of Cu/Mg-Al. From TOS study, this catalyst was comparatively stable for 10 h upon time-on-stream test.

In final summary, Cu/Mg-Al catalyst can be used as a promising catalyst in oxidative dehydrogenation of ethanol to acetaldehyde without any pre-reduction step. Moreover, it can be effectively employed in this reaction for the diluted ethanol at temperature range of $350-400^{o}$C.

5.2 Recommendations

1) The effect of Mg/Al ratio of LDHs on catalytic activity should be further investigated. It would affect the characteristics and catalytic performance in oxidative dehydrogenation of ethanol. The higher acetaldehyde yield would be obtained on a Mg-Al LDHs with suitable Mg/Al ratio.

2) The effect of copper loading on catalytic performance of Cu/Mg-Al should be investigated to understand the behavior of copper species on the surface. It might be play an important role on the reactivity of this catalyst in oxidative dehydrogenation of ethanol.

3) The other parameters on reaction condition should be studied such as WHSV and oxygen flow rate. Adjusting some parameters would promoting the acetaldehyde selectivity. The formation of byproduct, especially CO_2, would be decreased to obtain higher acetaldehyde yield.

4) The in-situ X-Ray diffraction (XRD) and in-situ X-Ray adsorption near-edge structure (XANES) at Cu edge should be provided to clarify the copper species on the catalyst surface during oxidative dehydrogenation reaction of ethanol.

5) According to the catalytic activity of LDHs at low temperature, it revealed higher ethanol conversion than the calcined catalyst. It is interesting to investigate the catalytic performance on liquid phase ethanol dehydrogenation at low temperature range.

6) The ethanol concentration of 95% (an azeotrope) should be studied in this reaction to investigate the effect of water content on both temperature program and time on stream (TOS).

7) The different method of metal modification, such as wet impregnation or ion-exchange, should be investigated. Because it tends affect the characteristics and catalytic activity.

APPENDIX

APPENDIX A

CALCULATION FOR CATALYST PREPAREATION

Calculation of metal loading

Preparations of V/Mg-Al, Mo/Mg-Al and Cu/Mg-Al catalyst by incipient wetness impregnation method are shown as follows

Reagent;　　- Vanadyl acetylacetonate ($OV(C_5H_7O_2)_2$)

Molecular weight	=	256.157	g/mol
V atomic weight	=	50.9415	g/mol

- Ammonium heptamolybdate tetrahydrate ($(NH_4)_6Mo_7O_{24}$)

Molecular weight	=	1235.86	g/mol
Mo atomic weight	=	95.94	g/mol

- Copper (II) nitrate hemi(pentahydrate) ($Cu(NO_3)_2 \cdot 2.5H_2O$)

Molecular weight	=	232.59	g/mol
Cu atomic weight	=	63.546	g/mol

- Support: Mg-Al mixed oxide derive from hydrotalcite

Based on 1g of catalyst required,

For V, the V/Mg-Al catalyst contain 5wt% of vanadium. So, the V/Mg-Al catalyst composition would be as follow:

Vanadium	=	0.05 g			
Mg-Al mixed oxide	=	1.00 – 0.05	=	0.95 g	

Vanadyl acetylacetonate (precursor) 1 mole contained 1 atom of V, so the amount of vanadyl acetylacetonate 265.16 g contained 50.9415 g of V.

$$\text{Required vanadyl acetylacetonate (g)} = \frac{265.16 \; g \; precursor}{50.9415 \; g \; V} \times 0.05 \; g \; V$$

$$= 0.2602 \; g \; precursor$$

For Mo, the Mo/Mg-Al catalyst contain 5wt% of vanadium. So, the Mo/Mg-Al catalyst composition would be as follow:

Molybdenum $\qquad$ = $\qquad$ 0.05 g

Mg-Al mixed oxide $\qquad$ = $\qquad$ 1.00 – 0.05 $\qquad$ = $\qquad$ 0.95 g

Ammonium heptamolybdate tetrahydrate (precursor) 1 mole contained 7 atom of Mo, so the amount of ammonium heptamolybdate tetrahydrate 1235.86 g contained 7 x 95.94 g of Mo.

$$\text{Required ammonium heptamolybdate tetrahydrate (g)}$$

$$= \frac{1235.86 \ g \ precursor}{7 \times 95.94 \ g \ Mo} \times 0.05 \ gMo$$

$$= 0.0920 \ g \ precursor$$

For Cu, the Cu/Mg-Al catalyst contain 5wt% of vanadium. So, the Cu/Mg-Al catalyst composition would be as follow:

Copper $\qquad$ = $\qquad$ 0.05 g

Mg-Al mixed oxide $\qquad$ = $\qquad$ 1.00 – 0.05 $\qquad$ = $\qquad$ 0.95 g

Copper (II) nitrate hemi(pentahydrate) (precursor) 1 mole contained 1 atom of Cu, so the amount of copper (II) nitrate hemi(pentahydrate) 232.59 g contained 63.546 g of Cu.

$$\text{Required copper (II)nitrate hemi(pentahydrate) (g)}$$

$$= \frac{232.59 \ g \ precursor}{63.546 \ g \ Cu} \times 0.05 \ g \ Cu$$

$$= 0.1830 \ g \ precursor$$

APPENDIX B

CALCULATION OF BASICITY

The basicity of catalyst was measured by CO_2-TPD method. Total basicity was calculated from the area under curve of CO_2-TPD profile of the catalyst sample with respect to the area under the standard calibration curve of CO_2 (from Micromeritic Chemisorp 2750) as following equations

$$\text{Total basicity (µmole)} = \frac{17.6 \times A}{W}$$

where:

A = area under curve of CO_2-TPD profile of the catalyst sample (unit area)

W= weight of catalyst sample (g)
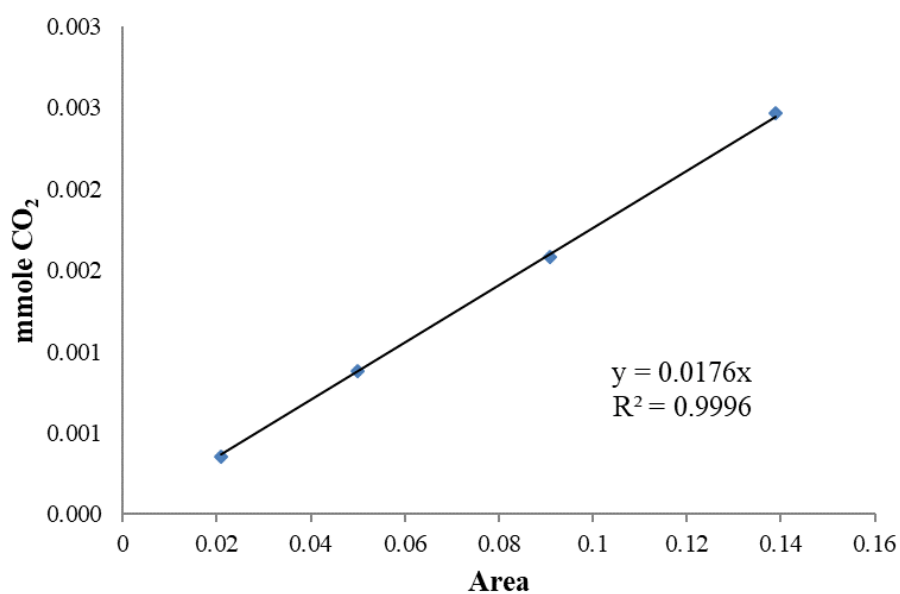
Figure B.1 calibration curve of CO_2 from Micromeritic Chemisorp 2750

APPENDIX C

GC CALIBRATION CURVES

The amount of reactant and products were quantitively analyzed by gas chromatography (GC). The quantity of ethanol and hydrocarbon product (ethylene, acetaldehyde, diethyl ether, acetic acid, ethyl acetate and n-butanol) were analyzed using GC with flame ionization detector (GC-FID) and DB-5 capillary column. The amount of CO and CO_2 were measured using GC thermal conductivity detector (GC-TCD) and Porapak Q column. The analytical grade chemicals and ultra-high purity gas were used as the standard for GC-FID and GC-TCD calibration, respectively. The GC operating conditions and calibration curves of each chemicals are shown in this appendix as follow.

Table C.1 the conditions used in GC-FID-14B and TCD 8A

Parameters	Condition
Width	5
Slope	1000
Drift	0
Minimum area	100
T.DBL	1000
Stop time	10
Attenuation	2
Speed	5
Method	Normalization
SPL.WT	100
IS.WT	1
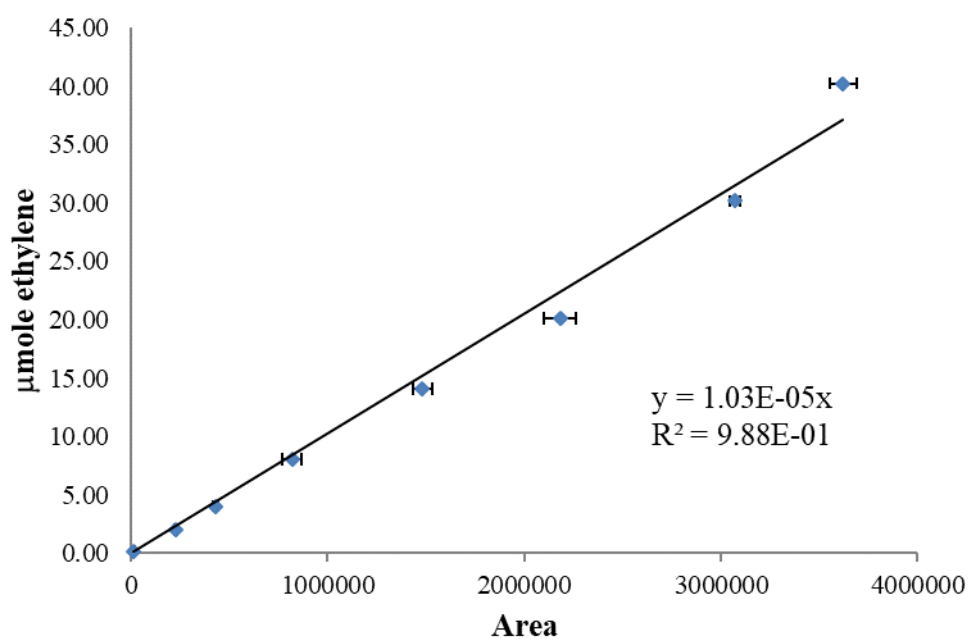
Figure C.1 the calibration curve of ethylene.

$$y = 1.03E-05x$$
$$R^2 = 9.88E-01$$
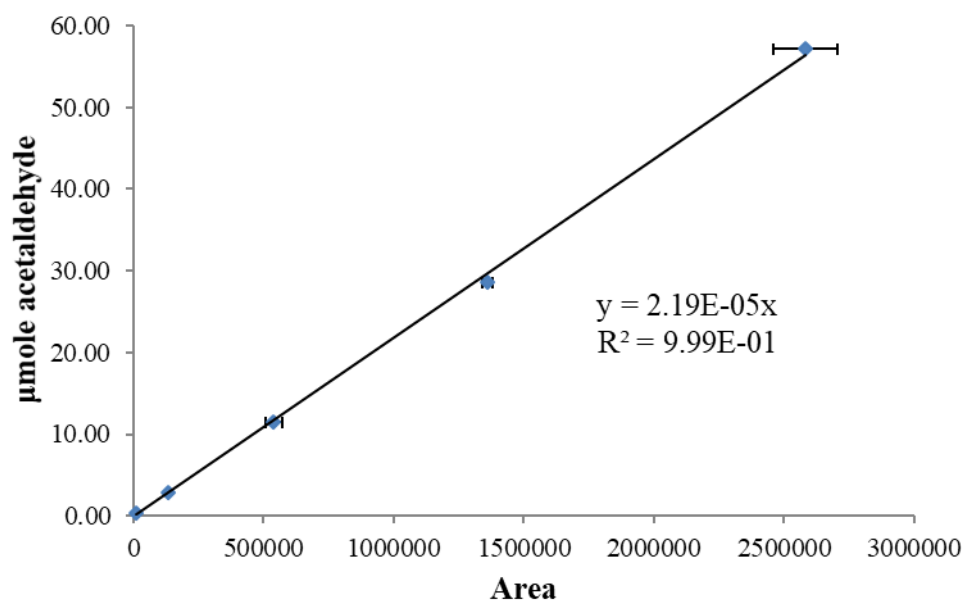
Figure C.2 the calibration curve of acetaldehyde.

$$y = 2.19E-05x$$
$$R^2 = 9.99E-01$$
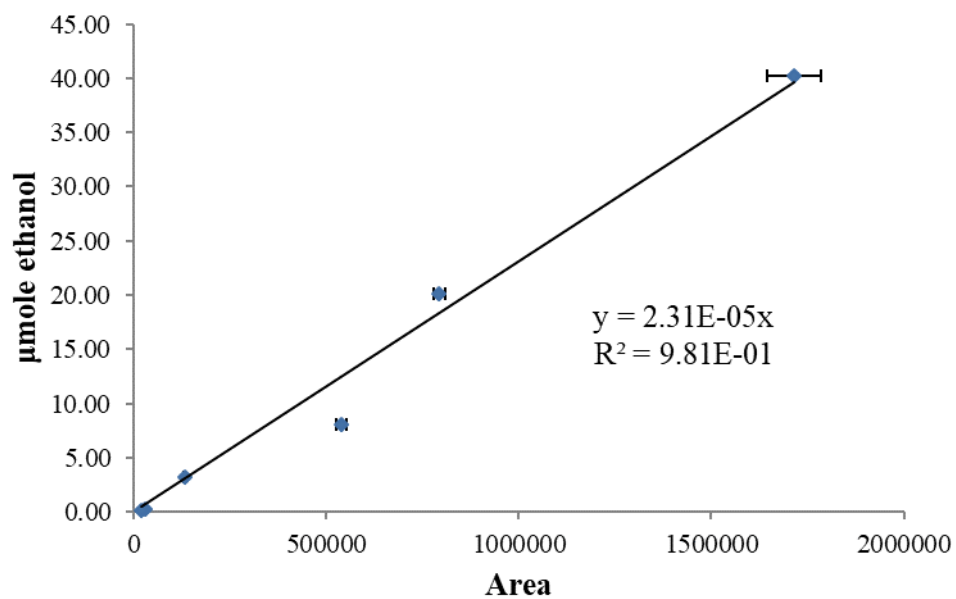
Figure C.3 the calibration curve of ethanol.
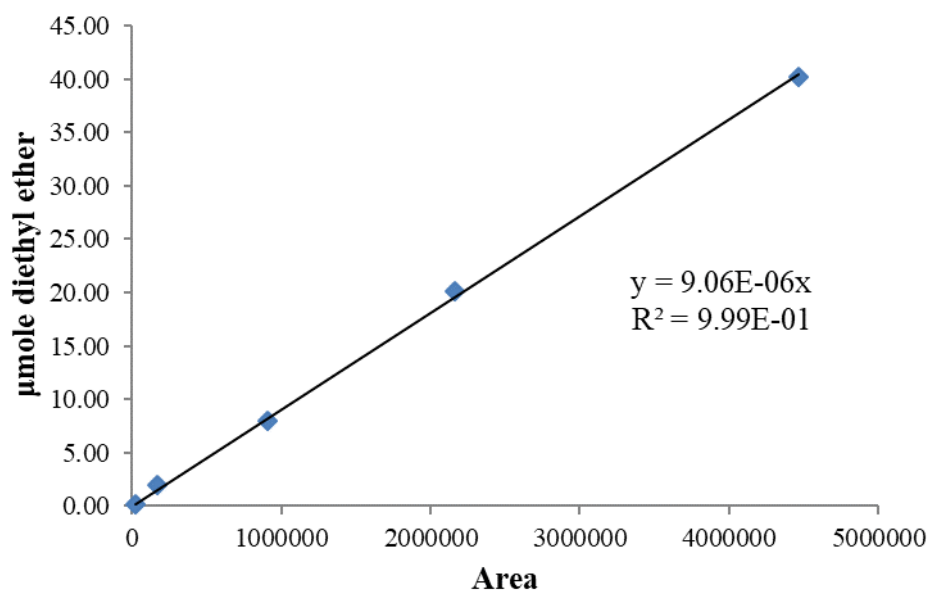
Figure C.4 the calibration curve of diethyl ether.
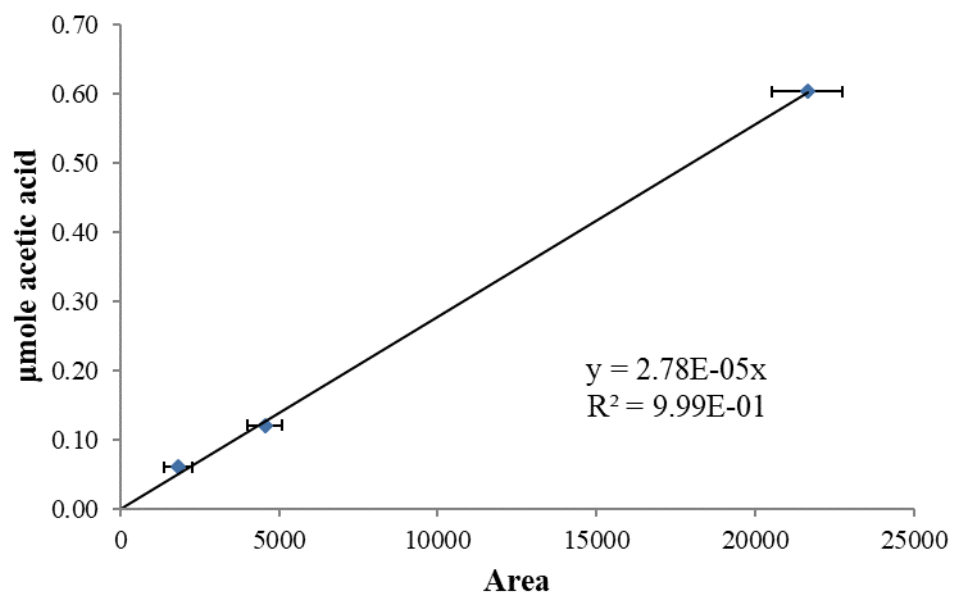
Figure C.5 the calibration curve of acetic acid.

$y = 2.78E\text{-}05x$
$R^2 = 9.99E\text{-}01$
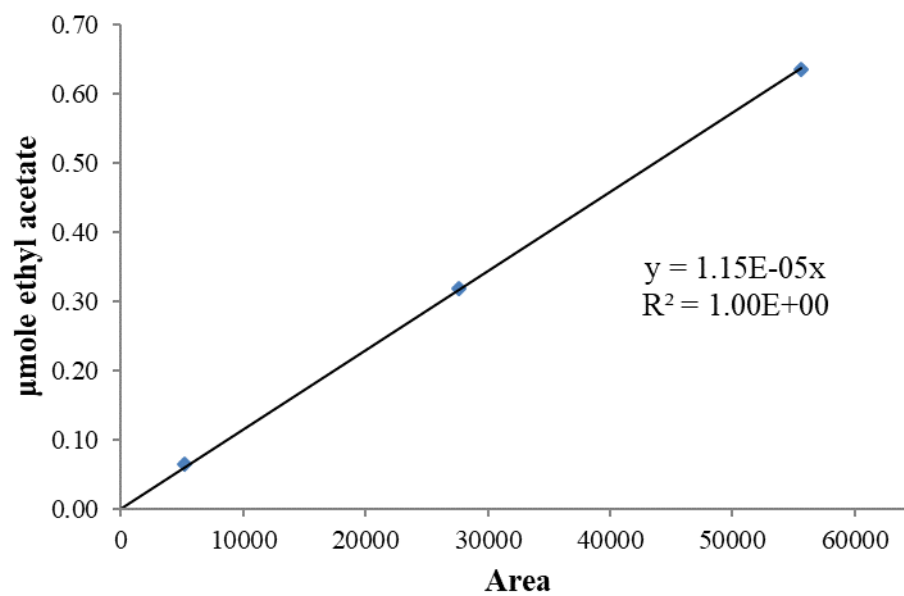
Figure C.6 the calibration curve of ethyl acetate.

$y = 1.15E\text{-}05x$
$R^2 = 1.00E\text{+}00$
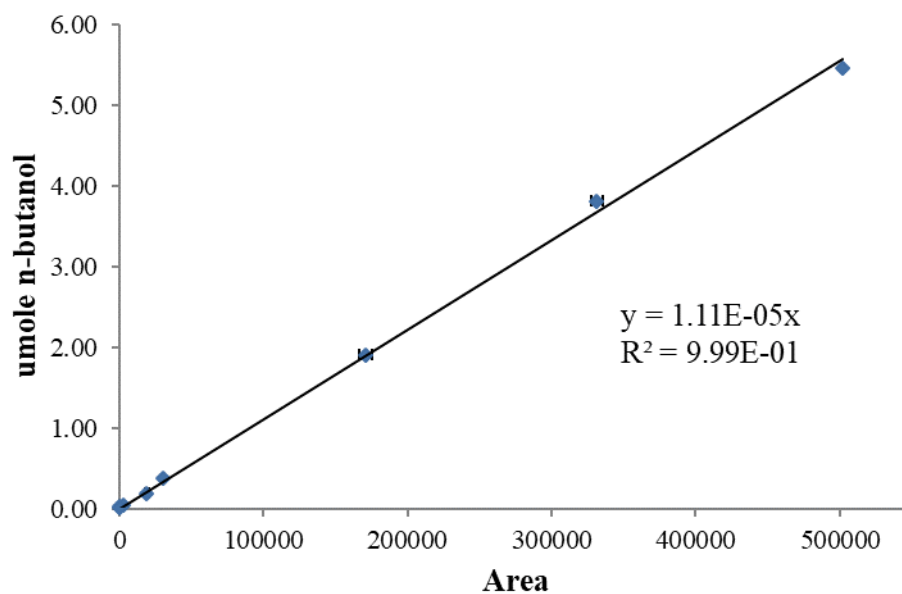
Figure C.7 the calibration curve of n-butanol.

$y = 1.11E-05x$
$R^2 = 9.99E-01$
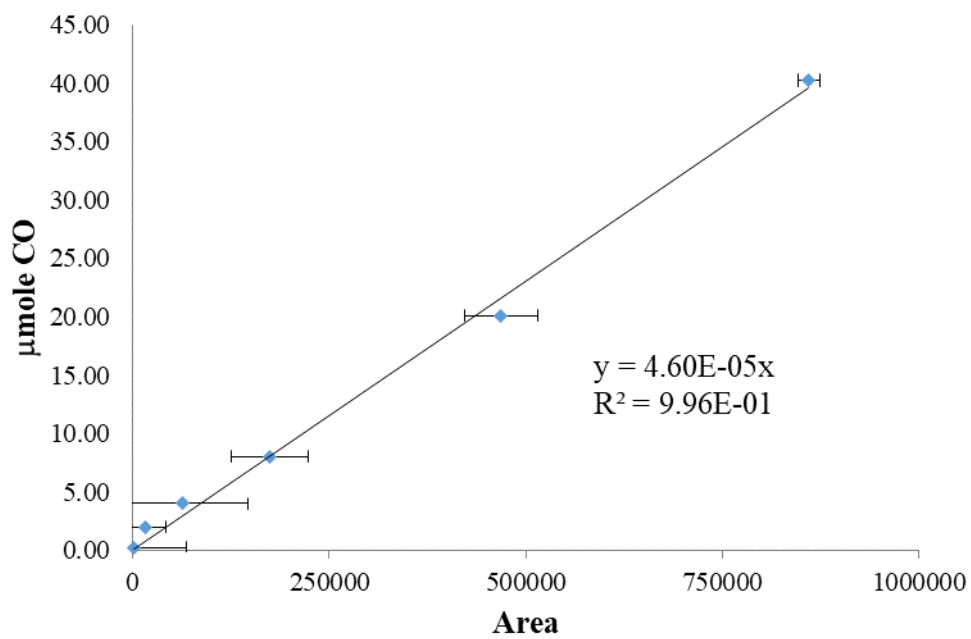
Figure C.8 the calibration curve of CO.

$y = 4.60E-05x$
$R^2 = 9.96E-01$
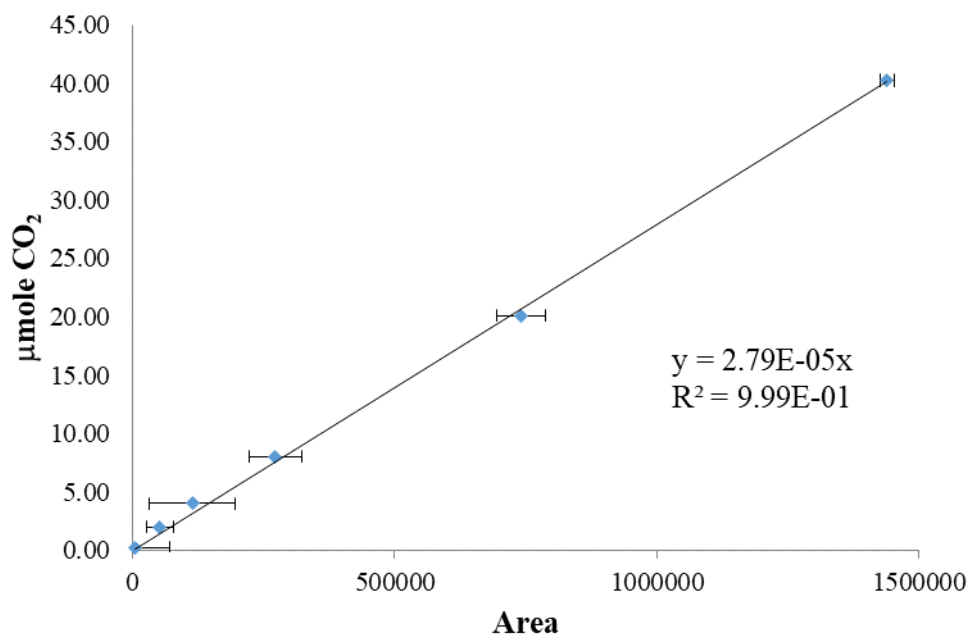
Figure C.9 the calibration curve of CO_2.

$$y = 2.79E\text{-}05x$$
$$R^2 = 9.99E\text{-}01$$

จุฬาลงกรณ์มหาวิทยาลัย

CHULALONGKORN UNIVERSITY
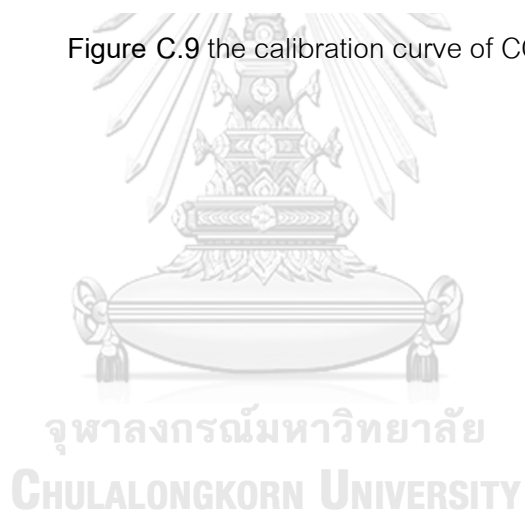
APPENDIX D

CALCULATION OF ETHANOL CONVERSION, PRODUCT SELECTIVITY AND PRODUCT YIELD

In the catalytic activity study, the ethanol conversion and products selectivity are the key parameters demonstrated the catalysts performance. The following calculations were used to determine those parameters in both dehydrogenation and oxidative dehydrogenation of ethanol.

Ethanol conversion

The conversion of ethanol is assigned as the amount of converted ethanol (mole) with respect to ethanol in feed as following equation.

$$\text{Ethanol conversion (\%)} = \frac{[\text{mole of ethanol in feed} - \text{mole of ethanol in product stream}] \times 100}{\text{mole of ethanol in feed}}$$

Product selectivity and yield

The products selectivity is assigned as the amount of product A formed (mole) with respect to total products (mole) as following equation

$$\text{Selectivity of A (\%)} = \frac{[\text{mole of product A}] \times 100}{\text{mole of total products}}$$

The product yield is defined by following equation

$$\text{Yield of A (\%)} = \frac{\text{Ethanol conversion (\%)} \times \text{Selectivity of A (\%)}}{100}$$

APPENDIX E

LIST OF PUBLICATIONS

1. Piriya Pinthong, Piyasan Praserthdam and Bunjerd Jongsomjit. Effect of Calcination Temperature on Mg-Al Layered Double Hydroxides (LDH) as Promising Catalysts in Oxidative Dehydrogenation of Ethanol to Acetaldehyde, Journal of Oleo Science, 68 (2019) 95-102. (Impact factor = 1.182, Q2 by SJR)

2. Piriya Pinthong, Piyasan Praserthdam and Bunjerd Jongsomjit. Oxidative dehydrogenation of ethanol over vanadium- and molybdenum-modified Mg-Al mixed oxide derived from hydrotalcite, Journal of Oleo Science, (In press). (Impact factor = 1.182, Q2 by SJR)
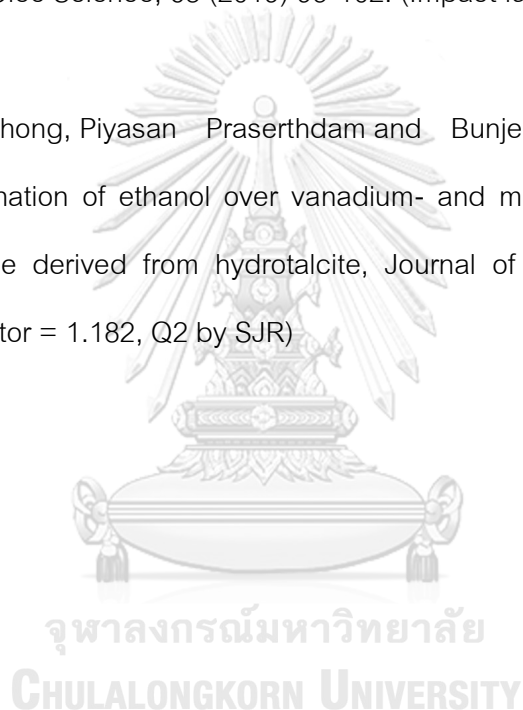
REFERENCES

1. Baltes, M., O. Collart, P. Van der Voort, and E.F. Vansant, *Synthesis of supported transition metal oxide catalysts by the designed deposition of acetylacetonate complexes.* Langmuir, 1999. **15**(18): p. 5841-5845.

2. Papong, S. and P. Malakul, *Life-cycle energy and environmental analysis of bioethanol production from cassava in Thailand.* Bioresource Technology, 2010. **101**(1, Supplement): p. S112-S118.

3. Kumar, S., R. Gupta, G. Kumar, D. Sahoo, and R.C. Kuhad, *Bioethanol production from Gracilaria verrucosa, a red alga, in a biorefinery approach.* Bioresource technology, 2013. **135**: p. 150-156.

4. Dias, M.O., M. Modesto, A.V. Ensinas, S.A. Nebra, R. Maciel Filho, and C.E. Rossell, *Improving bioethanol production from sugarcane: evaluation of distillation, thermal integration and cogeneration systems.* Energy, 2011. **36**(6): p. 3691-3703.

5. Llera, I., V. Mas, M. Bergamini, M. Laborde, and N. Amadeo, *Bio-ethanol steam reforming on Ni based catalyst. Kinetic study.* Chemical engineering science, 2012. **71**: p. 356-366.

6. Phung, T.K., L. Proietti Hernández, and G. Busca, *Conversion of ethanol over transition metal oxide catalysts: Effect of tungsta addition on catalytic behaviour of titania and zirconia.* Applied Catalysis A: General, 2015. **489**: p. 180-187.

7. Li, X. and E. Iglesia, *Selective Catalytic Oxidation of Ethanol to Acetic Acid on Dispersed Mo‑V‑Nb Mixed Oxides.* Chemistry–A European Journal, 2007. **13**(33): p. 9324-9330.

8. Krutpijit, C. and B. Jongsomjit, *Catalytic Ethanol dehydration over different acid-activated montmorillonite clays.* Journal of oleo science, 2016. **65**(4): p. 347-355.

9. Kamsuwan, T., P. Praserthdam, and B. Jongsomjit, *Diethyl ether production during catalytic dehydration of ethanol over Ru-and Pt-modified H-beta zeolite catalysts.* Journal of oleo science, 2017. **66**(2): p. 199-207.

10. Takei, T., N. Iguchi, and M. Haruta, *Synthesis of Acetoaldehyde, Acetic Acid, and Others by the Dehydrogenation and Oxidation of Ethanol.* Catalysis Surveys from Asia, 2011. **15**(2): p. 80-88.

11. Sato, A.G., D.P. Volanti, D.M. Meira, S. Damyanova, E. Longo, and J.M.C. Bueno, *Effect of the ZrO$_2$ phase on the structure and behavior of supported Cu catalysts for ethanol conversion.* Journal of Catalysis, 2013. **307**: p. 1-17.

12. Mallat, T. and A. Baiker, *Oxidation of Alcohols with Molecular Oxygen on Solid Catalysts.* Chemical Reviews, 2004. **104**(6): p. 3037-3058.

13. Shan, J., N. Janvelyan, H. Li, J. Liu, T.M. Egle, J. Ye, M.M. Biener, J. Biener, C.M. Friend, and M. Flytzani-Stephanopoulos, *Selective non-oxidative dehydrogenation of ethanol to acetaldehyde and hydrogen on highly dilute NiCu alloys.* Applied Catalysis B: Environmental, 2017. **205**: p. 541-550.

14. Autthanit, C., P. Praserthdam, and B. Jongsomjit, *Oxidative and non-oxidative dehydrogenation of ethanol to acetaldehyde over different VO$_x$/SBA-15 catalysts.* Journal of Environmental Chemical Engineering, 2018. **6**(5): p. 6516-6529.

15. Neramittagapong, A., W. Attaphaiboon, and S. Neramittagapong, *Acetaldehyde production from ethanol over Ni-based catalysts.* Chiang Mai J. Sci, 2008. **35**(1): p. 171-177.

16. Fan, D., D.-J. Dai, and H.-S. Wu, *Ethylene formation by catalytic dehydration of ethanol with industrial considerations.* Materials, 2012. **6**(1): p. 101-115.

17. Gomez, M.F., L.A. Arrua, and M.C. Abello, *Kinetic Study of Partial Oxidation of Ethanol over VMgO Catalyst.* Industrial & Engineering Chemistry Research, 1997. **36**(9): p. 3468-3472.

18. Tu, Y.-J. and Y.-W. Chen, *Effects of Alkali Metal Oxide Additives on Cu/SiO$_2$ Catalyst in the Dehydrogenation of Ethanol.* Industrial & Engineering Chemistry Research, 2001. **40**(25): p. 5889-5893.

19. Quaranta, N.E., J. Soria, V.C. Corberán, and J.L.G. Fierro, *Selective Oxidation of Ethanol to Acetaldehyde on V$_2$O$_5$/TiO$_2$/SiO$_2$ Catalysts.* Journal of Catalysis, 1997. **171**(1): p. 1-13.

20. Guan, Y. and E.J. Hensen, *Selective oxidation of ethanol to acetaldehyde by Au‑Ir catalysts.* Journal of catalysis, 2013. **305**: p. 135-145.

21. Liu, P., T. Li, H. Chen, and E.J. Hensen, *Optimization of Au^0–Cu^+ synergy in $Au/MgCuCr_2O_4$ catalysts for aerobic oxidation of ethanol to acetaldehyde.* Journal of Catalysis, 2017. **347**: p. 45-56.

22. Chen, K., A.T. Bell, and E. Iglesia, *The relationship between the electronic and redox properties of dispersed metal oxides and their turnover rates in oxidative dehydrogenation reactions.* Journal of Catalysis, 2002. **209**(1): p. 35-42.

23. Tichit, D., C. Gerardin, R. Durand, and B. Coq, *Layered double hydroxides: precursors for multifunctional catalysts.* Topics in catalysis, 2006. **39**(1-2): p. 89-96.

24. Sikander, U., S. Sufian, and M.A. Salam, *A review of hydrotalcite based catalysts for hydrogen production systems.* International Journal of Hydrogen Energy, 2017. **42**(31): p. 19851-19868.

25. Ramasamy, K.K., M. Gray, H. Job, D. Santosa, X.S. Li, A. Devaraj, A. Karkamkar, and Y. Wang, *Role of calcination temperature on the hydrotalcite derived MgO–Al_2O_3 in converting ethanol to butanol.* Topics in Catalysis, 2016. **59**(1): p. 46-54.

26. Holgado, M., V. Rives, and M. San Román, *Characterization of Ni–Mg–Al mixed oxides and their catalytic activity in oxidative dehydrogenation of n-butane and propene.* Applied Catalysis A: General, 2001. **214**(2): p. 219-228.

27. Holgado, M., F. Labajos, M. Montero, and V. Rives, *Thermal decomposition of Mg/V hydrotalcites and catalytic performance of the products in oxidative dehydrogenation reactions.* Materials research bulletin, 2003. **38**(14): p. 1879-1891.

28. Zhou, W., Q. Tao, J. Pan, J. Liu, J. Qian, M. He, and Q. Chen, *Effect of basicity on the catalytic properties of Ni-containing hydrotalcites in the aerobic oxidation of alcohol.* Journal of Molecular Catalysis A: Chemical, 2016. **425**: p. 255-265.

29. Pinthong, P., P. Praserthdam, and B. Jongsomjit, *Effect of Calcination Temperature on Mg-Al Layered Double Hydroxides (LDH) as Promising Catalysts in Oxidative*

Dehydrogenation of Ethanol to Acetaldehyde. Journal of oleo science, 2019. **68**(1): p. 95-102.

30. Bahranowski, K., G. Bueno, V.C. Corberán, F. Kooli, E. Serwicka, R. Valenzuela, and K. Wcisło, *Oxidative dehydrogenation of propane over calcined vanadate-exchanged Mg, Al-layered double hydroxides.* Applied Catalysis A: General, 1999. **185**(1): p. 65-73.

31. Mitchell, P. and S. Wass, *Propane dehydrogenation over molybdenum hydrotalcite catalysts.* Applied Catalysis A: General, 2002. **225**(1-2): p. 153-165.

32. Zǎvoianu, R., R. Bîrjega, O.D. Pavel, A. Cruceanu, and M. Alifanti, *Hydrotalcite like compounds with low Mo-loading active catalysts for selective oxidation of cyclohexene with hydrogen peroxide.* Applied Catalysis A: General, 2005. **286**(2): p. 211-220.

33. Malherbe, F., C. Depege, C. Forano, J. Besse, M. Atkins, B. Sharma, and S. Wade, *Alkoxylation reaction catalysed by layered double hydroxides.* Applied clay science, 1998. **13**(5-6): p. 451-466.

34. Inmanee, T., P. Pinthong, and B. Jongsomjit, *Effect of Calcination Temperatures and Mo Modification on Nanocrystalline (γ-χ)-Al$_2$O$_3$ Catalysts for Catalytic Ethanol Dehydration.* Journal of Nanomaterials, 2017. **2017**: p. 9.

35. Velu, S. and C.S. Swamy, *Selective C-alkylation of phenol with methanol over catalysts derived from copper-aluminium hydrotalcite-like compounds.* Applied Catalysis A: General, 1996. **145**(1): p. 141-153.

36. Velu, S. and C.S. Swamy, *Alkylation of phenol with 1-propanol and 2-propanol over catalysts derived from hydrotalcite-like anionic clays.* Catalysis Letters, 1996. **40**(3): p. 265-272.

37. Hosoglu, F., J. Faye, K. Mareseanu, G. Tesquet, P. Miquel, M. Capron, O. Gardoll, J.-F. Lamonier, C. Lamonier, and F. Dumeignil, *High resolution NMR unraveling Cu substitution of Mg in hydrotalcites–ethanol reactivity.* Applied Catalysis A: General, 2015. **504**: p. 533-541.

38. Kaneda, K., S. Ueno, and T. Imanaka, *Catalysis of transition metal-functionalized*

hydrotalcites for the Baeyer-Villiger oxidation of ketones in the presence of molecular oxygen and benzaldehyde. Journal of Molecular Catalysis A: Chemical, 1995. **102**(3): p. 135-138.

39. Ob-eye, J., P. Praserthdam, and B. Jongsomjit, *Dehydrogenation of Ethanol to Acetaldehyde over Different Metals Supported on Carbon Catalysts.* Catalysts, 2019. **9**(1): p. 66.

40. Pimentel, D. and T.W. Patzek, *Ethanol production using corn, switchgrass, and wood; biodiesel production using soybean and sunflower.* Natural resources research, 2005. **14**(1): p. 65-76.

41. Eckert, M., G. Fleischmann, R. Jira, H.M. Bolt, and K. Golka, *Acetaldehyde*, in *Ullmann's Encyclopedia of Industrial Chemistry*. 2002, Wiley-VCH: Weinhiem, Germany. p. 31-44.

42. Lanzafame, P., G. Centi, and S. Perathoner, *Catalysis for biomass and CO$_2$ use through solar energy: opening new scenarios for a sustainable and low-carbon chemical production.* Chem Soc Rev, 2014. **43**(22): p. 7562-80.

43. Sun, J. and Y. Wang, *Recent Advances in Catalytic Conversion of Ethanol to Chemicals.* ACS Catalysis, 2014. **4**(4): p. 1078-1090.

44. Holz, M.C., K. Tolle, and M. Muhler, *Gas-phase oxidation of ethanol over Au/TiO$_2$ catalysts to probe metal-support interactions.* Catalysis Science & Technology, 2014. **4**(10): p. 3495-3504.

45. Church, J.M. and H.K. Joshi, *Acetaldehyde by Dehydrogenation of Ethyl Alcohol.* Industrial & Engineering Chemistry, 1951. **43**(8): p. 1804-1811.

46. Allison, J.N. and W.A. Goddard, *Oxidative Dehydrogenation of Methanol to Formaldehyde.* Catalysis, 1985. **92**(127-135).

47. Chubar, N., V. Gerda, O. Megantari, M. Mičušík, M. Omastova, K. Heister, P. Man, and J. Fraissard, *Applications versus properties of Mg–Al layered double hydroxides provided by their syntheses methods: Alkoxide and alkoxide-free sol– gel syntheses and hydrothermal precipitation.* Chemical Engineering Journal, 2013. **234**: p. 284-299.

48.   Xu, Z.P., J. Zhang, M.O. Adebajo, H. Zhang, and C. Zhou, *Catalytic applications of layered double hydroxides and derivatives.* Applied Clay Science, 2011. **53**(2): p. 139-150.

49.   Zubitur, M., M.A. Gómez, and M. Cortázar, *Structural characterization and thermal decomposition of layered double hydroxide/poly(p-dioxanone) nanocomposites.* Polymer Degradation and Stability, 2009. **94**(5): p. 804-809.

50.   Forano, C., U. Costantino, V. Prévot, and C.T. Gueho, *Layered Double Hydroxides (LDH).* Developments in Clay Science, 2013. **5**: p. 745-782.

51.   Cavani, F., F. Trifirò, and A. Vaccari, *Hydrotalcite-type anionic clays: Preparation, properties and applications.* Catalysis Today, 1991. **11**(2): p. 173-301.

52.   Lopez, T., P. Bosch, E. Ramos, R. Gomez, O. Novaro, D. Acosta, and F. Figueras, *Synthesis and Characterization of Sol-Gel Hydrotalcites. Structure and Texture.* Langmuir, 1996. **12**(1): p. 189-192.

53.   Kovanda, F., D. Koloušek, Z. Cílová, and V. Hulínský, *Crystallization of synthetic hydrotalcite under hydrothermal conditions.* Applied clay science, 2005. **28**(1): p. 101-109.

54.   Sharma, S.K., P.K. Kushwaha, V.K. Srivastava, S.D. Bhatt, and R.V. Jasra, *Effect of hydrothermal conditions on structural and textural properties of synthetic hydrotalcites of varying Mg/Al ratio.* Industrial & engineering chemistry research, 2007. **46**(14): p. 4856-4865.

55.   Xu, Z.P., G. Stevenson, C.-Q. Lu, and G.Q. Lu, *Dispersion and size control of layered double hydroxide nanoparticles in aqueous solutions.* The Journal of Physical Chemistry B, 2006. **110**(34): p. 16923-16929.

56.   Meyn, M., K. Beneke, and G. Lagaly, *Anion-exchange reactions of layered double hydroxides.* Inorganic Chemistry, 1990. **29**(26): p. 5201-5207.

57.   Rives, V. and M.a. Angeles Ulibarri, *Layered double hydroxides (LDH) intercalated with metal coordination compounds and oxometalates.* Coordination Chemistry Reviews, 1999. **181**(1): p. 61-120.

58.   Gérardin, C., D. Kostadinova, N. Sanson, B. Coq, and D. Tichit, *Supported Metal*

Particles from LDH Nanocomposite Precursors: Control of the Metal Particle Size at Increasing Metal Content. Chemistry of Materials, 2005. **17**(25): p. 6473-6478.

59. Wu, G., L. Wang, D.G. Evans, and X. Duan, *Layered double hydroxides containing intercalated zinc sulfide nanoparticles: synthesis and characterization.* European journal of inorganic chemistry, 2006. **2006**(16): p. 3185-3196.

60. Kooli, F., V. Rives, and M. Ulibarri, *Preparation and study of decavanadate-pillared hydrotalcite-like anionic clays containing transition metal cations in the layers. 1. Samples containing nickel-aluminum prepared by anionic exchange and reconstruction.* Inorganic chemistry, 1995. **34**(21): p. 5114-5121.

61. Sato, T., T. Wakabayashi, and M. Shimada, *Adsorption of various anions by magnesium aluminum oxide of ($Mg_{0.7}Al_{0.3}O_{1.15}$).* Industrial & Engineering Chemistry Product Research and Development, 1986. **25**(1): p. 89-92.

62. Weckhuysen, B.M. and D.E. Keller, *Chemistry, spectroscopy and the role of supported vanadium oxides in heterogeneous catalysis.* Catalysis Today, 2003. **78**(1): p. 25-46.

63. Zhu, J., B. Rebenstorf, and S.L.T. Andersson, *Influence of phosphorus on the catalytic properties of V_2O_5/TiO_2 catalysts for toluene oxidation.* Journal of the Chemical Society, Faraday Transactions 1: Physical Chemistry in Condensed Phases, 1989. **85**(11): p. 3645-3662.

64. Spencer, N.D. and C.J. Pereira, *V_2O_5/SiO_2-catalyzed methane partial oxidation with molecular oxygen.* Journal of Catalysis, 1989. **116**(2): p. 399-406.

65. Baltes, M., O. Collart, P. Van Der Voort, and E. Vansant, *Synthesis of supported transition metal oxide catalysts by the designed deposition of acetylacetonate complexes.* Langmuir, 1999. **15**(18): p. 5841-5845.

66. Van Der Voort, P., M. Baltes, and E.F. Vansant, *Stabilized MCM-48/VO_x catalysts: synthesis, characterization and catalytic activity.* Catalysis today, 2001. **68**(1): p. 119-128.

67. Carrier, X., J.-F. Lambert, S. Kuba, H. Knözinger, and M. Che, *Influence of ageing on MoO_3 formation in the preparation of alumina-supported Mo catalysts.* Journal

of molecular structure, 2003. **656**(1): p. 231-238.

68. Kitano, T., S. Okazaki, T. Shishido, K. Teramura, and T. Tanaka, *Brønsted acid generation of alumina-supported molybdenum oxide calcined at high temperatures: Characterization by acid-catalyzed reactions and spectroscopic methods.* Journal of Molecular Catalysis A: Chemical, 2013. **371**(0): p. 21-28.

69. Abello, M.C., M.F. Gomez, M. Casella, O.A. Ferretti, M.A. Bañares, and J.L.G. Fierro, *Characterization and performance for propane oxidative dehydrogenation of Li-modified MoO₃/Al₂O₃ catalysts.* Applied Catalysis A: General, 2003. **251**(2): p. 435-447.

70. Lowenthal, E.E., S. Schwarz, and H.C. Foley, *Surface Chemistry of Rh-Mo/γ-Al₂O₃: An Analysis of Surface Acidity.* Journal of Catalysis, 1995. **156**(1): p. 96-105.

71. Han, Y., C. Lu, D. Xu, Y. Zhang, Y. Hu, and H. Huang, *Molybdenum oxide modified HZSM-5 catalyst: Surface acidity and catalytic performance for the dehydration of aqueous ethanol.* Applied Catalysis A: General, 2011. **396**(1): p. 8-13.

72. Forsyth, J.B. and S. Hull, *The effect of hydrostatic pressure on the ambient temperature structure of CuO.* Journal of Physics: Condensed Matter, 1991. **3**(28): p. 5257-5261.

73. Quesada, J., L. Faba, E. Díaz, and S. Ordóñez, *Copper‐Basic Sites Synergic Effect on the Ethanol Dehydrogenation and Condensation Reactions.* ChemCatChem, 2018. **10**(16): p. 3583-3592.

74. Earley, J.H., R.A. Bourne, M.J. Watson, and M. Poliakoff, *Continuous catalytic upgrading of ethanol to n-butanol and C₄ products over Cu/CeO₂ catalysts in supercritical CO₂.* Green Chemistry, 2015. **17**(5): p. 3018-3025.

75. Jiang, D., X. Wu, J. Mao, J. Ni, and X. Li, *Continuous catalytic upgrading of ethanol to n-butanol over Cu–CeO 2/AC catalysts.* Chemical Communications, 2016. **52**(95): p. 13749-13752.

76. Di Cosimo, J.I., Apesteguı, C. a, M. Ginés, and E. Iglesia, *Structural requirements and reaction pathways in condensation reactions of alcohols on MgyAlOₓ catalysts.* Journal of Catalysis, 2000. **190**(2): p. 261-275.

77. León, M., E. Díaz, and S. Ordóñez, *Ethanol catalytic condensation over Mg–Al mixed oxides derived from hydrotalcites.* Catalysis today, 2011. **164**(1): p. 436-442.

78. Poreddy, R., C. Engelbrekt, and A. Riisager, *Copper oxide as efficient catalyst for oxidative dehydrogenation of alcohols with air.* Catalysis Science & Technology, 2015. **5**(4): p. 2467-2477.

79. Janlamool, J. and B. Jongsomjit, *Oxidative dehydrogenation of ethanol over AgLi–Al_2O_3 catalysts containing different phases of alumina.* Catalysis Communications, 2015. **70**: p. 49-52.

80. Lippits, M.J. and B.E. Nieuwenhuys, *Direct conversion of ethanol into ethylene oxide on gold-based catalystsEffect of CeO_x and Li_2O addition on the selectivity.* Journal of Catalysis, 2010. **274**(2): p. 142-149.

81. Deo, G. and I.E. Wachs, *Reactivity of Supported Vanadium Oxide Catalysts: The Partial Oxidation of Methanol.* Journal of Catalysis, 1994. **146**(2): p. 323-334.

82. Arthit Neramittagapong, W.A., Sutasinee Neramittagapong, *Acetaldehyde Production from Ethanol over Ni-Based Catalysts.* Chiang Mai J. Sci., 2008. **35**(1): p. 171-177.

83. Ramaswamy, A.V., P. Ratnasamy, and L.M. Yeddanapalli, *CHANGES IN THE STRUCTURE OF A CATALYST DURING A CATALYTIC REACTION-DEHYDROGENATION OF CYCLOHEXANOL ON NICKEL OXIDE.* Current Science, 1970. **39**(14): p. 316-319.

84. Gucbilmez, Y., T. Dogu, and S. Balci, *Ethylene and Acetaldehyde Production by Selective Oxidation of Ethanol Using Mesoporous V-MCM-41 Catalysts.* Industrial & engineering chemistry research, 2006. **45**(10): p. 3496-3502.

85. Stošić, D., F. Hosoglu, S. Bennici, A. Travert, M. Capron, F. Dumeignil, J.L. Couturier, J.L. Dubois, and A. Auroux, *Methanol and ethanol reactivity in the presence of hydrotalcites with Mg/Al ratios varying from 2 to 7.* Catalysis Communications, 2017. **89**: p. 14-18.

86. Campisano, I.S.P., C.B. Rodella, Z.S.B. Sousa, C.A. Henriques, and V. Teixeira da

Silva, *Influence of thermal treatment conditions on the characteristics of Cu-based metal oxides derived from hydrotalcite-like compounds and their performance in bio-ethanol dehydrogenation to acetaldehyde.* Catalysis Today.

87. Hidalgo, J.M., Z. Tišler, D. Kubička, K. Raabova, and R. Bulanek, *(V)/Hydrotalcite, (V)/Al$_2$O$_3$, (V)/TiO$_2$ and (V)/SBA-15 catalysts for the partial oxidation of ethanol to acetaldehyde.* Journal of Molecular Catalysis A: Chemical, 2016. **420**: p. 178-189.

88. Ramasamy, K.K., M. Gray, H. Job, D. Santosa, X.S. Li, A. Devaraj, A. Karkamkar, and Y. Wang, *Role of Calcination Temperature on the Hydrotalcite Derived MgO–Al$_2$O$_3$ in Converting Ethanol to Butanol.* Topics in Catalysis, 2016. **59**(1): p. 46-54.

89. Abd El-Raady, A.A., N.E. Fouad, M.A. Mohamed, and S.A. Halawy, *Effect of the Preparation Methodof Al–Mg–O Catalysts on the Selective Decomposition of Ethanol.* Monatshefte für Chemie/Chemical Monthly, 2002. **133**(10): p. 1351-1361.

90. Mitran, G., T. Cacciaguerra, S. Loridant, D. Tichit, and I.-C. Marcu, *Oxidative dehydrogenation of propane over cobalt-containing mixed oxides obtained from LDH precursors.* Applied Catalysis A: General, 2012. **417**: p. 153-162.

91. Dula, R., K. Wcisło, J. Stoch, B. Grzybowska, E. Serwicka, F. Kooli, K. Bahranowski, and A. Gaweł, *Layered double hydroxide-derived vanadium catalysts for oxidative dehydrogenation of propane: Influence of interlayer-doping versus layer-doping.* Applied Catalysis A: General, 2002. **230**(1): p. 281-291.

92. Mészáros, S., J. Halász, Z. Kónya, P. Sipos, and I. Pálinkó, *Reconstruction of calcined MgAl- and NiMgAl-layered double hydroxides during glycerol dehydration and their recycling characteristics.* Applied Clay Science, 2013. **80-81**: p. 245-248.

93. A. Aramendia, M., Y. Aviles, V. Borau, J. M. Luque, J. M. Marinas, J. R. Ruiz, and F. J. Urbano, *Thermal decomposition of Mg/Al and Mg/Ga layered-double hydroxides: a spectroscopic study.* Journal of Materials Chemistry, 1999. **9**(7): p. 1603-1607.

94. Dixit, M., M. Mishra, P.A. Joshi, and D.O. Shah, *Physico-chemical and catalytic properties of Mg–Al hydrotalcite and Mg–Al mixed oxide supported copper*

catalysts. Journal of Industrial and Engineering Chemistry, 2013. **19**(2): p. 458-468.

95.   Yang, W., Y. Kim, P.K.T. Liu, M. Sahimi, and T.T. Tsotsis, *A study by in situ techniques of the thermal evolution of the structure of a Mg–Al–CO₃ layered double hydroxide.* Chemical Engineering Science, 2002. **57**(15): p. 2945-2953.

96.   Li, F., X. Jiang, D.G. Evans, and X. Duan, *Structure and basicity of mesoporous materials from Mg/Al/In layered double hydroxides prepared by separate nucleation and aging steps method.* Journal of Porous Materials, 2005. **12**(1): p. 55-63.

97.   Dai, W.-L., Y. Cao, L.-P. Ren, X.-L. Yang, J.-H. Xu, H.-X. Li, H.-Y. He, and K.-N. Fan, *Ag–SiO₂–Al₂O₃ composite as highly active catalyst for the formation of formaldehyde from the partial oxidation of methanol.* Journal of Catalysis, 2004. **228**(1): p. 80-91.

98.   Nair, H., J.E. Gatt, J.T. Miller, and C.D. Baertsch, *Mechanistic insights into the formation of acetaldehyde and diethyl ether from ethanol over supported VOₓ, MoOₓ, and WOₓ catalysts.* Journal of Catalysis, 2011. **279**(1): p. 144-154.

99.   Blokhina, A.S., I.A. Kurzina, V.I. Sobolev, K.Y. Koltunov, G.V. Mamontov, and O.V. Vodyankina, *Selective oxidation of alcohols over Si₃N₄-supported silver catalysts.* Kinetics and Catalysis, 2012. **53**(4): p. 477-481.

100.   Pavel, O.D., D. Tichit, and I.-C. Marcu, *Acido-basic and catalytic properties of transition-metal containing Mg–Al hydrotalcites and their corresponding mixed oxides.* Applied Clay Science, 2012. **61**: p. 52-58.

101.   Di Cosimo, J., V. Dıez, M. Xu, E. Iglesia, and C. Apesteguıa, *Structure and surface and catalytic properties of Mg-Al basic oxides.* Journal of Catalysis, 1998. **178**(2): p. 499-510.

102.   Constantino, V.R.L. and T.J. Pinnavaia, *Basic Properties of Mg²⁺₁₋ₓAl³⁺ₓ Layered Double Hydroxides Intercalated by Carbonate, Hydroxide, Chloride, and Sulfate Anions.* Inorganic Chemistry, 1995. **34**(4): p. 883-892.

103.   Idriss, H. and E. Seebauer, *Reactions of ethanol over metal oxides.* Journal of Molecular Catalysis A: Chemical, 2000. **152**(1-2): p. 201-212.

104. Zhou, H., J. Wang, X. Chen, C.-L. O'Young, and S.L. Suib, *Studies of oxidative dehydrogenation of ethanol over manganese oxide octahedral molecular sieve catalysts.* Microporous and Mesoporous Materials, 1998. **21**(4-6): p. 315-324.

105. Santacesaria, E., A. Sorrentino, R. Tesser, M. Di Serio, and A. Ruggiero, *Oxidative dehydrogenation of ethanol to acetaldehyde on V_2O_5/TiO_2-SiO_2 catalysts obtained by grafting vanadium and titanium alkoxides on silica.* Journal of Molecular Catalysis A: Chemical, 2003. **204**: p. 617-627.

106. Mielby, J., J.O. Abildstrøm, F. Wang, T. Kasama, C. Weidenthaler, and S. Kegnæs, *Oxidation of Bioethanol using Zeolite‐Encapsulated Gold Nanoparticles.* Angewandte Chemie, 2014. **126**(46): p. 12721-12724.

107. Sobolev, V.I., K.Y. Koltunov, O.A. Simakova, A.-R. Leino, and D.Y. Murzin, *Low temperature gas-phase oxidation of ethanol over Au/TiO_2.* Applied Catalysis A: General, 2012. **433**: p. 88-95.

108. Zhang, M., F. Yu, J. Li, K. Chen, Y. Yao, P. Li, M. Zhu, Y. Shi, Q. Wang, and X. Guo, *High CO Methanation Performance of Two-Dimensional Ni/MgAl Layered Double Oxide with Enhanced Oxygen Vacancies via Flash Nanoprecipitation.* Catalysts, 2018. **8**(9): p. 363.

109. Gazzoli, D., S. De Rossi, G. Ferraris, M. Valigi, L. Ferrari, and S. Selci, *Morphological and textural characterization of vanadium oxide supported on zirconia by ionic exchange.* Applied Surface Science, 2008. **255**(5, Part 1): p. 2012-2019.

110. Li, X., L. Wang, Q. Xia, Z. Liu, and Z. Li, *Catalytic oxidation of toluene over copper and manganese based catalysts: Effect of water vapor.* Catalysis Communications, 2011. **14**(1): p. 15-19.

111. Leofanti, G., M. Padovan, G. Tozzola, and B. Venturelli, *Surface area and pore texture of catalysts.* Catalysis Today, 1998. **41**(1): p. 207-219.

112. Caro, C., K. Thirunavukkarasu, M. Anilkumar, N. Shiju, and G. Rothenberg, *Selective Autooxidation of Ethanol over Titania‐Supported Molybdenum Oxide Catalysts: Structure and Reactivity.* Advanced synthesis & catalysis, 2012. **354**(7):

p. 1327-1336.

113. Janlamool, J. and B. Jongsomjit, *Catalytic Ethanol Dehydration to Ethylene over Nanocrystalline χ- and γ-Al$_2$O$_3$ Catalysts.* Journal of Oleo Science, 2017. **66**(9): p. 1029-1039.

114. Andrushkevich, T.V., V.V. Kaichev, Y.A. Chesalov, A.A. Saraev, and V.I. Buktiyarov, *Selective oxidation of ethanol over vanadia-based catalysts: The influence of support material and reaction mechanism.* Catalysis Today, 2017. **279**: p. 95-106.

115. Campisano, I.S.P., C.B. Rodella, Z.S.B. Sousa, C.A. Henriques, and V. Teixeira da Silva, *Influence of thermal treatment conditions on the characteristics of Cu-based metal oxides derived from hydrotalcite-like compounds and their performance in bio-ethanol dehydrogenation to acetaldehyde.* Catalysis Today, 2018. **306**: p. 111-120.

116. Ahmed, R., C. Sinnathambi, and D. Subbarao, *Kinetics of de-coking of spent reforming catalyst.* Journal of Applied Sciences, 2011. **11**(7): p. 1225-1230.

117. Nagaraja, B.M., A.H. Padmasri, P. Seetharamulu, K. Hari Prasad Reddy, B. David Raju, and K.S. Rama Rao, *A highly active Cu-MgO-Cr$_2$O$_3$ catalyst for simultaneous synthesis of furfuryl alcohol and cyclohexanone by a novel coupling route— Combination of furfural hydrogenation and cyclohexanol dehydrogenation.* Journal of Molecular Catalysis A: Chemical, 2007. **278**(1): p. 29-37.

118. Krutpijit, C. and B. Jongsomjit, *Effect of HCl Loading and Ethanol Concentration over HCl-Activated Clay Catalysts for Ethanol Dehydration to Ethylene.* Journal of oleo science, 2017. **66**(12): p. 1355-1364.

119. Wu, L., T. Zhou, Q. Cui, H. Wang, Y. Hu, and H. Huang, *The catalytic dehydration of bio-ethanol to ethylene on SAPO-34 catalysts.* Petroleum Science and Technology, 2013. **31**(22): p. 2414-2421.

120. Golay, S., R. Doepper, and A. Renken, *Reactor performance enhancement under periodic operation for the ethanol dehydration over γ-alumina, a reaction with a stop-effect.* Chemical Engineering Science, 1999. **54**(20): p. 4469-4474.

121. Chen, G., S. Li, F. Jiao, and Q. Yuan, *Catalytic dehydration of bioethanol to*

*ethylene over TiO$_2$/**γ**-Al$_2$O$_3$ catalysts in microchannel reactors.* Catalysis Today, 2007. **125**(1-2): p. 111-119.

VITA

NAME   Piriya Pinthong

DATE OF BIRTH   20 February 1985

PLACE OF BIRTH   Bangkok, Thailand

INSTITUTIONS ATTENDED   M.Eng. (Chemical Engineering), Kasetsart University

                           B.S. (Industrial Chemistry), Kasetsart University

HOME ADDRESS   33 Soi Phiboonsongkram 2, Phiboonsongkram Rd.,

                           Nonthaburi, Thailand

PUBLICATION   1. Piriya Pinthong, Piyasan Praserthdam and Bunjerd

                           Jongsomjit. Effect of Calcination Temperature on Mg-Al

                           Layered Double Hydroxides (LDH) as Promising Catalysts in

                           Oxidative Dehydrogenation of Ethanol to Acetaldehyde,

                           Journal of Oleo Science, 68 (2019) 95-102.

                           2. Piriya Pinthong, Piyasan Praserthdam and Bunjerd

                           Jongsomjit. Oxidative dehydrogenation of ethanol over

                           vanadium- and molybdenum-modified Mg-Al mixed oxide

                           derived from hydrotalcite, Journal of Oleo Science, In press.